A STUDY OF THE ENERGY LEVELS OF ^{18}Ne, ^{22}Mg, ^{26}Si, ^{30}S, ^{34}Ar, AND ^{38}Ca BY THE (p,t) REACTION

By

Robert Alton Paddock

A THESIS

Submitted to
Michigan State University
in partial fulfillment of the requirements
for the degree of

DOCTOR OF PHILOSOPHY

Department of Physics

1969

ABSTRACT

A STUDY OF THE ENERGY LEVELS OF ^{18}Ne, ^{22}Mg, ^{26}Si, ^{30}S, ^{34}Ar, AND ^{38}Ca BY THE (p,t) REACTION

By

Robert Alton Paddock

A study of the (p,t) reaction on the even-even N=Z nuclei in the 2s1d shell has been carried out. This reaction has been used to study the energy levels of ^{18}Ne, ^{22}Mg, ^{26}Si, ^{30}S, ^{34}Ar and ^{38}Ca. Until recently little has been reported about these nuclei. Except for a few scattered reports of (p,t) experiments, only the (^{3}He,n) and (^{3}He,nγ) reactions have been used to study these nuclei. The excited states that were observed are reported along with the spin and parity assignments when possible.

The two nucleon transfer distorted wave theory of N. K. Glendenning has been studied with respect to these (p,t) reactions. It was found that the shapes of the predicted angular distributions are primarily dependent on the orbital angular momentum transfer and the optical model parameters. This fact was used to make the spin-parity assignments. It was also found that the magnitudes of the predicted cross-sections are strongly dependent on not only the optical model parameters, but

also the bound state parameters of the transferred neutrons and the configuration mixing in the initial and final nuclear wave functions.

It is concluded that the (p,t) reaction is useful to study the energy levels of nuclei two nucleons away from stability. It is also concluded that the two nucleon transfer distorted wave theory is useful to predict the general shapes of angular distributions but that the magnitudes are too dependent on parameters which are not well known to be predicted successfully.

A STUDY OF THE ENERGY LEVELS OF ^{18}Ne, ^{22}Mg, ^{26}Si, ^{30}S, ^{34}Ar, AND ^{38}Ca BY THE (p,t) REACTION

By

Robert Alton Paddock

A THESIS

Submitted to
Michigan State University
in partial fulfillment of the requirements
for the degree of

DOCTOR OF PHILOSOPHY

Department of Physics

1969

ACKNOWLEDGMENTS

I would first of all like to thank Dr. Walter Benenson for suggesting these experiments as a thesis topic and his help in carrying out the experimental work. I would also like to thank Dr. B. Preedom for his helpful discussions on the distorted wave method. My thanks go to Dr. K. Koltveit for his aid in my understanding of parentage factors. I would also like to thank Dr. W. Gerace for making a copy of the code TWOFRM available to the M.S.U. Cyclotron Laboratory, and Professor R. M. Drisko for making a copy of the FORTRAN-IV version of the JULIE available. Special thanks go to Dr. P. Locard and Mr. Ivan Proctor for their help in taking the data as well as to the entire staff of the Cyclotron Laboratory. I must also thank Mr. P. Plauger, whose relativistic kinematics computer routine was used throughout the analysis of the experimental data.

I would also like to acknowledge the financial support of the National Science Foundation and Michigan State University throughout my graduate work.

Very special thanks to my wife, Connie, for her understanding through the past two years, and for the typing of the rough copies of this thesis.

TABLE OF CONTENTS

LIST OF TABLES

LIST OF FIGURES

CHAPTER 1

INTRODUCTION

The two nucleon transfer reaction has been studied for the particular case of the (p,t) reaction. The targets studied were the even-even, N=Z nuclei in the 2s1d shell. In particular, the targets were ^{20}Ne, ^{24}Mg, ^{28}Si, ^{32}S, ^{36}Ar and ^{40}Ca, which all have $J^{\pi}=0^{+}$ ground states. These (p,t) reactions reach states in nuclei which are two nucleons away from stability. Until recently these nuclei had not been studied to any great extent. The same nuclei can in general also be reached by the (^{3}He,n) reaction, and recently work has been done in this area. Reports of the study of these nuclei with the (p,t) reaction have been scattered and sparce until now. This is most probably due to the large negative Q-values (~-20MeV) and small cross-sections involved, which necessitates a high energy, high intensity proton beam of good resolution such as the Michigan State University Sector Focused Cyclotron is capable of producing.

The (p,t) reaction and other two nucleon transfer reactions have been previously used to study nuclei in the light mass region by experimenters such as Cerny and his co-workers(Ce64, Fl68, Ga64). This reaction has

also been used in the medium to heavy mass region by experimenters such as Hintz and his co-workers[Ba64a, Ba65, Ba68, Ma66b, Re67]. These workers have all reported that the shapes of the angular distributions of the tritons are very much characteristic of the orbital angular momentun transfer of the reaction.

The two nucleon transfer reaction in general and the (p,t) reaction in particular have some very restrictive selection rules (see Chapter 2) which make spin-parity assignments to the final nuclear states quite unambiguous. This is primarily based on the fact that the shapes of the angular distributions of the tritons from the (p,t) reaction are to a great extent dominated by the orbital angular momentum transfer of the reaction. This dependence will be further investigated in later chapters of this work.

Two nucleon transfer theories have been developed which allow the (p,t) reaction to be treated by the direct reaction distorted wave method (see Chapter 3). It was therefore decided to study such a theory, in particular the theory of Glendenning[Gl65], and to investigate the ability of this theory to predict the observed angular distributions. In particular, the dependence of such a theory on the initial and final state wave functions and the bound state wave functions has been studied in Chapter 7.

CHAPTER 2

SELECTION RULES FOR (p,t)

The two nucleon transfer reaction in general and the two neutron pickup reaction in particular have some very special and restrictive selection rules. These rules have been discussed in detail elsewhere (Hi64, G165, Ba64a, G162), and only those applying to (p,t) in particular will be discussed here. Let us denote the angular momentum and isospin of the target as J_A and T_A respectively. The final nucleus will be denoted by J_B and T_B. The orbital angular momentum, spin and total angular momentum of the transferred neutrons will be denoted by ℓ_1, s_1, j_1 and ℓ_2, s_2, j_2. The transferred quantum numbers will be designated by L, S, J and T. We can then write:

$$\vec{S}=\vec{s}_1+\vec{s}_2 \qquad \vec{L}=\vec{\ell}_1+\vec{\ell}_2=\vec{\Lambda}+\vec{\lambda} \qquad \vec{J}=\vec{L}+\vec{S} \tag{2.1}$$

Here we have denoted the orbital angular momentum of the relative and center of mass coordinates of the transferred pair by λ and Λ respectively. This possibility of the relative motion of the two transferred particles

is something which does not arise in single nucleon transfer such as (p,d).

Conservation of angular momentum yields the following restriction, or selection rule.

$$|J_A-J_B| \leq J \leq (J_A+J_B) \tag{2.2}$$

Unless a single step direct interaction model is assumed for the transfer process, the quantity J may not be a good quantum number. Along with equation (2.2), there is also the following restriction on the parity change during the reaction.

$$\Delta\pi=(-1)^{\ell_1+\ell_2}=(-1)^{\Lambda+\lambda} \tag{2.3}$$

We note from equation (2.3) that if both neutrons are picked up from the same shell ($\ell_1=\ell_2$), then $\Delta\pi=+1$. Also, from the Pauli Principle, J must be even. If $\Delta\pi=-1$, then the two neutrons must come from shells of different parity ($\pi=(-1)^{\ell}$). The isospin of two neutrons must be 1, since each has isospin t=1/2 and projection $\tau=+1/2$. Therefore, the following restriction on isospin is imposed.

$$|T_A-T_B| \leq 1 \leq (T_A+T_B) \tag{2.4}$$

In this work, we will be concerned with even-even N=Z targets so that in all cases studied $J_A=0$,

$\tau_A=+1$, and $T_A=0$. Equation (2.2) and (2.4) then leads to the following:

$$J_B=J \qquad T_B=1 \tag{2.5}$$

A neutron seniority selection rule can also be defined. Neutron seniority is related to the number of neutrons not coupled in pairs to zero angular momentum. Since the pickup of two neutrons can break at most two pairs, the following restriction holds.

$$\Delta\nu_n=0,\pm2 \tag{2.6}$$

Seniority is not necessarily a good quantum number and thus this selection rule may not be applicable to the reaction as a whole although it must apply to the individual components of the wave functions which are responsible for the process.

There are also certain approximate selection rules that arise based on some specific properties of the triton. The two neutrons bound in the triton are mostly (~95%)[B162] in a state of relative spatial symmetry (λ even) with S=0. Then according to equation (2.1), J=L, and equations (2.2), (2.3) and (2.5) become:

$$|J_A-J_B|\leq L\leq(J_A+J_B) \tag{2.6}$$

$$\Delta\pi=(-1)^{\Lambda} \tag{2.7}$$

$$J_B = L \text{ for } J_A = 0 \tag{2.8}$$

We will find later that the shape of the angular distribution is very much dominated by the orbital angular momentum transfer L and therefore equation (2.8) makes the spin assignment of the final state unique for the (p,t) reactions as opposed to the case of (p,d) where $J = L \pm 1/2$

If it is further assumed that the neutrons are in a relative s-state ($\lambda = 0$) in the triton, then $L = \Lambda$ and we get the following approximate selection rule from equation (2.7).

$$\Delta\pi = (-1)^L = (-1)^J \tag{2.9}$$

We note that the approximate selection rule of equation (2.9) restricts the nuclear states that can be excited by the (p,t) reaction.

CHAPTER 3

TWO NEUTRON PICKUP AND THE DISTORTED WAVE METHOD

3.1 The Distorted Wave Method

The details of the distorted wave method of calculating direct reaction processes have been discussed by Satchler and others[Sa64, Ba62]. Only those parts of the theory pertinent to applying it to the particular case of two nucleon pickup will be discussed here.

We denote the general reaction as follows:

$$A(a,b)B \tag{3.1}$$

We denote the spins and projections of the particles by J_A, J_B, s_a, s_b, M_A, M_B, m_a and m_b. Following the procedure of Satchler[Sa64], the differential cross-section for such a reaction can be written as follows:

$$\frac{d\sigma}{d\Omega} = \frac{\mu_a \mu_b}{(2\pi\hbar^2)^2} \frac{k_b}{k_a} \frac{\sum_{M_B M_A m_b m_a} |T|^2}{(2J_A+1)(2s_a+1)} \tag{3.1.2}$$

The reduced masses are denoted by μ and k denotes the asymptotic relative momenta. The quantity T is called

the transition amplitude and is defined in equation (3.1.3).

$$T=\langle J_B M_B, s_b m_b, \vec{k}_b | V | J_A M_A, s_a m_a, \vec{k}_a \rangle \qquad (3.1.3)$$

V is the interaction which causes the reaction, i.e. carries the system from one elastic scattering state to another. In the distorted wave formalism of reference Sa64, T can be written as follows:

$$T_{DW} = \mathcal{J} \sum_{\substack{m_a' \\ m_b'}} \int d\vec{r}_{aA} \int d\vec{r}_{bB}\, \chi^{(-)*}_{m_b' m_b}(\vec{k}_b, \vec{r}_b) \qquad (3.1.4)$$

$$\langle J_B M_B s_b m_b' | V | J_A M_A s_a m_a' \rangle \chi^{(+)}_{m_a' m_a}(\vec{k}_a, \vec{r}_a)$$

$\mathcal{J}$ denotes the Jacobian of the transformation from the individual coordinates to the relative coordinate $\vec{r}_{aA}$ and $\vec{r}_{bB}$.

It is convenient to expand the matrix element of equation (3.1.4) in terms corresponding to particular angular momentum transfer. We define the transferred quantities as follows:

$$\vec{J}=\vec{J}_B-\vec{J}_A, \quad \vec{S}=\vec{s}_a-\vec{s}_b, \quad \vec{J}=\vec{L}+\vec{S} \qquad (3.1.5)$$

We write the expansion as follows including the appropriate Clebsh-Gordan coupling coefficients.

$$\mathcal{J} \langle J_B M_B, s_b m_b | V | J_A M_A, s_a m_a \rangle \equiv \mathcal{J}\mathcal{M} \qquad (3.1.6)$$

$$= \sum_{LSJ} \langle J_A\ J\ M_A,\ M_B - M_A | J_B M_B \rangle \langle L\ S\ M,\ m_a - m_b | J,\ M_B - M_A \rangle$$

$$\langle s_a\ s_b\ m_a - m_b | S,\ m_a - m_b \rangle (-1)^{s_b - m_b}\ i^L\ A_{LSJ}(Bb, Aa)$$

$$f_{LSJ,M}(\vec{r}_{bB},\ \vec{r}_{aA})\ ;\ \text{where } M = M_B + m_b - M_A - m_a$$

The product $A_{LSJ} f_{LSJ,M}$ is often called the form factor for the reaction. We substitute this expansion into equation (3.1.4) and define a reduced amplitude β as in equation (13) of reference Sa64.

$$T_{DW} = \sum_J (2J+1)^{1/2} \langle J_A J M_A,\ M_B - M_A | J_B M_B \rangle \qquad (3.1.7)$$

$$\sum_{LS} A_{LSJ}\ \beta_{SJ}^{LMm_b m_a}(\vec{k}_b, \vec{k}_a)$$

Taking the absolute square of T_{DW} and summing over the projections indicated in equation (3.1.2), along with symmetry and completeness relations for the Clebsh-Gordan coefficients from reference Ro67, we get:

$$\Sigma |T_{DW}|^2 = \sum_{JMm_b m_a} (2J_B+1) \left| \sum_{LS} A_{LSJ}\ \beta_{SJ}^{LMm_b m_a} \right|^2 \qquad (3.1.8)$$

Substitution into equation (3.1.2) gives the following expression for the differential cross-section.

$$\frac{d\sigma}{d\Omega} = \frac{\mu_a \mu_b}{(2\pi\hbar^2)^2} \frac{k_b}{k_a} \frac{(2J_B+1)}{(2J_A+1)(2s_a+1)} \sum_{JMm_b m_a} \left| \sum_{LS} A_{LSJ} \beta_{SJ}^{LMm_b m_a} \right|^2 \tag{3.1.9}$$

If only one L and S are important, this reduces to the following:

$$\frac{d\sigma}{d\Omega} = \frac{2J_B+1}{2J_A+1} \sum_J \frac{|A_{LSJ}|^2}{(2s_a+1)} \sigma_{LSJ}(\theta) \tag{3.1.10}$$

Where we have defined the reduced cross-section as follows:

$$\sigma_{LSJ}(\theta) = \frac{\mu_a \mu_b}{(2\pi\hbar^2)^2} \frac{k_b}{k_a} \sum_{Mm_b m_a} \left| \beta_{SJ}^{LMm_b m_a} \right|^2 \tag{3.1.11}$$

It is this reduced cross-section that is calculated by a distorted wave computer code such as JULIE(Ba62). The method of calculating the β_{SJ}^{L}'s has previously been described(Sa64, Ba62) and will not be discussed here. The β_{SJ}^{L}'s are actually calculated in a zero range approximation where $f_{LSJ,M}(\vec{r}_{bB},\vec{r}_{aA})$ is replaced by a purely radial function F_{LSJ}, a spherical harmonic Y_L^{M*} and a three dimensional δ-function in $\vec{r}_{bB}$ and $\vec{r}_{aA}$.

3.2 The Two Neutron Pickup Matrix Element

We now must evaluate the matrix element η of equation (3.1.6) explicitly for the two neutron pickup

reaction. The method of dealing with this matrix element for the case of two nucleon transfer has been developed by several workers(Gl65, Li64, Ba64b, He64a, Ab66, Li66, Br67). We will follow the method of Glendenning(Gl65) along with some of the details, extensions and notation of Jaffe and Gerace(Ja68).

We denote the pair of transferred neutrons as x and write:

$$b=a+x \qquad A=B+x \tag{3.2.1}$$

The interaction responsible for the reaction is assumed to be the interaction of a with x. We assume the interaction is central and is a function of the separation between the center of mass of a and the center of mass of x.

$$V=V(r_{ax}) \tag{3.2.2}$$

Following the procedure of reference (Ba62), we write the matrix element more explicitly as follows:

$$\mathcal{M} = \int d\xi_B \, d\xi_a \, d\xi_x \, \psi^*_{J_B M_B}(\xi_B) \, \psi^*_{s_b m_b}(\vec{r}_{ax},\xi_a,\xi_x) \, V(r_{ax})$$

$$\psi_{J_A M_A}(\xi_B,\vec{r}_{xB},\xi_x) \, \psi_{s_a m_a}(\xi_a) \tag{3.2.3}$$

The ξ's denote the internal coordinates (spin and spatial if appropriate) of the respective particles. We assume

$V(r_{ax})$ does not effect $\psi_{J_A M_A}$ and $\psi_{J_B M_B}$ so that we can consider the integral over $d\xi_B$ separately.

$$G_{AB}^{(M_A-M_B)}(\vec{r}_{xB},\xi_x) \equiv \int d\xi_B \; \psi^*_{J_B M_B}(\xi_B)\; \psi_{J_A M_A}(\xi_a,\vec{r}_{xB},\xi_x) \tag{3.2.4}$$

G_{AB} is then expanded in terms of normalized two particle eigenfunctions of some potential well. In particular, we choose the product wave functions of the two neutrons to be transferred denoted by coordinates and spins $\vec{r}_{1B}$, $\vec{r}_{2B}$, $\vec{\sigma}$, and $\vec{\sigma}_2$ (Ja68).

$$G_{AB}^{(M_A-M_B)} = \sum_{\substack{\alpha\beta \\ LSJ}} {}^{b}\gamma_\alpha\gamma_\beta LSJ \langle J_B J, M_B \; M_A-M_B | J_B M_A\rangle \; \Phi^{(M_A-M_B)}_{\gamma_\alpha\gamma_\beta LSJ}(\vec{r}_{1B},\vec{r}_{2B},\vec{\sigma}_1,\vec{\sigma}_2) \tag{3.2.5}$$

$$\Phi^{(M_A-M_B)}_{\gamma_\alpha\gamma_\beta LSJ} = \sum_M [\phi_{\gamma_\alpha \ell_\alpha}(\vec{r}_{1B})\phi_{\gamma_\beta \ell_\beta}(\vec{r}_{2B})]_L^{-M} \; \chi_S^{M_A-M_B+M}(\vec{\sigma}_1,\vec{\sigma}_2) \; \langle LS, -M \; M_A-M_B+M | J \; M_A-M_B\rangle \tag{3.2.6}$$

The brackets [ ] denote vector coupling of the orbital parts of the two neutron wave functions, and χ_S is the coupled spin part. The Clebsh-Gordan coefficient assures the proper coupling to a specific total angular momentum J,M. We note here that Φ is an L-S coupled two particle

wave function. The sum over α and β implies a sum over all configurations of the two neutrons needed to describe this overlap G_{AB}.

Since the interaction is assumed to depend on the center of mass coordinate of the two neutrons, we must perform a transformation to the coordinates of the product wave function Φ. This is most easily carried out with harmonic oscillator wave functions where the transformation coefficients are calculable in closed form. We expand the ϕ's in terms of harmonic oscillator wave function $\Theta_{n\ell}(\alpha,\vec{r})$ where α is the usual oscillator strength parameter.

$$\phi_{\gamma\ell}(\vec{r}) = \sum_{\mu} a^{\mu}_{\gamma}\ \Theta_{\mu\ell}(\alpha,\vec{r}) \qquad (3.2.7)$$

Equation (3.2.6) becomes:

$$\Phi^{(M_A-M_B)}_{\gamma_\alpha\gamma_\beta LSJ} = \sum_{M}\sum_{\mu\nu} a^{\mu}_{\gamma_\alpha}\ a^{\nu}_{\gamma_\beta}\ [\Theta_{\mu\ell_\alpha}(\alpha,\vec{r}_{1B})\Theta_{\nu\ell_\beta}(\alpha,\vec{r}_{2B})]^{-M}_{L}$$
$$\chi_S^{M_A-M_B+M}(\vec{\sigma}_1,\vec{\sigma}_2) \langle L\ S,\ -M,\ M_A-M_B+M \mid J\ M_A-M_B\rangle \qquad (3.2.8)$$

The well known Moshinsky-Talmi transformation can now be applied to the oscillator wave functions to transform them to relative and center of mass coordinates (Mo59, Br60, La60).

$$\Phi = \sum_{M,\,\mu\nu} a^{\mu}_{\gamma_\alpha}\, a^{\nu}_{\gamma_\beta} \sum_{n\lambda N\Lambda} \langle n\lambda,\, N\Lambda,\, L|\mu\ell_\alpha,\, \nu\ell_\beta,\, L\rangle$$

$$[\Theta_{n\lambda}(\alpha/2,\, \vec{r}_{12})\, \Theta_{N\Lambda}(2\alpha,\, \vec{r}_{xB})]^{-M}_{L}$$

$$\chi^{M_A-M_B+M}_{S}(\vec{\sigma}_1,\vec{\sigma}_2)\, \langle LS,\, -M\ M_A-M_B+M|J\ M_A-M_B\rangle \tag{3.2.9}$$

$N\Lambda$ and $n\lambda$ are the principle and orbital angular momentum quantum numbers associated with the center of mass and relative coordinates respectively. The following restriction on these quantum numbers holds:

$$2(n+N)+\lambda+\Lambda=2(\mu+\nu)+\ell_\alpha+\ell_\beta \tag{3.2.10}$$

The expression for the matrix elements of equation (3.2.3) now can be written as follows:

$$\mathcal{M} = \int d\xi_a\, d\xi_x \sum_{LSJ}{}^{\alpha\beta} b_{\gamma_\alpha\gamma_\beta LSJ}\, \langle J_B\ J,\, M_B,\, M_A-M_B|J_A\ M_A\rangle$$

$$\sum_{M,\,\mu\nu} a^{\mu}_{\gamma_\alpha}\, a^{\nu}_{\gamma_\beta} \sum_{n\lambda N\Lambda} \langle n\lambda,\, N\Lambda,\, L|\mu\ell_\alpha,\, \nu\ell_\beta,\, L\rangle$$

$$[\Theta_{n\lambda}(\alpha/2,\, \vec{r}_{12})\, \Theta_{N\Lambda}(2\alpha,\, \vec{r}_{xB})]^{-M}_{L}\, \chi^{M_A-M_B+M}_{S}(\vec{\sigma}_1,\vec{\sigma}_2)$$

$$\langle LS,\, -M,\, M_A-M_B + M|J\ M_A-M_B\rangle\, \psi^{*}_{S_b m_b}(\vec{r}_{ax},\, \xi_a,\, \xi_x)$$

$$V(r_{ax})\, \psi_{s_a m_a}(\xi_a) \tag{3.2.11}$$

Explicitly, the remaining wave functions can be written as follows for the specific case of (p,t).

$$\psi_{s_a m_a}(\xi_a) = \chi^{m_a}_{s_a}(\vec{\sigma}_a) \quad ; \text{ proton spin wave function} \tag{3.2.12}$$

$$\chi^{M_A-M_B+M}_{S}(\vec{\sigma}_1,\vec{\sigma}_2) = \sum_{m_1 m_2} \langle s_1 s_2 m_1 m_2 | S\ M_A-M_B+M\rangle \chi^{m_1}_{s_1}(\vec{\sigma}_1)\ \chi^{m_2}_{s_2}(\vec{\sigma}_2) \tag{3.2.13}$$

The wave function of the triton is assumed for simplicity to be a Gaussian as suggested in references G165 and Ja68.

$$\psi_{S_b m_b} = N\, e^{-\eta^2(r_{12}^2 + r_{2p}^2 + r_{p1}^2)} \times (\text{spin function}) \tag{3.2.14}$$

This Gaussian wave function can be easily separated, in terms of harmonic oscillator functions, into the relative coordinates of neutrons 1 and 2, and the separation between the proton and the center of mass of 1 and 2 (particle x)[G165].

$$\psi_{s_b m_b}(r_{ax}, \xi_a, \xi_x) = \Theta_{00}(3\eta^2, \vec{r}_{12})\ \Theta_{00}(4\eta^2, \vec{r}_{ax})$$

$$\langle s_p S'\ m_p m' | s_b m_b \rangle\ \chi^{m_b}_{s_p}(\vec{\sigma}_p) \sum_{m'_1\ m'_2}$$

$$\langle s'_1\ s'_2\ m'_1\ m'_2\ |S' m' \rangle\ \chi^{m'_1}_{s'_1}(\vec{\sigma}_1)\ \chi^{m'_2}_{s'_2}(\vec{\sigma}_2) \quad (3.2.15)$$

We restrict S' to be zero as was discussed in Chapter 2. The relative orbital angular momentum of the two neutrons in the triton is also zero indicated by the first factor of equation (3.2.15) and mentioned in Chapter 2.

In order to evaluate $\mathcal{N}$, the integral indicated in equation (3.2.11) must be carried out. We note that $\int d\xi_a\ d\xi_x$ implies $\int d\vec{r}_{12}\ d\vec{\sigma}_a\ d\vec{\sigma}_1\ d\vec{\sigma}_2$. This total integral will involve the following integral.

$$\int \Theta_{00}(3\eta^2, \vec{r}_{12})\ \Theta_{n\lambda}(\alpha/2, \vec{r}_{12}) d\vec{r}_{12} = \delta_{\lambda 0}\ \Omega_n(\alpha, \eta) \quad (3.2.16)$$

This definition of Ω_n is equivalent to the one of Glendenning[G165]. Making the explicit substitution of equations (3.2.12), (3.2.13) and (3.2.15) into equation (3.2.11), the integral can be evaluated making use of the orthonormality of the spin wave functions and the completeness of the Clebsh-Gordan coefficients. We note that the total projection (-M) of the coupled oscillator wave functions can be assigned to $\Theta_{N\Lambda}$ since λ=0 only

for $\Theta_{n\lambda}$ and thus $\Theta_{n\lambda}$ can carry no projection. Also since $\lambda=0$, then Λ must equal L. At the same time, we factor the oscillator wave function into two parts.

$$\Theta_{NL}^{-M}(2\alpha, \vec{r}_{xB}) = R_{NL}(2\alpha r_{xB}^2)\, Y_L^{-M}(\hat{r}_{xB}) \qquad (3.2.17)$$

Evaluating the integral of equation (3.2.11) we get:

$$\mathcal{M} = \sum_{LSJ}^{\alpha\beta} b_{\gamma_\alpha\gamma_\beta LSJ} \langle J_B J\ M_B M_b - M_B \mid J_A M_A\rangle\, A'_{\gamma_\alpha\gamma_\beta L}(r_{xB})$$

$$\sum_{M} Y_L^{-M}(\hat{r}_{xB}) \langle LS,\ -M\ M_A - M_B + M \mid J\ M_A - M_B\rangle$$

$$\langle s_a\ 0\ m_a\ 0 \mid s_b m_b\rangle\, V(r_{ax})\, \Theta^*_{00}(4\eta^2, \vec{r}_{ax})\, \delta_{S,0} \qquad (3.2.18)$$

$$A'_{\gamma_\alpha\gamma_\beta L} = \sum_{\mu\nu} a^{\mu}_{\gamma_\alpha}\, a^{\nu}_{\gamma_\beta} \sum_{nN} \langle n0,\ NL,\ L \mid \mu\ell_\alpha,\ \nu\ell_\beta,\ L\rangle$$

$$\Omega_n(\alpha, \eta)\, R_{NL}(2\alpha r_{xB}^2) \qquad (3.2.19)$$

Using the symmetry properties of the Clebsh-Gordan coefficients and some properties of the spherical harmonics, equation (3.2.18) can be put into a form that can be compared with equation (3.1.6). From this comparison, we can identify $A_{LSJ}\, f_{LSJ,M}$.

$$A_{LSJ}\ f_{LSJ,M} = \mathcal{J} \sum_{\alpha\beta} b_{\gamma_\alpha\gamma_\beta LSJ}\ A'_{\gamma_\alpha\gamma_\beta L}(r_{xB})\ Y_L^{M*}(\hat{r}_{xB})$$

$$V(r_{ax})\ \Theta_{00}^*(4\eta^2, \vec{r}_{ax})$$

$$\delta_{S,O}(-1)^{J_A-J_B+s_a-s_b}\ (-1)^{L+S-J}$$

$$i^L \left(\frac{2s_b+1}{2S+1}\right)^{1/2} \left(\frac{2J_A+1}{2J_B+1}\right)^{1/2}$$

where $M = M_B - M_A - m_a + m_b$

(3.2.20)

The zero range approximation must now be made in order to be able to apply a zero range distorted wave computer code such as JULIE to this theory.

$$V(r_{ax})\Theta_{00}^*(4\eta^2, \vec{r}_{ax}) \approx D_0\ \delta(\vec{r}_{ax}) \qquad (3.2.21)$$

In order to evaluate $\delta(\vec{r}_{ax})$ and the Jacobian $\mathcal{J}$, we write down the geometric relationships in analogy with the results of reference Ba62.

$$\mathcal{J} = \left[\frac{b\ A}{x\left(B+b\right)}\right]^3 = c^3 \qquad (3.2.22)$$

$$\vec{r}_{ax} = -c\left(\frac{\eta_B}{\eta_A}\vec{r}_{bB} - \vec{r}_{aA}\right) \qquad (3.2.23)$$

The quantities denoted by $\mathcal{m}$ represent the masses of the respective particles. Equation (3.2.23) then can be used to evaluate $\delta(\vec{r}_{ax})$.

$$\delta(\vec{r}_{ax}) = (1/c^3)\delta(\frac{\mathcal{m}_B}{\mathcal{m}_A}\vec{r}_{bB} - \vec{r}_{aA})$$

$$= (1/\mathcal{g})\delta(\frac{\mathcal{m}_B}{\mathcal{m}_A}\vec{r}_{bB} - \vec{r}_{aA}) \qquad (3.2.24)$$

When $\vec{r}_{ax}$ goes to zero then $\vec{r}_{x\beta}=\vec{r}_{bB}$. The form factor of equation (3.2.20) with this zero range approximation can then be written as follows:

$$A_{LSJ} = D_0\ \delta_{S,0}\ (-1)^{L+S-J}\ (-1)^{J_A-J_B+s_a-s_b}\ i^L$$

$$\left(\frac{2s_b+1}{2S+1}\right)^{1/2}\left(\frac{2J_A+1}{2J_B+1}\right)^{1/2} \qquad (3.2.25)$$

$$f_{LSJ,M} = \sum_{\alpha\beta}\ b_{\gamma_\alpha\gamma_\beta LSJ}\ A'_{\gamma_\alpha\gamma_\beta L}(r_{bB})\ Y_L^{M*}(\hat{r}_{bB})$$

$$\delta(\frac{\mathcal{m}_B}{\mathcal{m}_A}\vec{r}_{bB} - \vec{r}_{aA}) \qquad (3.2.26)$$

The separation into A_{LSJ} and $f_{LSJ,M}$ is an arbitrary separation for convenience. We now identify $\sum_{\alpha\beta} b_{\gamma_\alpha\gamma_\beta LSJ}\ A'_{\gamma_\alpha\gamma_\alpha L}$ with the F_{LSJ} mentioned at the end

of section 3.2 as the radial form factors which must be read into the distorted wave code JULIE to calculate the $\sigma_{LSJ}(\theta)$ of equation (3.1.11). According to equation (3.1.10), $|A_{LSJ}|^2$ is needed to evaluate the cross-section.

$$|A_{LSJ}|^2 = D_0^2 \frac{2s_b+1}{2S+1} \frac{2J_A+1}{2J_B+1} \quad ; S=0 \qquad (3.2.27)$$

Since S=0, then J=L is the only allowed value. Also for the case of (p,t) which we are considering, $s_a=s_b=1/2$, and equation (3.1.10) becomes:

$$\frac{d\sigma}{d\Omega}_{(p,t)} = D_0^2 \, \sigma_{L0L}(\theta) \qquad (3.2.28)$$

According to reference Ba62, for the particular normalization used in the code JULIE, equation (3.2.28) becomes:

$$\frac{d\sigma}{d\Omega}_{(p,t)} = \frac{D_0^2}{5014} \, \sigma_{L0L}(\text{JULIE}), \text{ [mb/st]} \qquad (3.2.29)$$

3.3 The (p,t) Form Factor

The zero range form factor, F_{LSJ}, that must be input into a distorted wave computer code such as JULIE was calculated in section 3.2.

$$F_{LSJ}(r) = \sum_{\alpha\beta} {}^{b}\gamma_\alpha\gamma_\beta LSJ \; A'_{\gamma_\alpha\gamma_\beta L}(r) \qquad (3.3.1)$$

$$A'_{\gamma_\alpha \gamma_\beta L}(r) = \sum_{\mu\nu} a^{\mu}_{\gamma_\alpha} a^{\nu}_{\gamma_\beta} \sum_{nN} \langle n0,\ NL,\ L \mid \mu\ell_\alpha,\ \nu\ell_\beta,\ L\rangle$$

$$\Omega_n(\alpha,n)\ R_{NL}(2\alpha r^2) \qquad (3.3.2)$$

For reasons that will become evident in section 3.4, we introduce the following factor.

$$\begin{bmatrix} \ell_\alpha & s_\alpha & j_\alpha \\ \ell_\beta & s_\beta & j_\beta \\ L & S & J \end{bmatrix} = \qquad (3.3.3)$$

$$[(2j_2+1)(2j_B+1)(2S+1)(2L+1)]^{1/2}$$

$$\times \begin{Bmatrix} \ell_\alpha & s_\alpha & j_\alpha \\ \ell_\beta & s_\beta & j_\beta \\ L & S & J \end{Bmatrix}$$

The symbol { } is the Wigner 9-J symbol for recoupling four angular momenta[Br62, Sh63]. We rewrite equation (3.3.1).

$$F_{LSJ}(r) = \sum_{\alpha\beta} B_{\gamma_\alpha \gamma_\beta j_\alpha j_\beta J}\ A_{\gamma_\alpha \gamma_\beta LSJ}(r) \qquad (3.3.4)$$

$$A_{\gamma_\alpha \gamma_\beta LSJ} = \begin{bmatrix} \ell_\alpha & s_\alpha & j_\alpha \\ \ell_\beta & s_\beta & j_\beta \\ L & S & J \end{bmatrix} A'_{\gamma_\alpha \gamma_\beta L} \qquad (3.3.5)$$

$$B_{\gamma_\alpha \gamma_\beta j_\alpha j_\beta J} = b_{\gamma_\alpha \gamma_\beta LSJ} \begin{bmatrix} \ell_\alpha & s_\alpha & j_\alpha \\ \ell_\beta & s_\beta & j_\beta \\ L & S & J \end{bmatrix}^{-1} \quad (3.3.6)$$

These B's (or b's) contain spectroscopic information (see section 3.4) and are often called parentage factors. The A's contain the radial dependence and are made up of the radial wave functions of the center of mass of the two neutrons weighted by the overlap of their relative motion with the relative motion of the neutrons in the triton. It is these A's that are calculated by the computer code TWOFRM written by Dr. W. J. Gerace at Princeton University. The code uses eigenfunctions of a real Woods-Saxon well with a spin-orbit term. The triton size parameter η is fixed at 0.242f as suggested by Glendenning[G165].

3.4 The Two Neutron Parentage Factor

The parentage factors are needed to calculate the total form factor. They enter as weighting factors in a sum over all possible neutron configurations in the target nucleus from which two neutrons can be picked up to reach a particular state in the final nucleus.

In section 3.2, the parentage factors were introduced in the expansion of the overlap of the target and residual nuclei.

$$\sum_{\alpha\beta} b_{\gamma_\alpha\gamma_\beta LSJ} \langle J_B\ J\ M_B\ M_A-M_B \mid J_A\ M_A\rangle\ \Phi^{(M_A-M_B)}_{\gamma_\alpha\gamma_\beta LSJ}(\vec{r}_{xB},\xi_x)$$

$$= \int d\xi_B\ \psi^*_{J_B M_B}(\xi_B)\ \psi_{J_A M_A}(\xi_B,\ \vec{r}_{xB},\ \xi_x) \qquad (3.4.1)$$

In order to solve this equation for the parentage factors, we multiply both sides of the equation by (3.4.2).

$$\langle J_B\ J'\ M_B\ M_A-M_B \mid J_A\ M_A\rangle\ \ \Phi^{(M_A-M_B)*}_{\gamma'_\alpha\ \gamma'_\beta\ L'S'J'} \qquad (3.4.2)$$

Then we integrate over $d\vec{r}_{xB}\ d\xi_x$ and finally sum over the spin projections of the initial and final nuclei.

$$b_{\gamma_\alpha\gamma_\beta LSJ} = \int [\psi^*_{J_B}(\xi_B)\ \Phi^*_{\gamma_\alpha\gamma_\beta LSJ}(\xi_B,\ \vec{r}_{xB})]_{J_A}$$

$$\psi_{J_A}(\xi_B\vec{r}_{xB},\ \xi_x)d\xi_B\ d\vec{r}_{xB}\ d\xi_x \qquad (3.4.3)$$

The square brackets denote vector coupling.

We can now interprete the b's as a measure of how much the final nucleus plus the two neutrons looks like the target nucleus. The b's are then a measure of the probability of picking two particular neutrons out of the target and reaching a particular final state of the residual nucleus. The "cross-section" for this component of the reaction is thus proportional to the square of b.

In actuality there may be several possible neutrons which are available to be picked up in this one

manner, so we must multiply the "cross-section" for this part of the reaction by the number of ways that the neutrons can be picked up in this manner. If both neutrons are picked up from a group of N identical neutrons (such as from the same shell model orbit containing N neutrons), then this factor is the combinatorial factor denoted by $\binom{N}{2}$. The general expression for a combination factor is given in equation (3.4.4).

$$\binom{n}{m} = \frac{n!}{(n-m)!m!} \tag{3.4.4}$$

If the two neutrons are picked up from different groups (such as from different shell model orbits), then this factor is just $2N_\alpha N_\beta$ where N_α (N_β) is the number of neutrons in the α (β) group. The 2 comes from the possibility that either neutron can come from either group and yet the final configuration will be the same. More formally it is an antisymmetrization factor. We denote this statistical factor in general by $g_{\gamma_\alpha \gamma_\beta}$.

$$\begin{aligned} g_{\gamma_\alpha \gamma_\beta} &= \binom{N}{2} = \frac{N(N-1)}{2} \quad ; \gamma_\alpha = \gamma_\beta \quad N_\alpha = N_\beta = N \\ &= 2N_\alpha N_\beta \quad ; \gamma_\alpha \neq \gamma_\beta \end{aligned} \tag{3.4.5}$$

If the "cross-section" must be multiplied by g then b must be multiplied by $g^{1/2}$.

$$b_{\gamma_\alpha\gamma_\beta LSJ} = g^{1/2}_{\gamma_\alpha\gamma_\beta} \langle \psi_{J_B}, \Phi_{\gamma_\alpha\gamma_\beta LSJ}, J_A \mid \psi_{J_A} \rangle \quad (3.4.6)$$

We have essentially rewritten equation (3.4.3) in a simplified notation and included the statistical factor. We see that the $b_{\gamma_\alpha\gamma_\beta LSJ}$'s are analogous to the $\beta_{\gamma LSJT}$'s of Glendenning[(Gl65)]. In order to proceed further with the calculation of the parentage factors we must choose a particular model with which to describe the wave functions of equation (3.4.6). We choose a j-j coupled shell model since it is quite often used and its concept is fairly easy to grasp. Since $\Phi_{\gamma_\alpha\gamma_\beta LSJ}$ is a L-S coupled two particle wave function, we must transform it to j-j coupling. We make use of the Wigner 9-J coefficients[(Br62, Sh63)].

$$\Phi_{\gamma_\alpha\gamma_\beta LSJ} = \sum_{j_\alpha j_\beta} \begin{bmatrix} \ell_\alpha & s_\alpha & j_\alpha \\ \ell_\beta & s_\beta & j_\beta \\ L & S & J \end{bmatrix} \Phi_{\gamma_\alpha\gamma_\beta j_\alpha j_\beta J} \quad (3.4.7)$$

The coefficients [ ] are related to the Wigner 9-J coefficients as in equation (3.3.3) and are real. Applying this transformation and interpreting the sum over j_α and j_β as being included in the sum over α and β of equation (3.4.1), we get the following:

$$B_{\gamma_\alpha \gamma_\beta j_\alpha j_\beta J} = g^{1/2}_{\gamma_\alpha \gamma_\beta} \langle \psi_{J_B}, \Phi_{\gamma_\alpha \gamma_\beta j_\alpha j_\beta J}; J_A \mid \psi_{J_A} \rangle \tag{3.4.8}$$

We have used the B's as defined in equation (3.3.6).

In order to calculate the parentage factors, we must consider the particular shell model space used in calculating $|\psi_A\rangle$ and $|\psi_B\rangle$. As an example we will consider the case where the nucleons are limited to two shells outside a closed core. This will allow the possibility of picking up the nucleons from either the same shell or two different shells. Therefore, such an example will cover the essentials of this type calculation since in a direct reaction description of two nucleon pickup these are the only two possibilities. So far we have avoided the explicit introduction of isospin since we are primarily concerned in this work with two identical particles which we know are neutrons. Often shell model wave functions are calculated with isospin explicitly included (see reference G164 for example), therefore we will now introduce isospin.

In the example we have chosen to consider, the wave function of the target nucleus can be written as in equation (3.4.9).

$$|\psi_A\rangle = \sum_{\alpha\beta} C^A_{\alpha\beta} \left[|\gamma_\alpha^{N_{A\alpha}} J_{A\alpha} T_{A\alpha} \chi_{A\alpha}\rangle |\gamma_\beta^{N_{A\beta}} J_{A\beta} T_{A\beta} \chi_{A\beta}\rangle \right]^{\tau_A}_{J_A T_A} |\text{core}\rangle \tag{3.4.9}$$

The first factor represents the two active shells, the shells outside the closed core. Here γ represents the particular shell (such as $1d_{5/2}$, $2s_{1/2}$, or $1d_{3/2}$) and N is the number of nucleons in that shell. There is, of course, the restriction that $N_{A\alpha}+N_{A\beta}$ equals the number of nucleons outside the core. J, T, and χ represent respectively the angular momentum, isospin and any other quantum numbers which might be needed to make the description of the state unique. The core is assumed to have zero angular momentum, isospin and isospin projection, and therefore J_A, T_A and τ_A are the quantum numbers of the total nuclear state. The total wave function must have definite isospin projection τ_A but the individual active shells do not. The square brackets denote vector coupling, and $\sum_{\alpha\beta}$ represents a sum over all different possible configurations of the active nucleons in these two shells with amplitude $C^A_{\alpha\beta}$. The final state can be written in the same way.

$$|\psi_B> = \sum_{\alpha\beta} C^B_{\alpha\beta} \left[|\gamma_\alpha^{N_{B\alpha}} J_{B\alpha}\ T_{B\alpha}\ \chi_{B\alpha}> \right.$$

$$\left. |\gamma_\beta^{N_{B\beta}} J_{B\beta}\ T_{B\beta}\ \chi_{B\beta}> \right]^{\tau_B}_{J_B T_B} |\ \text{core}> \qquad (3.4.10)$$

For two nucleon pickup when the core is not effected, we have the following obvious restriction.

$$N_{A\alpha} + N_{A\beta} = N_{B\alpha} + N_{B\beta} + 2 \qquad (3.4.11)$$

In order to proceed further, we consider two possible cases.

Case I $N_{A\beta} = N_{B\beta}$, $N_{A\alpha} = N_{B\alpha} + 2$

In this case both particles came from the same shell. In order to proceed we must decouple the nucleons to be transferred from the target wave functions by means of a fractional parentage expansion defined in the following equation.

$$|\gamma^N\ J\ T\ \chi> = \sum_{J'T'\chi'} <\gamma^{N-1} J'T'\chi',\ \gamma jt|\}\gamma^N\ J\ T\ \chi>$$

$$[\,|\gamma^{N-1}\ J'T'\chi'>|\gamma jt>\,]_{JT\chi} \qquad (3.4.12)$$

The coefficients $< |\} >$ are called coefficients of fractional parentage (c.f.p.). C.f.p.'s such as these are described in reference Sh63 and others. We have chosen an unconventional brief notation for the c.f.p.'s. Applying equation (3.4.12) twice to one typical term of equation (3.4.10) and dropping the core since we have assumed it will overlap exactly with the core of the residual nucleus, we get the following:

$$|\psi_A>_{\alpha\beta} = C^A_{\alpha\beta} \sum_{\substack{J'T'\chi' \\ J''T''\chi''}} <\gamma_\alpha^{N_{A\alpha}-1}\ J',\ \gamma_\alpha|\}\gamma_\alpha^{N_{A\alpha}}\ J_{A\alpha}>$$

$$<\gamma_\alpha^{N_{A\alpha}-2}\ J'',\ \gamma_\alpha|\}\gamma_\alpha^{N_{A\alpha}-1}\ J'>$$

$$\Big\{[\{|\gamma_\alpha^{N_{A\alpha}-2}\ J'>|\gamma_\alpha>\}_{J'}$$

$$|\gamma_\alpha>]_{J_{A\alpha}}|\gamma_\beta^{N_{A\beta}}\ J_{A\beta}>\Big\}^{T_A}_{J_A T_A} \qquad (3.4.14)$$

In this case all three brackets denote vector coupling in the order indicated, and for ease of writing, we have suppressed many of the essential quantum numbers. We must now recouple these wave functions in such a way that we can identify the coupled pair to be transferred. Such a transformation(Sh63) will involve the Racah W-functions, and can be written as follows in our notation.

$$[\{|\ell_1>|\ell_2>\}_{L_{12}}|\ell_3>]_L = \sum_{L_{23}} (2L_{12}+1)^{1/2}(2L_{23}+1)^{1/2}$$

$$W(\ell_1\ell_2L\ell_3;\ L_{12}L_{23})$$

$$[|\ell_1>\{|\ell_2>|\ell_3>\}_{L_{23}}]_L$$

(3.4.14)

Applying the recoupling transformation to both angular momentum and isospin, equation (3.4.13) becomes:

$$|\psi_A>_{\alpha\beta} = C^A_{\alpha\beta} \sum_{\substack{J'T'\chi' \\ J''T''\chi'' \\ J'''T'''}} < | \} >< | \} > [(2J'+1)(2J'''+1)$$

$$(2T'+1)(2T'''+1)]^{1/2} \; W(J''j_\alpha J_{A\alpha} j_\alpha; J'J''')$$

$$W(T''t_\alpha T_{A\alpha} t_\alpha;\; T'T''') \left\{ [|\gamma_\alpha^{N_{A\alpha}-2} \; J''> \right.$$

$$\left. \{|\gamma_\alpha>|\gamma_\alpha>\}_{J'''}]_{J_{A\alpha}} |\gamma_\alpha^{N_{A\beta}} \; J_{A\beta}> \right\}^{\tau_A}_{J_A T_A} \qquad (3.4.15)$$

We can simplify the above expression by defining what might be called a two particle c.f.p. similar to the definition of reference Sh63.

$$<\gamma^{N-2} \; J_1 T_1 \chi_1,\; \gamma^2 \; J_2 T_2 | \} \gamma^N \; JT\chi> =$$

$$\sum_{J'T'\chi'} <\gamma^{N-1} \; J'T'\chi',\; \gamma jt | \} \gamma^N \; JT\chi>$$

$$<\gamma^{N-2} \; J_1 T_1 \chi_1,\; \gamma jt | \} \gamma^{N-1} \; J'T'\chi'>$$

$$[(2J'+1)(2J_2+1)(2T'+1)(2T_2+1)]^{1/2}$$

$$W(J_1 jJj;\; J'J_2)\; W(T_1 tTt;\; T'T_2) \qquad (3.4.16)$$

We introduce this two particle c.f.p. into equation (3.4.15).

$$|\psi_A>_{\alpha\beta} = C^A_{\alpha\beta} \sum_{\substack{J''T''\chi'' \\ J'''T'''}} \tag{3.4.17}$$

$$<\gamma_\alpha^{N_{A\alpha}-2} J''T''\chi'', \gamma_\alpha^2 J'''T''' | \}\gamma_\alpha^{N_{A\alpha}} J_{A\alpha}T_{A\alpha}\chi_{A\alpha}>$$

$$\left\{[|\gamma_\alpha^{N_{A\alpha}-2} J''>\{|\gamma_\alpha>|\gamma_\alpha>\}_{J'''}]_{J_{A\alpha}} |\gamma^{N_{A\beta}} J_{A\beta}>\right\}^{T_A}_{J_A T_A}$$

We now must recouple again to completely separate out the coupled pair of nucleons. Another form of the recoupling transformation is needed[Sh63] which written in our notation is as follows:

$$[\{|\ell_1>|\ell_2>\}_{L_{12}} |\ell_3>]_L = \sum_{L_{13}} (2L_{13}+1)^{1/2}(2L_{13}+1)^{1/2}$$

$$(-1)^{\ell_1+2\ell_2+2\ell_3+L_{12}+L_{13}+L} W(\ell_2\ell_1 L\ell_3; L_{12}\ L_{13})$$

$$[\{|\ell_1>|\ell_3>\}_{L_{13}} |\ell_2>]_L \tag{3.4.18}$$

We apply this recoupling transformation to both angular momentum and isospin in equation (3.4.17).

$$|\psi_A\rangle_{\alpha\beta} = C^A_{\alpha\beta} \sum_{\substack{J''T''\chi'' \\ J'''T'''J^{iv}T^{iv}}} \langle 2 \text{ particle c.f.p.}\rangle$$

$$(-1)^{J''+2(J'''+J_{A\beta})+J_{A\alpha}+J^{iv}+J_A}$$

$$(-1)^{T''+2(T'''+T_{A\beta})+T_{A\alpha}+T^{iv}+T_A}$$

$$[(2J_{A\alpha}+1)(2J^{iv}+1)(2T_{A\alpha}+1)(2T^{iv}+1)]^{1/2}$$

$$W(J''' \; J'' \; J_A \; J_{A\beta}; \; J_{A\alpha} \; J^{iv})$$

$$W(T''' \; T'' \; T_A \; T_{A\beta}; \; T_{A\alpha} \; T^{iv})$$

$$\tau_{iv} \sum_{\tau'''} \langle T^{iv} \; T''' \; \tau^{iv} \; \tau'''|T_A \; \tau_A\rangle$$

$$[\{|\gamma_\alpha^{N_{A\alpha}-2} \; J''\rangle|\gamma_\beta^{N_{A\beta}} \; J_{A\beta}\rangle\}^{\tau^{iv}}_{J^{iv}}$$

$$\{|\gamma_\alpha\rangle|\gamma_\alpha\rangle\}^{\tau'''}_{J'''} \;]^{\tau_A}_{J_A T_A} \qquad (3.4.19)$$

Since isospin projection is important here (i.e. $(T''')_Z \equiv \tau''' = -1$ for two protons, $\tau''' = 0$ for a proton and a neutron, and $\tau''' = +1$ for two neutrons), we have included it explicitly with the proper Clebsh-Gordan coupling coefficient.

We now must write down an explicit form for the other wave functions needed to evaluate the overlap and

thus the parentage factor of equation (3.4.8). For the case of both nucleons coming from the same shell we know the overlap will vanish unless the two nucleons come from the particular shell γ_α.

$$|\Phi\rangle = \{|\gamma_\alpha j_\alpha t_\alpha\rangle|\gamma_\alpha j_\alpha t_\alpha\rangle\}^{\tau}_{JT} \qquad (3.4.20)$$

In equation (3.4.20) J, T and τ are the transferred quantum numbers in the pickup reaction. The only term in the expansion of the final state wave function that could possibly overlap with the particular part of the target wave function which we have uncoupled can be written as follows.

$$|\psi_B\rangle_{\alpha\beta} = C^B_{\alpha\beta} \{|\gamma_\alpha^{N_{A\alpha}-2} J_{B\alpha}\ T_{B\alpha}\ \chi_{B\alpha}\rangle \qquad (3.4.21)$$

$$|\gamma_\beta^{N_{A\beta}}\ J_{B\beta}\ T_{B\beta}\ \chi_{B\beta}\rangle\}^{\tau_B}_{J_B T_B}$$

We combine this with equation (3.4.20).

$$|\psi_B\ \Phi,\ J_A\rangle_{\alpha\beta} = C^B_{\alpha\beta} [\{|\gamma_\alpha^{N_{A\alpha}-2}\ J_{B\beta}\rangle|\gamma_\beta^{N_{A\beta}}\ J_{B\beta}\rangle\}^{\tau_B}_{J_B T_B}$$

$$\{|\gamma_\alpha\rangle|\gamma_\alpha\rangle\}^{\tau}_{JT}]^{\tau_A}_{J_A T_A} \qquad (3.4.22)$$

Again, we have suppressed some essential quantum numbers in equation (3.4.22) for brevity.

The overlap described in equation (3.4.8) can now be easily carried out for these two typical terms. The complete result is given in equation (3.4.23).

$$
\begin{aligned}
B_{\gamma_\alpha \gamma_\beta j_\alpha j_\beta JT} = {} & C^{A}_{\alpha\beta}\; C^{B*}_{\alpha\beta} \left(\frac{N_{A\alpha}(N_{A\alpha}-1)}{2}\right)^{1/2} \qquad (3.4.23)\\
& \langle \gamma_\alpha^{N_{A\alpha}-2}\; J_{B\alpha}\; T_{B\alpha}\; \chi_{B\alpha},\; \gamma_\alpha^2\; J\; T| \}\gamma_\alpha^{N_{A\alpha}}\; J_{A\alpha}\; T_{A\alpha}\; \chi_{A\alpha}\rangle \\
& (-1)^{J_{B\alpha}+2(J+J_{B\beta})+J_{A\alpha}+J_B+J_A} \\
& (-1)^{T_{B\alpha}+2(T+T_{B\beta})+T_{A\alpha}+T_B+T_A} \\
& W(J\; J_{B\alpha}\; J_A\; J_{B\beta};\; J_{A\alpha}\; J_B) \\
& W(T\; T_{B\alpha}\; T_A\; T_{B\beta};\; T_{A\alpha}\; T_B) \\
& \langle T_B\; T\; \tau_B\; \tau|\; T_A\; \tau_A\rangle\; \delta(J_{A\beta},\; J_{B\beta})\; \delta(T_{A\beta},\; T_{B\beta})
\end{aligned}
$$

The total parentage factor will be the sum of terms like equation (3.4.23) for each component of $|\psi_A\rangle$ that overlaps with a component of $|\psi_B\rangle$ plus two nucleons in the same shell γ_α.

Case II $N_{A\alpha}=N_{B\alpha}+1$, $N_{A\beta}=N_{B\beta}+1$

In this case the two particles came from two different shells. Again a c.f.p. expansion can be applied to $|\psi_A>$, but this time just once to each active shell.

$$|\psi_A>_{\alpha\beta} = C_{\alpha\beta} \sum_{\substack{J_\alpha' T_\alpha' \chi_\alpha' \\ J_\beta' T_\beta' \chi_\beta'}} <\gamma_\alpha^{N_{A\alpha}-1} J_\alpha', \gamma_\alpha | \} \gamma_\alpha^{N_{A\alpha}} J_{A\alpha}>$$

$$<\gamma_\beta^{N_{A\beta}-1} J_\beta', \gamma_\beta | \} \gamma_\beta^{N_{A\beta}} J_{A\beta}>$$

$$[\{ |\gamma_\alpha^{N_{A\alpha}-1} J_\alpha'> |\gamma_\alpha> \}_{J_{A\alpha}}$$

$$\{ |\gamma_\beta^{N_{A\beta}-1} J_\beta'> |\gamma_\alpha> \}_{J_{A\beta}}]_{J_A} \qquad (3.4.24)$$

Some essential quantum numbers have been suppressed for brevity.

We now must reorder the coupling in order to identify the coupled pair to be transferred. This can be done by using the Wigner-9J coefficients. The form of the recoupling transformation has already been written down in equation (3.4.7).

$$|\psi_A>_{\alpha\beta} = \sum_{\substack{J_\alpha' T_\alpha' \chi_\alpha' \\ J_\beta' T_\beta' \chi_\beta' \\ J' T' J''' T'''}} < | \} >< | \} > \begin{bmatrix} J_\alpha' & J_\beta' & J'' \\ j_\alpha & j_\alpha & J''' \\ J_{A\alpha} & J_{A\beta} & J_A \end{bmatrix}$$

$$\begin{bmatrix} T_\alpha' & T_\beta' & T'' \\ t_\alpha & t_\beta & T''' \\ T_{A\alpha} & T_{A\beta} & T_A \end{bmatrix} \sum_{\tau'' \tau'''} <T'' T''' \tau'' \tau''' | T_A \tau_A>$$

$$[\{|\gamma_\alpha^{N_{A\alpha}-1} J_\alpha'> |\gamma_\beta^{N_{A\beta}-1} J_\beta'>\}^{\tau''}_{J'' T''}$$

$$\{|\gamma_\alpha> |\gamma_\beta>\}^{\tau'''}_{J''' T'''}]^{\tau_A}_{J_A T_A} \qquad (3.4.25)$$

As in case I, we have included the isospin Clebsh-Gordan coefficient to take care of the necessary specific isospin projection.

Now we write down the explicit form of the other wave functions needed to evaluate the overlap and thus the parentage factor of equation (3.4.8).

$$|\Phi>_{\alpha\beta} = \{|\gamma_\alpha j_\alpha t_\alpha> |\gamma_\beta j_\beta t_\beta>\}^{\tau}_{JT} \qquad (3.4.26)$$

$$|\psi_B>_{\alpha\beta} = C^B_{\alpha\beta} \{|\gamma_\alpha^{N_{A\alpha}-1} J_{B\alpha} T_{B\alpha} \chi_{B\alpha}> |\gamma_\beta^{N_{A\beta}-1} J_{B\beta} T_{B\beta} \chi_{B\beta}>\}^{\tau_B}_{J_B T_B}$$

(3.4.27)

$$|\psi_B, \Phi; J_A\rangle_{\alpha\beta} = C^B_{\alpha\beta} \left[\{|\gamma_\alpha^{N_{A\alpha}-1} J_{B\alpha}\rangle |\gamma_\beta^{N_{A\beta}-1} J_{B\beta}\rangle\}^{\tau_B}_{J_B T_B}\right.$$

$$\left. \{|\gamma_\alpha\rangle|\gamma_\beta\rangle\}^{\tau}_{J_T}\right]^{\tau_A}_{J_A T_A} \qquad (3.4.28)$$

The overlap can now easily be performed.

$$B_{\gamma_\alpha\gamma_\beta j_\alpha j_\beta JT} = (2N_{A\alpha}N_{A\beta})^{1/2} C^A_{\alpha\beta} C^B_{\alpha\beta} \langle T_B T \; \tau_B \tau \mid T_A \tau_A\rangle$$

$$\langle\gamma_\alpha^{N_{A\alpha}-1} J_{B\alpha} \; T_{B\alpha} \; \chi_{B\alpha}, \; \gamma_\alpha j_\alpha t_\alpha|\}\gamma_\alpha^{N_{A\alpha}} J_{A\alpha} \; T_{A\alpha} \; \chi_{A\alpha}\rangle$$

$$\langle\gamma_\beta^{N_{A\beta}-1} J_{B\beta} \; T_{B\beta} \; \chi_{B\beta}, \; \gamma_\beta j_\beta t_\beta|\}\gamma_\beta^{N_{A\beta}} J_{A\beta} \; T_{A\beta} \; \chi_{A\beta}\rangle$$

$$\begin{bmatrix} J_{B\alpha} & J_{B\beta} & J_B \\ j_\alpha & j_\beta & J \\ J_{A\alpha} & J_{A\beta} & J_A \end{bmatrix} \begin{bmatrix} T_{B\alpha} & T_{B\beta} & T_B \\ t_\alpha & t_\beta & T \\ T_{A\alpha} & T_{A\beta} & T_A \end{bmatrix} \qquad (3.4.29)$$

The total parentage factor will be a sum of terms like equation (3.4.29) for each component of $|\psi_A\rangle$ which overlaps with a component $|\psi_B\rangle$ plus one nucleon in shell γ_α and one in γ_β . We note that for the (p,t) reaction, when the transferred particles are neutrons, τ=+1, and T=1.

Some of the parentage factors can be expressed in simple closed form. In particular, for some cases where isospin is not explicitly included in the wave functions

and seniority (ν) is the only other quantum number necessary to describe completely the nuclear states involved, Glendenning[G165] has given explicit expressions for the two particle c.f.p.'s.

When isospin is not included, and two identical particles are taken from the same shell, and there is only one active shell so that $J_{B\alpha}=J_B$, $J_{A\alpha}=J_A$ and the β components are included in the closed core, case I reduces to the following:

$$B_{\gamma_\alpha \gamma_\beta j_\alpha j_\beta J} = C_\alpha^A \; C_\alpha^{B*} \left(\frac{N_{A\alpha}(N_{A\alpha}-1)}{2}\right)^{1/2} \qquad (3.4.30)$$

$$<\gamma_\alpha^{N_{A\alpha}-2} \; J_B \; \nu_B, \; \gamma_\alpha^2 \; J \,|\}\, \gamma_\alpha^{N_{A\alpha}} \; J_A \; \nu_A>$$

For the situation where $N_{A\alpha}$ is even, $J_A=0$, and $\nu_A=0$ and therefore $J_B=J$, this c.f.p. has the following value[G165].

$$<\gamma^{N-2} \; J \; \nu, \; \gamma^2 \; J \,|\}\, \gamma^N \; 00> = \left(\frac{2(N-2)}{(N-1)} \; \frac{2J+1}{(2j-1)(2j+1)}\right)^{1/2}; \quad \text{for } \nu=2, \; J\neq 0$$

$$= \left(\frac{3j+3-N}{(N-1)(2j+1)}\right)^{1/2}; \quad \text{for } \nu=0, \; J=0 \qquad (3.4.31)$$

Since isospin is not included in this case, N is the number of particles in the active shell of the same type as those that are being transferred. For this simple case the parentage factor becomes:

$$B_{\gamma_\alpha \gamma_\alpha j_\alpha j_\alpha 0} = C^A_\alpha \, C^{B*}_\alpha \left(\frac{N_{A\alpha}(2j_\alpha + 3 - N_{A\alpha})}{2(2j_\alpha + 1)} \right)^{1/2}; \quad \nu = 0, \; J = 0$$

$$B_{\gamma_\alpha \gamma_\alpha j_\alpha j_\alpha J} = C^A_\alpha \, C^{B*}_\alpha \left(\frac{N_{A\alpha}(N_{A\alpha} - 2)(2J+1)}{(2j_\alpha - 1)(2j_\alpha + 1)} \right)^{1/2}; \quad \nu = 2, \; J \neq 0$$

(3.4.32)

When isospin is not included, and the two particles are taken from different shells, case II reduces to the following:

$$B_{\gamma_\alpha \gamma_\beta j_\alpha j_\beta J} = (2N_{A\alpha} N_{A\beta})^{1/2} \, C^A_{\alpha\beta} \, C^{B*}_{\alpha\beta} \qquad (3.4.33)$$

$$\langle \gamma_\alpha^{N_{A\alpha}-1} \; J_{B\alpha} \; \nu_{B\alpha}, \; \gamma_\alpha \; j_\alpha | \} \gamma_\alpha^{N_{A\alpha}} \; J_{A\alpha} \; \nu_{A\alpha} \rangle$$

$$\langle \gamma_\beta^{N_{A\beta}-1} \; J_{B\beta} \; \nu_{B\beta}, \; \gamma_\beta \; j_\beta | \} \gamma_\beta^{N_{A\beta}} \; J_{A\beta} \; \nu_{A\beta} \rangle$$

$$\begin{bmatrix} J_{B\alpha} & J_{B\beta} & J_B \\ j_\alpha & j_\beta & J \\ J_{A\alpha} & J_{A\beta} & J_A \end{bmatrix}$$

In the case of an even-even target with each shell coupled to zero angular momentum and seniority zero ($N_{A\alpha}$ and $N_{A\beta}$ even, $J_A=0$, $J_{A\alpha}=0$, $J_{A\beta}=0$, $\nu_{A\alpha}=0$, $\nu_{A\beta}=0$) then $J_B=J$, $J_{B\alpha}=j_\alpha$ and $J_{B\beta}=j_\beta$. The necessary c.f.p.'s are then trivial(Sh63).

$$\langle \gamma^{N-1}\ j\ \nu,\ \gamma_j\ |\}\ \gamma^N\ 00\rangle = \delta_{\nu 1} \qquad (3.4.34)$$

The parentage factor for this simple case can then be written as follows:

$$B_{\gamma_\alpha \gamma_\beta j_\alpha j_\beta J} = (2N_{A\alpha}N_{A\beta})^{1/2}\ C^A_{\alpha\beta}\ C^{B^*}_{\alpha\beta} \qquad (3.4.35)$$

$$\begin{bmatrix} j_\alpha & j_\beta & J \\ j_\alpha & j_\beta & J \\ 0 & 0 & 0 \end{bmatrix} \delta(\nu_{B\alpha},1)\ \delta(\nu_{B\beta},1)$$

This particular Wigner 9-J coefficient can be evaluated using relationships from reference Br62.

$$B_{\gamma_\alpha \gamma_\beta j_\alpha j_\beta J} = C^A_{\alpha\beta}\ \ C^{B^*}_{\alpha\beta} \left(\frac{2N_{A\alpha}N_{A\beta}(2J+1)}{(2j_\alpha+1)(2j_\beta+1)}\right)^{1/2}$$

$$\delta(\nu_{B\alpha},1)\ \delta(\nu_{B\beta},1) \qquad (3.4.36)$$

We emphasize again that parentage factors for configuration mixed wave functions consisting of combinations of the above type configurations must be summed over all combinations of components of $|\psi_A\rangle$ and ($|\psi_B\rangle$+2 nucleons) which overlap. The relative phase of the components (i.e. the phases of the $C_{\alpha\beta}$'s) of the wave functions contributing are important since they add coherently in

calculating the B's and the B's add coherently in calculating the sum of equation (3.3.4) to form the total form factor.

CHAPTER 4

THE EXPERIMENT

4.1 The Proton Beam

The Michigan State University Sector Focused Cyclotron was used to provide a beam of protons of energy 40 MeV to 45 MeV. The beam was energy analyzed and spatially defined by two 45° bending magnets and three pairs of slits. The beam resolution was ~40 keV, as calculated from the measured magnetic fields and slit apertures. The details of this transport system have been discussed in reference Ma67.

After analysis, the beam was bent through 22 1/2° and sent through a shielding wall to an experimental vault and a 36" scattering chamber. Quadrupole focusing magnets were used at appropriate locations along the evacuated beam line. The magnetic fields of the analyzing magnets were measured by N.M.R. probes and from these measurements the proton energy was calculated. The magnitudes of the quadrupole fields were also calculated for the particular beam energy used. Fine adjustments in some of the quadrupoles were made by visual observation of the beam spot on plastic scintilators in the beam line.

Particular attention was paid to the beam spot at the target position in the scattering chamber.

4.2 The Faraday Cup and Charge Collection

The beam exiting from the back of the scattering chamber was stopped and collected in an aluminum Faraday cup. The beam current was monitored, and the total charge collected was measured with an ELCOR model A310B current indicator and integrator.

The beam current was varied depending upon the particular scattering angle. At forward angles the elastic proton counting rate and the counting rate capability of the electronics limited the usable beam current to as little as 5 n.A. in some cases. At backward angles the beam current was generally limited by the cyclotron to about 500 n.A. The normal range of the beam current was 50 n.A. to 250 n.A.

4.3 The Scattering Chamber

A 36" diameter evacuated scattering chamber was used. The target post at the center was capable of supporting either a ladder for solid foil targets or a gas cell target. The detector telescope was mounted on a remotely movable arm and, in the case of foil targets, a monitor counter was mounted on a relocatable stationary arm. The position of the movable arm had a remote read

out which was accurate and reproducible to about 0.15°. A viewing port in the side of the chamber allowed visual inspection of the beam spot on the plastic scintilator at the position of the target by means of a closed circuit television system.

4.4 Targets

The ^{20}Ne target was a 3" diameter gas cell with 1/2 mil Kapton* windows. The gas was natural neon which is about 90.9% ^{20}Ne. The gas pressure was maintained at about 28 cm. of Hg and was monitored throughout the runs with a mercury manometer.

The ^{24}Mg target was a self supporting foil of magnesium metal enriched to 99.96% ^{24}Mg. This foil was obtained from Union Carbide at the Oak Ridge National Laboratory. It was reported to be 566 $\mu g/cm^2$ thick, and this thickness was used in normalizing the cross-sections obtained. For this purpose the thickness was assumed to be accurate to ±5%.

The ^{28}Si target was a self supporting foil of natural silicon metal (92.21% ^{28}Si). This foil was also obtained from Union Carbide. Its thickness was determined by measuring the energy loss of alpha particles from a natural source when they passed through the foil. The results were compared with range tables(Wi66) to

*E. I. DuPont de Nemours, Wilmington, Del.

determine the thickness. The thickness was found to be 687 $\mu g/cm^2$ and an accuracy of ±5% was assumed for normalization purposes.

The ^{32}S target was a 5" diameter gas cell with 1/2 mil Kapton windows. The gas was natural H_2S (~95.0% ^{32}S) at a pressure of about 21 cm. of Hg. The pressure was monitored throughout the runs with a mercury manometer.

Two different ^{36}Ar targets were used. Both were 3" gas cells filled with argon gas enriched to >99% ^{36}Ar. The first cell was a sealed cell, with 1/2 mil Havar windows and a pressure of 45.1±1.0 cm. of Hg, built by R. L. Kozub[Ko67]. The thick windows (10 mg/cm^2) caused some problems in triton resolution. The second cell had 1/2 mil Kapton windows (~1.7 mg/cm^2) and a pressure of 26 cm. of Hg. Better resolution was obtained with this target and so it was used for energy calibration purposes. It also served as a check on the actual gas pressure of the sealed cell which was over a year old.

The ^{40}Ca target was a self supporting foil of natural calcium (96.97% ^{40}Ca). This foil was prepared by evaporating in vacuum calcium metal onto a tantalum backing. Upon cooling, the calcium foil was easily removed. The thickness was measured with alpha particles in the same way as described for the ^{28}Si target. Its thickness was found to be 863 $\mu g/cm^2$ and an error of ±4%

was assumed for normalization purposes. A thinner target (~690 $\mu g/cm^2$) was used for some runs, but all the data was normalized to the first target.

4.5 The Detector Telescope

The detector telescope was made up of two silicon surface barrier transmission mounted ORTEC counters. The first counter was relatively thin and will be designated the ΔE counter. The second was thicker and will be called the E counter. The particular counters used depended on the specific experiment. In the ^{36}Ar, ^{24}Mg, and ^{28}Si experiments, both triton and the helium-3 data was taken. In order to allow the ^{3}He's to reach the E counter the ΔE counter was chosen to be 160 microns thick and was kept at a bias of 50 to 75 volts. The E counter was 2000 microns thick and was at 475 volts bias. In the ^{20}Ne experiment, both deuteron and triton data was taken. In order to stop the deuterons the E counter was made up of two 2000 micron counters at 475 volts bias. The ΔE counter was 260 microns thick and at 100 volts bias. In the ^{32}S and ^{40}Ca experiments, only triton data was taken. The ΔE counter was 260 microns thick at 100 to 125 volts and the E counter was 1000 microns thick at 275 to 475 volts bias.

The experiments involving foil targets required only one collimator in front of the detectors. These

collimators were made of 50 to 90 mil tantalum located at 8 to 11 inches from the target. Both round apertures of 160 mil diameter and oval apertures of 75x170 mils, 100x210 mils, and 125x210 mils were used. The oval collimators were smaller in the horizontal direction in order to minimize kinematic broadening and yet increase the effective solid angle.

When gas cell targets were used, two collimators were needed to define the volume of gas that is to be considered the target. Brass plates on the sides of the telescope were also needed to prevent particles scattering from the cell windows and other regions of the gas from entering to detector system. The front collimator nearest the gas cell was a tall brass slit with a full width of about 125 mils. The back collimators were the same ones previously mentioned for foil targets and were located from 9 to 12 1/2 inches from the center of the cell. The front collimator was from 5 to 8 1/2 inches ahead of the back collimator.

The monitor counter which was used with foil targets consisted of a NaI crystal and a photomultiplier tube. It was held as a fixed angle and a single channel analyzer (SCA) was set with its window about the elastically scattered proton peak. In this way the output of the SCA was proportional to the product of the beam current and the effective target thickness. This output was scaled

and used to calculate the relative cross-section for solid foil targets as will be described later.

4.6 Dead Time Corrections

The dead time of the pulse analyzing system was taken account of in two different ways. When a monitor counter was used, the output of the SCA was scaled and also fed into channel zero of the pulse height analyzer. The ratio of these two numbers then gave a measure of the fraction of counts lost.

In the case where a monitor was not used, the signal from the beam current monitoring meter was sent to a voltage to frequency convertor which gave out pulses at a rate proportional to beam intensity. These pulses were then scaled and sent to channel zero of the analyzer. In the same way as with the monitor counter, a measure of lost counts was obtained. This is not as good a method as a monitor counter since the beam current meter cannot follow microscopic time structure in the beam intensity, but if dead times were kept small, the method was adequate.

4.7 Electronics and Particle Identification

Bombarding a target with 40 MeV protons produces a large number of nuclear reactions. Because of this, some method must be used to identify the particular

products of the reaction of interest, in this case tritons. The method chosen for these experiments depends on the difference in energy lost in the ΔE counter for particles of different mass and charge but the same kinetic energy.

The experiment with the ^{36}Ar, ^{24}Mg and ^{28}Si targets employed the ORTEC model 423 particle identifier which is based on the technique developed by Goulding et al.(Go64). The total energy spectrum, gated by the particle identifier output, was analyzed and stored in a NUCLEAR DATA 160 pulse height analyzer. Figure 1 shows a block diagram of the electronics involved. Figure 2 shows a sample spectrum from the particle identifier.

The experiments with ^{20}Ne and ^{40}Ca targets used a different method of particle identification also based on the differential energy loss. The signals from the ΔE and E counters were summed (called the Σ signal) at the detector telescope and all three pulses (ΔE, E and Σ) were passed through charge sensitive preamplifiers and sent to the data acquisition area. Figure 3 shows this summing circuit. Using an electronic setup similar to the previous method, a slow coincidence was required between the ΔE and E signals. This coincidence was used to gate the ΔE and Σ signals. These two signals then went to a NORTHERN SCIENTIFIC dual 4096 analogy to digital converter (ADC). An S.D.S. Sigma-7 on-line computer and

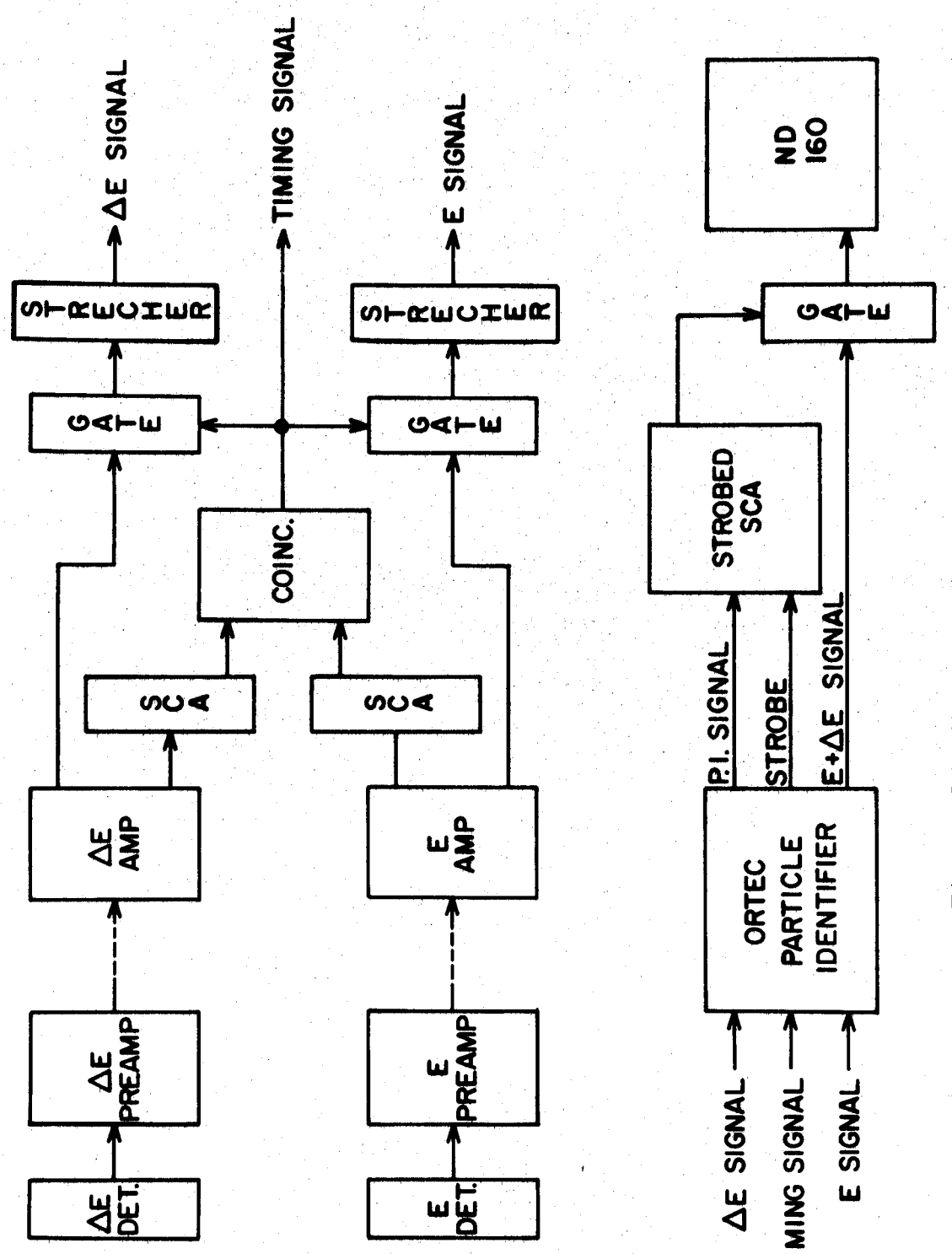

Figure 1.--Experimental electronics.

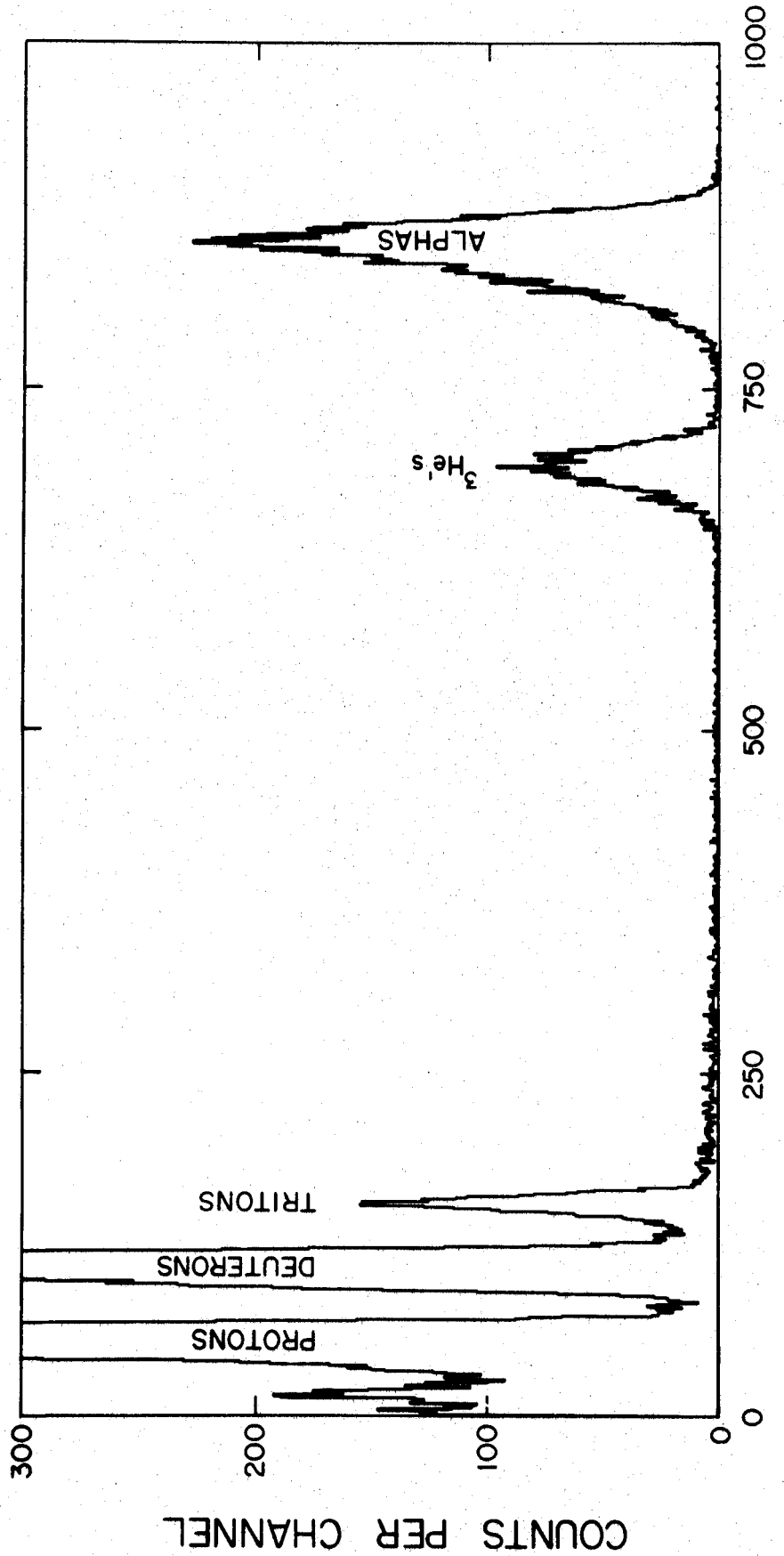

Figure 2.--Particle identification spectrum.

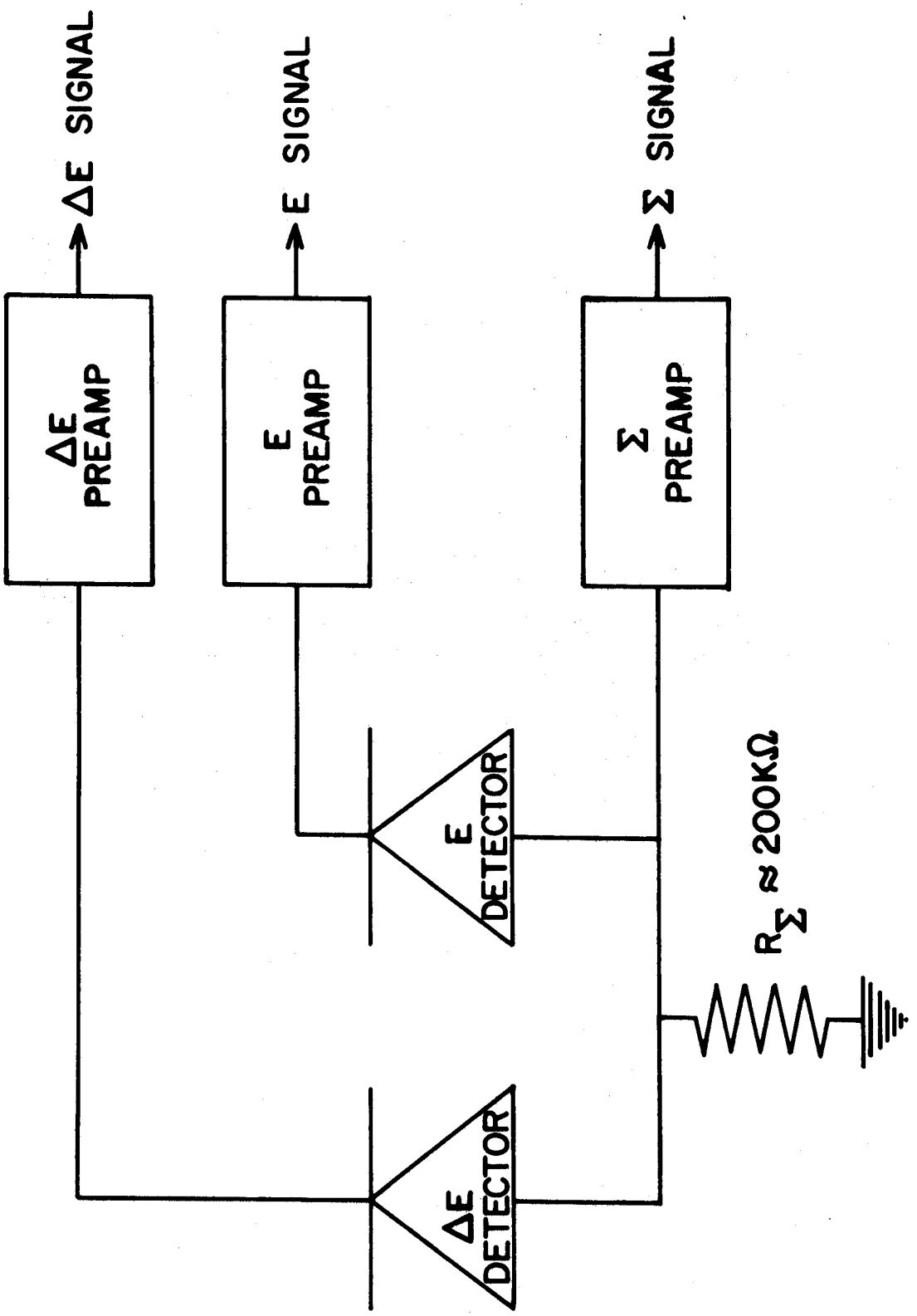

Figure 3.--Summing circuit.

the data acquisition computer code TOOTSIE(Ba69) were used to analyze the digital signals from the ADC. TOOTSIE displays, on a cathode ray screen, ΔE versus Σ. Due to the difference in energy loss (ΔE signal) of particles of different charge and mass for the same energy (Σ signal), the different particles fall into bands on the two dimensional plot. Figure 4 shows such a two dimensional plot. This particular spectrum was not taken during the present experiments. The code then allows gate lines to be introduced in the form of polynomial fits to designated points. These gate lines are then used to route the Σ signal to any of four 2048 channel spectrum.

In the case of the ^{32}S experiment, two detector telescopes, placed 10° apart on the scattering chamber arm, were used. The particle identification system using the on line computer was used. After the coincidence and linear gates the ΔE and Σ signals from the two telescopes were mixed and sent to the ADC, along with a routing signal taken from the coincidence modules.

4.8 Triton Energy Spectra and Energy Resolution

In the earlier experiments (Ar, Mg, Si), the electronic limitation on the resolution was measured by introducing a pulser signal, through a 1 or 2 pf. capacitor, into the preamps. It was found to be equivalent to

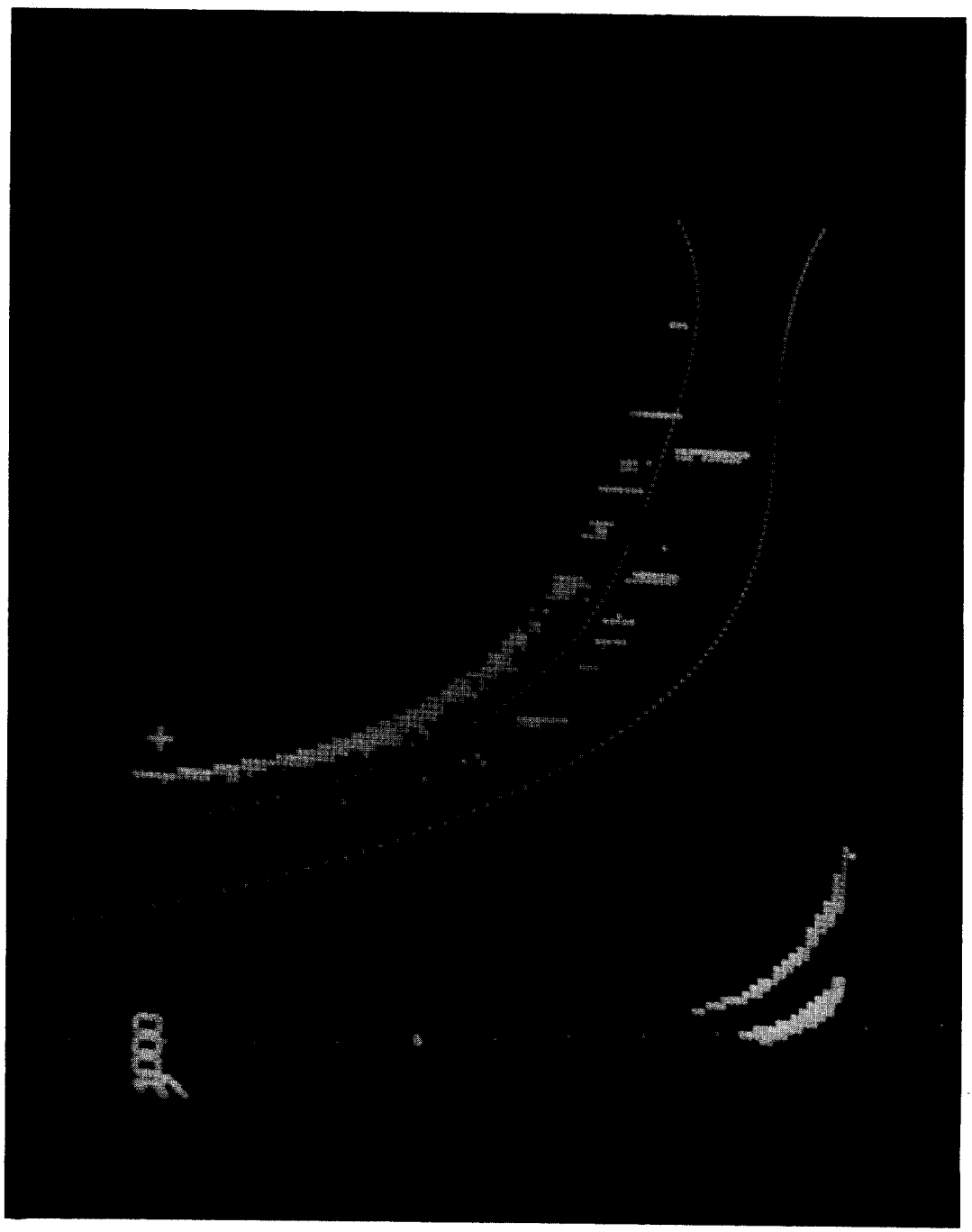

Figure 4.--Two dimensional TOOTSIE display.

45 to 65 keV full width at half maximum (FWHM). In the later experiments when the total energy signal (Σ) was taken from the summing circuit at the detector telescope, electronic contributions were reduced to 30 to 40 keV FWHM.

The over all experimental resolution varied with the particular target, counters, and electronic configuration. For the ^{20}Ne and ^{32}S cases the resolution was about 90 keV FWHM. The ^{24}Mg experiment had about 120 keV. The ^{28}Si case was about 140 keV. The ^{36}Ar gas cell with the thick Havar windows gave 155 keV, while the cell with Kapton windows gave 100 keV. The ^{40}Ca experiment had about 60 keV overall resolution. Figures 5, 6 and 7 show sample triton energy spectra for each target.

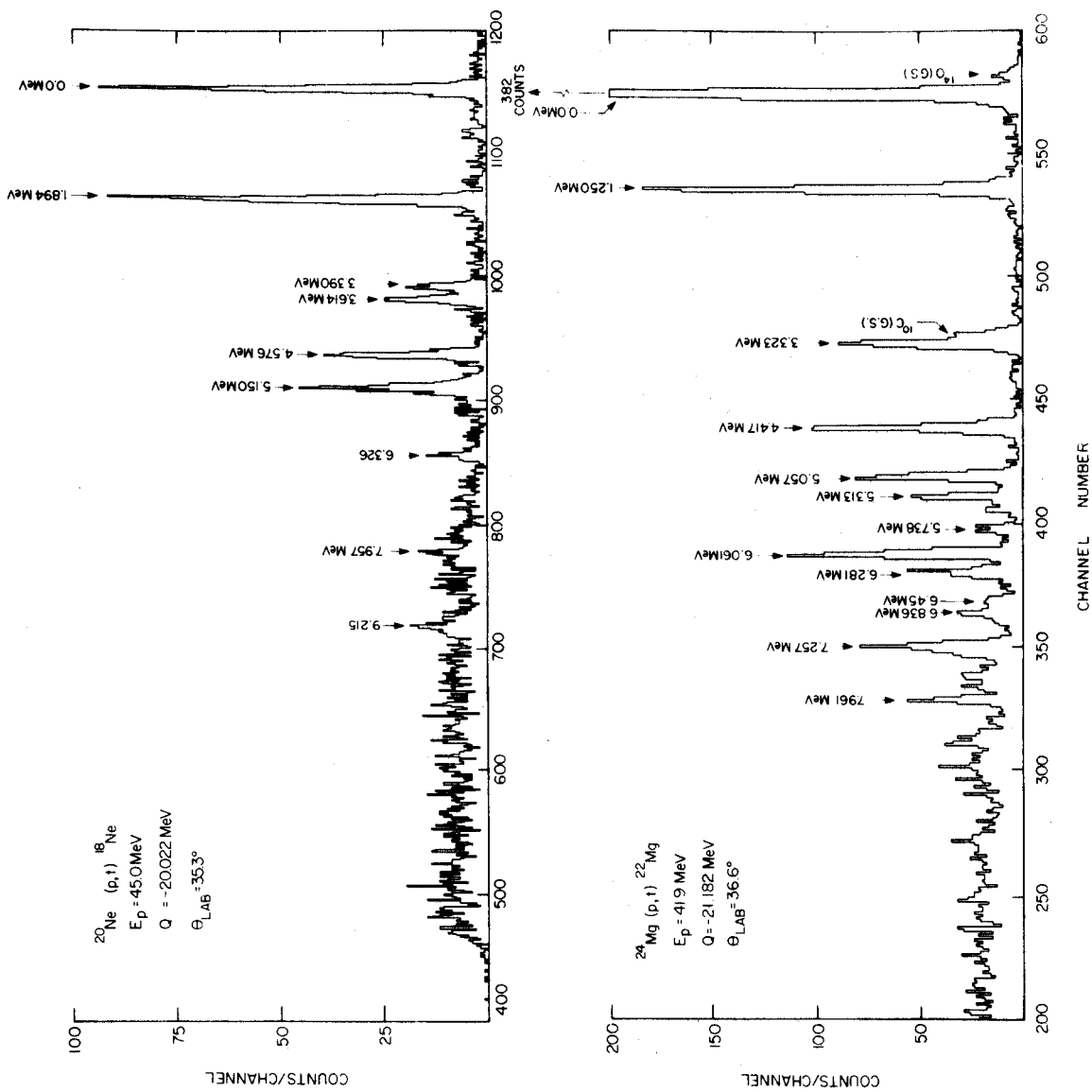

Figure 5.--Triton spectra from $^{20}Ne(p,t)^{18}Ne$ and $^{24}Mg(p,t)^{22}Mg$.

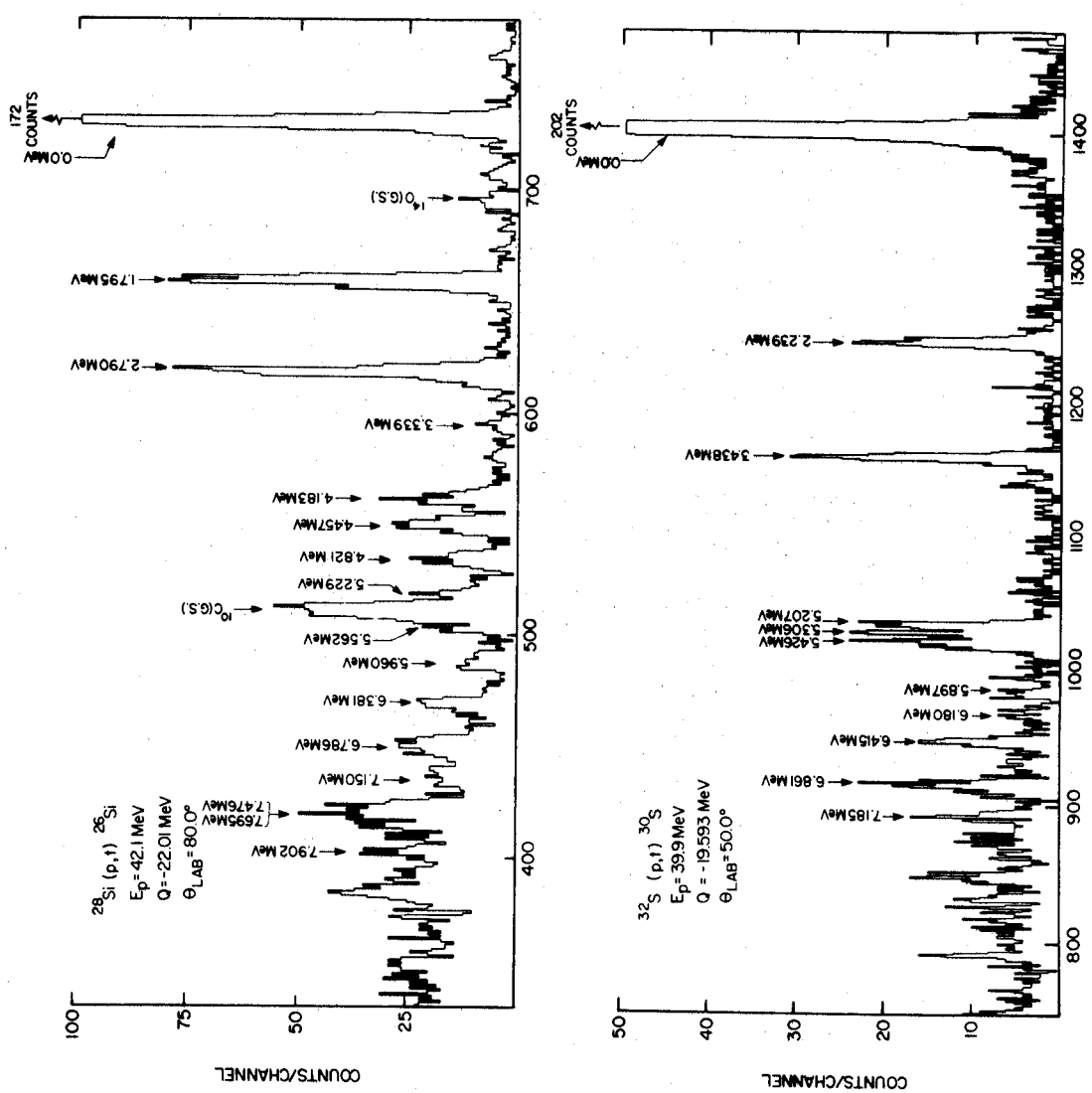

Figure 6.--Triton spectra from ^{28}Si(p,t)^{26}Si and ^{32}S(p,t)^{30}S.

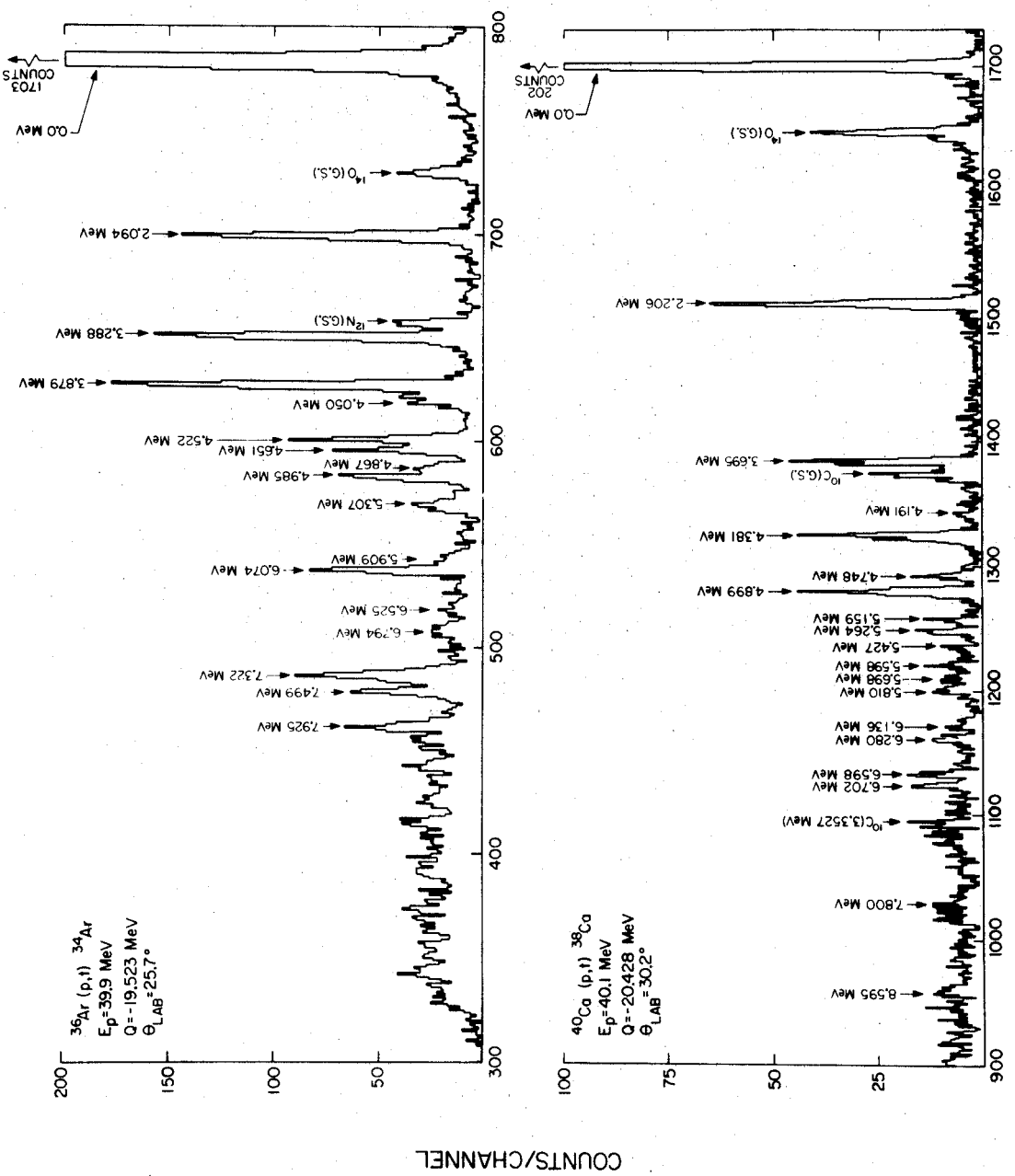

Figure 7.--Triton spectra from $^{36}Ar(p,t)^{34}Ar$ and $^{40}Ca(p,t)^{38}Ca$.

CHAPTER 5

DATA REDUCTION

The one dimensional triton spectra stored in the ND-160 were dumped directly into the Sigma-7 and punched on cards in the form of binary coded compressed data decks. The data acquisition task TOOTSIE punched out such data decks directly. The spectra were also plotted by the Sigma-7 in the form of semi-log histogram plots. Listings of the data were also obtained. From the plots and listings, the first and last channels of each peak along with the associated backgrounds were picked out by visual inspection. This information was put on punched cards and a simple Fortran computer code used these along with the data decks to calculate areas of peaks, statistical errors and centroids. The statistical error was taken to be simply $[(N+B)+B]^{1/2}/N$ where N is the net counts in the peak after the substaction of B background counts. The centroid was calculated using only the top two-thirds of the peak for peaks over 25 counts high to eliminate contributions from tails due to straggling in the target and other effects. In the case of smaller peaks, statistics did not seem to warrant this approach

and the total peak was used to calculate the centroid. The results were output on punched cards.

These cards, along with data on the proton energy, scattering angles, and particle masses went into a second simply Fortran computer code which used peaks designated as being known to set up an energy calibration curve. The calibration peaks were usually taken to be tritons from the (p,t) ground state transitions to ^{10}C, ^{12}N, and ^{14}O as well as the first excited state of ^{10}C at 3.3527 MeV[Pa69]. If the ground state Q-value of the reaction being studied was well known, these triton peaks were also used as calibration points. The C, N and O peaks came either from impurities in the target, or from a different target such as Mylar, air or carbon dioxide of a thickness comparable to the target being studied. The calibration curves and kinematics were used to calculate the excitation energies for the peaks corresponding to the states in the final nucleus.

The same peak cards along with geometry and target data and data concerning individual runs such as integrated beam current, target angle, monitor counts and detector telescope angle were entered into another Fortran computer code. This code calculated the center of mass scattering angles and differential cross-sections. The formula used in calculating the cross-section for

the foil targets is given in equation (5.1), equation (5.2) gives the formula used with gas targets.

$$\frac{d\sigma}{d\Omega}(\theta) = \mathcal{J} \frac{N\ f_{DT}\ \sin\theta_t\ M}{C\ \rho dx\ (A/R^2)} (2.66015 \times 10^{-16})\ [mb/st] \tag{5.1}$$

$$\frac{d\sigma}{d\Omega}(\theta) = \mathcal{J} \frac{N\ f_{DT}\ \sin\theta\ T}{C\ n\ P\ G} (1.65894 \times 10^{-12})\ [mb/st] \tag{5.2}$$

In the above formula, $\mathcal{J}$ is the Jacobian of the transformation to center of mass coordinates, N is the number of counts in the peak, f_{DT} is the dead time correction factor, θ is the scattering angle, θ_t is the target angle, M is the atomic mass of the target material in A.M.U., T is the gas temperature in °K, C is the integrated beam current in Coulombs, ρdx is the target thickness in g/cm^2, (A/R^2) is the detector solid angle, n is the number of target nucleons per molecule of gas, P is the gas pressure in cm. of Hg, and G is the G-factor in cm. The G-factor is that defined and discussed in detail by Silverstein(Si59). It is expressed as a sum of a series of terms. Only the first two, which do not depend on the shape of the angular distribution, were needed for the present data.

When a monitor counter was used, the relative cross-section was calculated by the expression given in equation (5.3).

$$\frac{d\sigma}{d\Omega}(\theta)_{rel.} = N\ f_{DT}/(\text{Monitor Counts}) \qquad (5.3)$$

An average normalization factor was then calculated by comparison with the results of equation (5.1).

The resulting angular distribution and excitation energies of the states observed are given in the Appendices.

CHAPTER 6

EXPERIMENTAL RESULTS

6.1 The Ground State Transitions

The targets studied in these experiments were all even-even N=Z nuclei with $J^{\pi}=0^{+}$ ground states. The residual nuclei following the (p,t) reaction are then also even-even nuclei, and therefore, according to the independent particle shell model[Ro67], have $J^{\pi}=0^{+}$ ground states also. From the selection rule of equation (2.2), the angular momentum transfer, J must be zero. Applying the approximate selection rule of equation (2.6) the orbital angular momentum transfer L must also be zero. Therefore, all the ground state transitions should show L=0 character. Inspection of the data shows that all six angular distributions are indeed similar (see Chapter 7). In Chapter 7 it will be shown that the general properties of the L=0 transitions are predicted by distorted wave calculations.

Directly from the experimental data several characteristics of the L=0 shape for the targets studied can be noted. This is a definite maximum in the range of 23 1/2° to 27 1/2°. This is truly the second maximum since the distorted wave calculations of Chapter 7

indicates a maximum at 0°. There is another definite maximum in the range of 47 1/2° to 59 1/2°. Another maximum is also indicated further back at 75° to 95° but the data do not cover this maximum in detail.

6.2 The Transition to the First Excited States

The angular distributions for the transitions to the first excited states in all six nuclei are similar. The distorted wave calculations of Chapter 7 show that this shape corresponds to L=2, and application of the selection rule of equations (2.8) and (2.9) indicates a spin-partiy assignment of 2^+ for all the first excited states. The lowest excited state being a 2^+ for even-even nuclei is typical for even-even nuclei in this mass region.

Experimentally the L=2 angular distributions have the following properties. They exhibit a peak or plateau (washed out peak) in the region between 30° and 45°, and a peak at 65° to 75°.

6.3 Other Transitions

The predominant dependence of the angular distributions on L and the restrictive selection rules for (p,t) outlined in Chapter 2 allow spin-parity assignments to be made for some other excited states of the residual nuclei. This dependence will be investigated

further in Chapter 7. Such assignments can be based on comparison with either the experimental L=0 and L=2 shapes, or the distorted wave predictions.

The residual nuclei studied in these experiments can in general only be studied by two nucleon transfer reactions since they are all two nucleons away from stability. Until recently these nuclei have not been studied much at all. Except for the case of a few low lying levels in some of the nuclei, the only previous experiments studying these nuclei have employed the (^{3}He,n) and the (^{3}He,nγ) reactions. The Q-values for these reactions are on the order of -1 MeV as opposed to the -20 MeV for the (p,t) reactions. This small Q-value makes the (^{3}He,n) reaction possible with lower energy accelerator, but high resolution in work involving neutron detection is difficult.

Tables 1 through 6 show the energy levels seen in this experiment as well as the J^π assignments for levels where the experimental angular distributions were clear enough to indicate the L-transfer. The distorted wave calculations for reactions leading to these states, and the basis for the J^π assignments will be discussed in Chapter 7. Also shown are the levels seen by other workers and their J^π assignments. Values in parentheses represent tentative assignments, double parentheses indicate that the assignment is extremely tentative. In

TABLE 1.--Energy levels of ^{18}Ne.

(this work)		(other works)		
Energy (MeV)	J^π	Energy (MeV)	J^π	References*
		M.E.=		(Ma65)
		5.3193		
		±.0047		
0.0	0^+	0.0	0^+	$(Fa68)^t(O168)^t(Sh68)$ (To68)
				$(Kr66)_{J\pi}$(Ga61)
1.894	2^+	1.8872	2^+	$(Fa68)^t(Gi68)_E$(Sh68) (To68)
±.010		±.0002		$(Kr66)_{J\pi}$
		3.356	$((0^+))$	(Sh68)
		±.002		
3.390	(4^+)	3.3762	4^+	(Sh69a) $(Fa68)^t(Gi68)_E(Sh68)_{J\pi}$
±.014		±.0004		(To68)
		3.5763	(0)	(Gi68)
		±.0020		
3.614	0^+	3.6164	2^+	(Sh69a) $(Fa68)^t(Gi68)_{EJ\pi}$
±.013		±.0006		(Sh68) (To68)
4.576	1^-	4.550		$(Fa68)^t$(To68) $(Ad67)_E$
±.017		±.015		
5.150				
±.014				
6.326				
±.018				
7.957				
±.025				
9.215				
±.020				

*See text for explanation of notation.

TABLE 2.--Energy levels of ^{22}Mg.

(this work)		(other works)		
Energy (MeV)	J^π	Energy (MeV)	J^π	References*
M.E.=		M.E.=		$(Ce66)^t$
-0.4123		-0.380		
±.0097		±.050		
0.0	0^+	0.0	0^+	(En67)
1.250	2^+	1.2450	2^+	$(Sh68)_{J\pi}(Ga67)^t(O167)_E(Be66)$
±.008		±.0006		$(Ce66)^t$
3.323	(4^+)	3.353	(4^+)	$(Sh68)_{J\pi}(Ga67)^t_E(Be66)$ $(Ce66)^t$
±.021		±.045		
4.417	(2^+)	4.38	(2^+)	$(Sh68)_{EJ\pi}(Ga67)^t$
±.027				
5.057	(2^+)	5.04	$(2^+,3^-)$	(Sh68)
±.031				
5.313		5.29	$(2^+,3^-,4^+)$	(Sh68)
±.032				
		5.44	$(2^+,3^-,4^+)$	(Sh68)
5.738		5.70	$((0^+))$	(Sh68)
±.035				
6.061	0^+			
±.037				
6.281				
±.033				
6.645				
±.044				
6.836				
±.044				
7.252				
±.044				
7.961				
±.049				

*See text for explanation of notation.

TABLE 3.--Energy levels of ^{26}Si.

(this work)		(other works)		
Energy (MeV)	J^π	Energy (MeV)	J^π	References*
		M.E.= -7.141 ±.011		(En67)
0.0	0^+	0.0	0^+	(Ad68) (Ha68) $(Da67)^t_{J\pi}$ (Mc67) (M167) (Mc65) (AJ60)
1.795 ±.011	2^+	1.79 ±.01	2^+	(Ha68) $(Ro68)_{EJ}$ $(Da67)^t_\pi$ (M167) (AJ60)
2.790 ±.012	(2^+)	2.78 ±.01	2^+	(Ha68) $(Ro68)_E$ $(Da67)^t_{J\pi}$ (Mc67) (M167) (Mc65) (AJ60)
3.339 ±.019		3.32 ±.02	(0)	(Ha68) $(Ro68)_{EJ}$ (Mc67) (Mc65)
		(3.770) (±.040)		(Ha68) $(Mc67)_E$
		3.745 ±.050	(2^+)	$(Da67)^t$
		3.890 ±.040	?	$(Ro68)_J$ $(Mc67)_E$
4.183 ±.011	(2^+)	4.160 ±.040	(2)	(Ha68) $(Ro68)_J$ (Mc67)
4.457 ±.013	$(2^+,3^+)$	4.425 ±.050	(2^+)	(Ha68) $(Da67)^t_{EJ\pi}$
4.821 ±.013				
5.229 ±.012				
5.562 ±.028				
5.960 ±.022				
6.381 ±.020				
6.786 ±.029				
7.150 ±.015				
7.476 ±.020				
7.695 ±.031				
7.902 ±.021				

*See text for explanation of notation.

(this work)		(other works)		References
Energy (MeV)	J^{π}	Energy (MeV)	J^{π}	
		5.480 ±.015		(Sh68)
		5.548 ±.024		(Sh68)
		(5.657) (±.028)		(Sh68)
		5.825 ±.019		(Sh68)
5.897 ±.027				
		6.014 ±.012		(Sh68)
(6.108) (±.029)		6.095 ±.010		(Sh68)
(6.223) (±.030)		6.233 ±.010		(Sh68)
6.415 ±.040				
6.681 ±.040				
7.185 ±.035				
7.570 ±.045				

TABLE 5.--Energy levels of ^{34}Ar.

(this work)		(other works)		
Energy (MeV)	J^{π}	Energy (MeV)	J^{π}	References*
M.E.=		M.E.=		(En67)
-18.370		-18.394		
±.011		±.013		
0.0	0^+	0.0	0^+	(Ha68) (Mc67) (M167) (M166)
2.094	2^+	2.058		(Ha68) (Mc67) $(M167)_E$
±.011		±.035		
3.288	2^+	3.30		$(Ha68)_E$(Mc67)
±.014		±.03		
3.879	0^+	3.90		(Ha68)
±.015		±.03		
4.050		4.05		(Ha68)
±.014		±.03		
		4.15		(Ha68)
		±.03		
4.522				
±.014				
4.651				
±.014				
4.867				
±.014				
4.985				
±.014				
5.307				
±.013				
5.909				
±.012				
6.074				
±.011				
6.525				
±.009				
6.794				
±.011				
7.322				
±.006				
7.499				
±.004				
7.925				
±.005				

*See text for explanation of notation.

(this work)		(other works)		
Energy (MeV)	J^{π}	Energy (MeV)	J^{π}	References*
5.264 ±.005				
5.427 ±.006				
5.598 ±.007				
5.698 ±.010				
5.810 ±.005				
6.136 ±.006				
6.280 ±.008	(0^{+})			
6.598 ±.007				
6.702 ±.010				
6.768 ±.015				
6.801 ±.012				
(7.208) (±.015)				
7.800 ±.012				
8.595 ±.010				

order to limit these tables to a convenient size, only the more recent references are given. The excitation energy listed is usually taken from the reference with the smallest quoted error. Correspondence with levels seen in the present work is made whenever possible. This correspondence, of course, may not always be correct. All references are to (^{3}He,n) or (^{3}He,nγ) work unless followed by a t, in which case the (p,t) reaction was used. The subscripts J, π, or E indicate that the spin, parity, or energy assignment was taken from that reference if it is not the only one. The mass excess (M.E.) quoted are sometimes averages of several experiments taken from the compilations of Mattauch et al.(Ma65) and Endt and Van der Leun(En67).

A consolidation of the results of the present experiments and the results of other workers are given in Figures 8 through 13. These level diagrams are not necessarily complete since there is some ambiguity as to which states seen by different experimenters are the same. These diagrams do give a general idea of the extent to which the level structures of these six nuclei are known. Also given in these figures are the low lying levels of the mirror nuclei. The levels of ^{18}O are taken from F. D. Lee, et al.(Le67) and the references therein. The levels of ^{22}Ne are taken from references La62, Aj59, Pe64, and Bu67. The levels of ^{26}Mg, ^{30}Si,

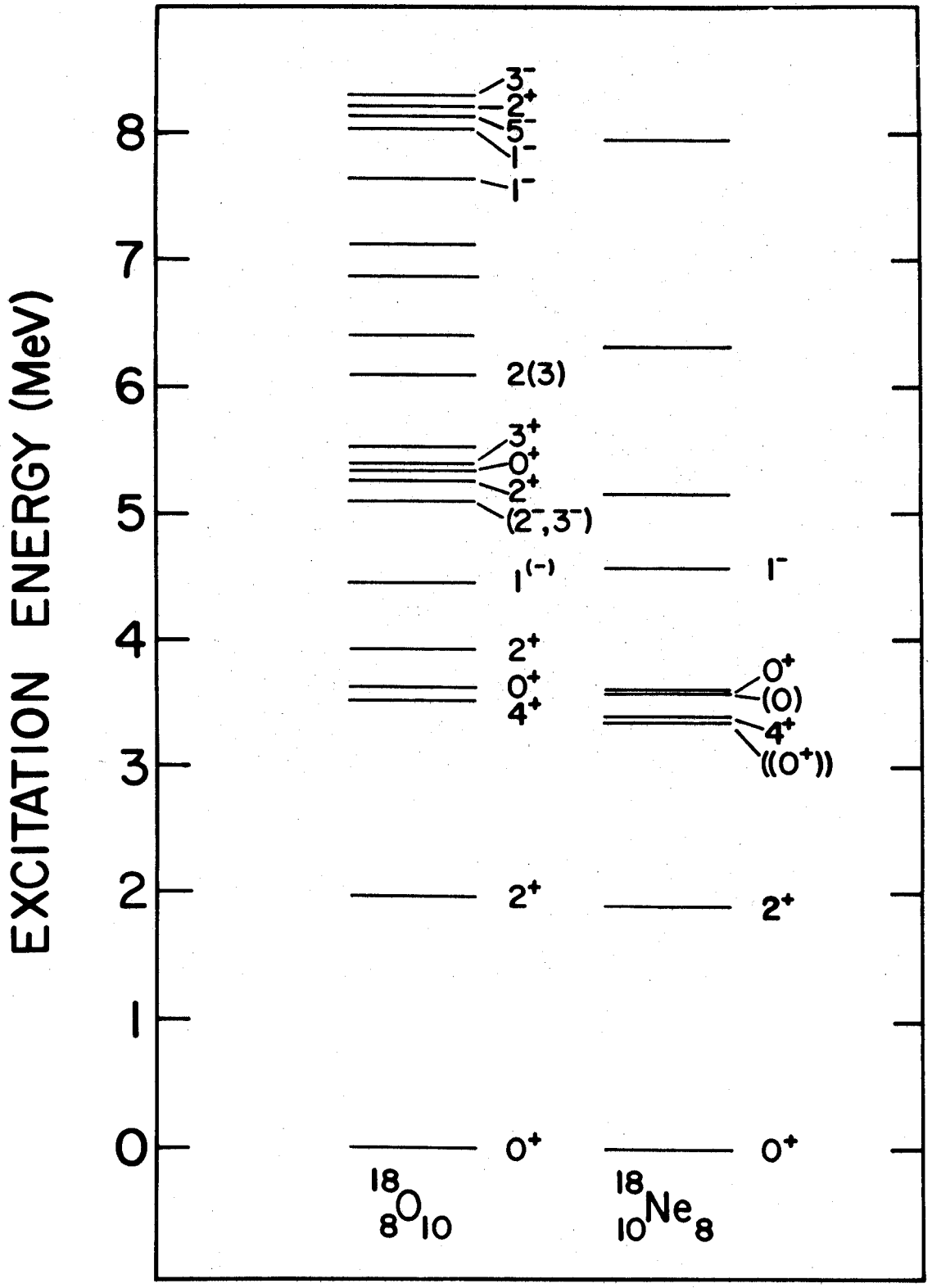

Figure 8.--Energy levels of ^{18}O and ^{18}Ne.

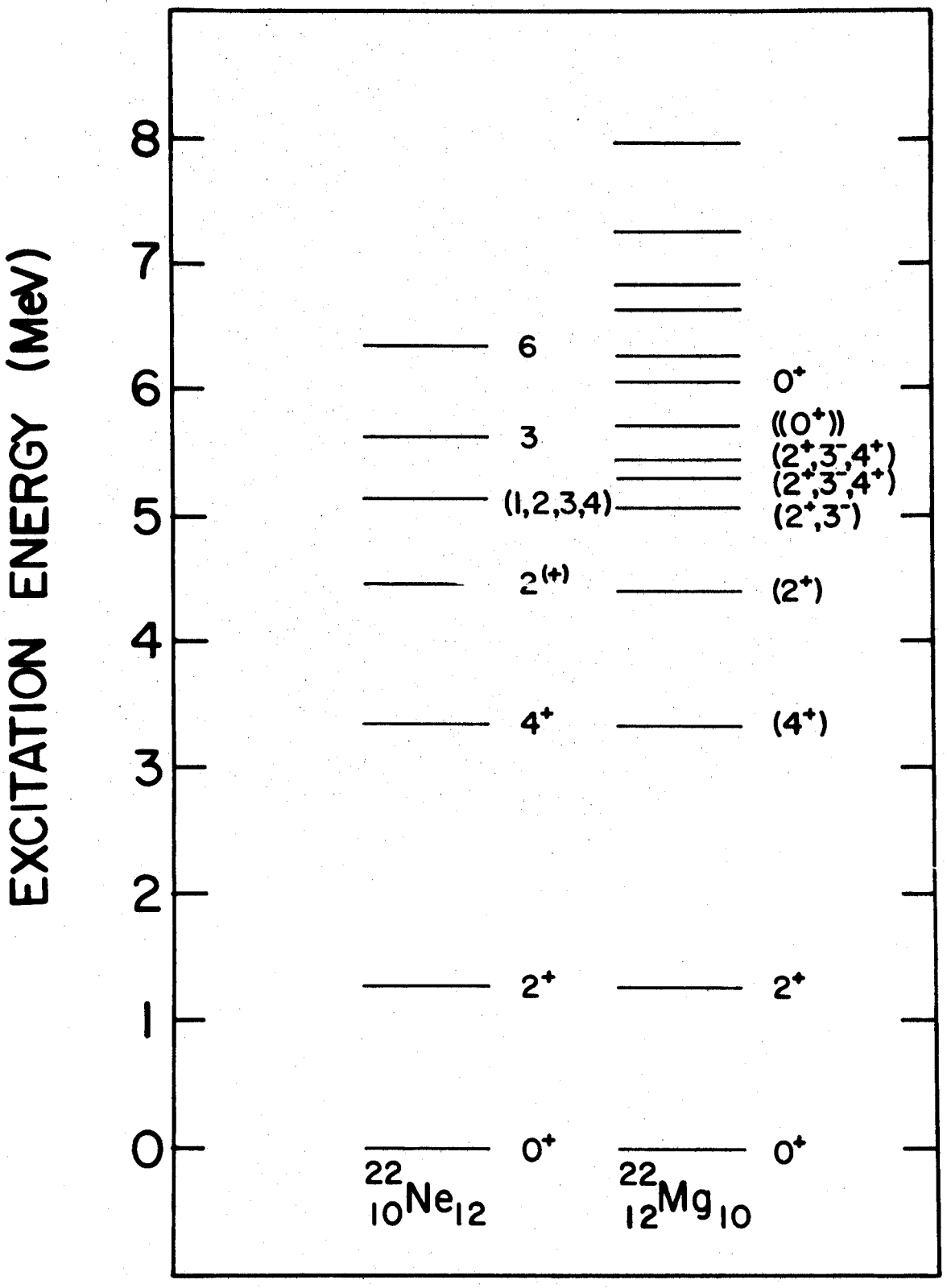

Figure 9.--Energy levels of ^{22}Ne and ^{22}Mg.

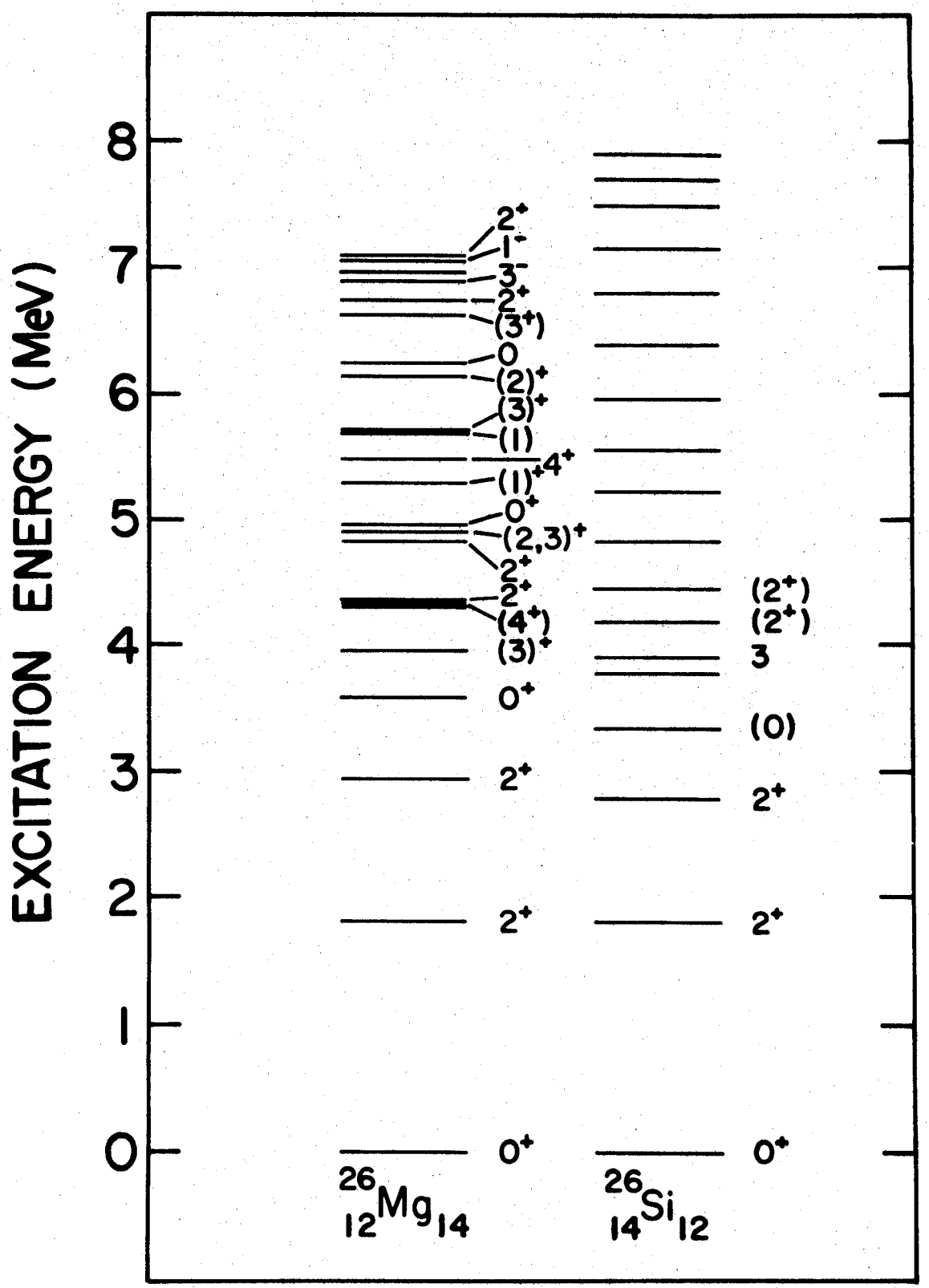

Figure 10.--Energy levels of ^{26}Mg and ^{26}Si.

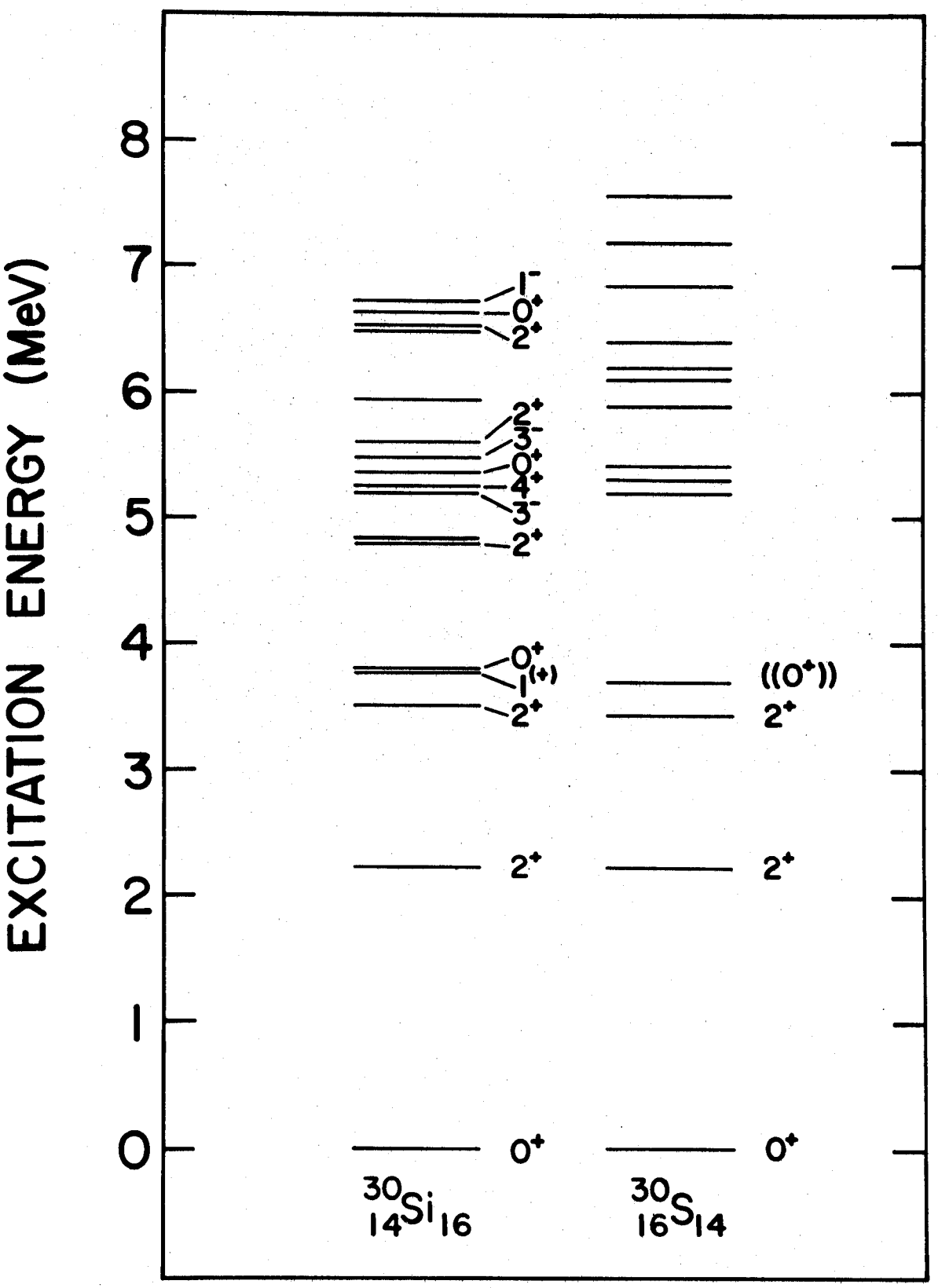

Figure 11.--Energy levels of ^{30}Si and ^{30}S.

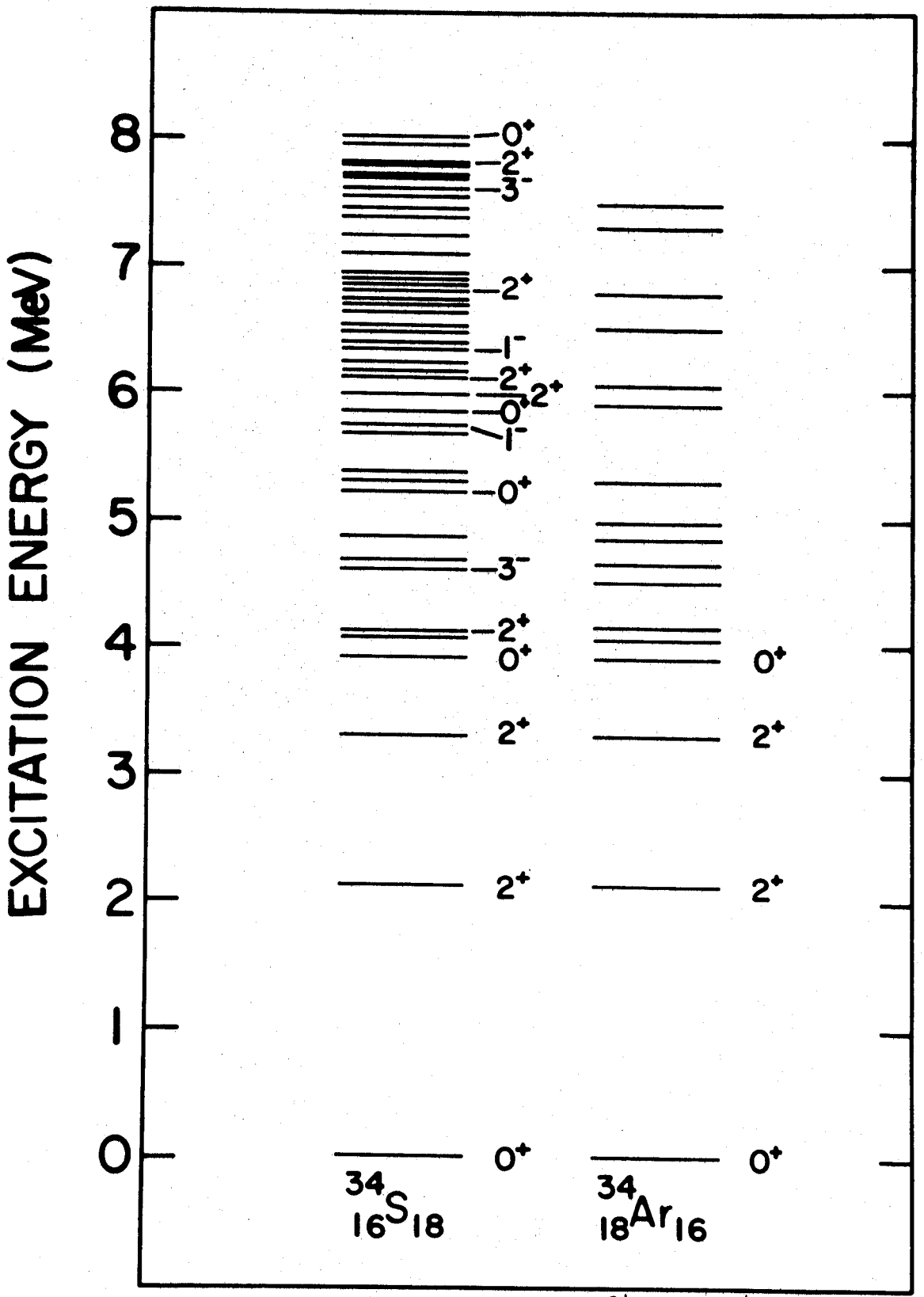

Figure 12.--Energy levels of ^{34}S and ^{34}Ar.

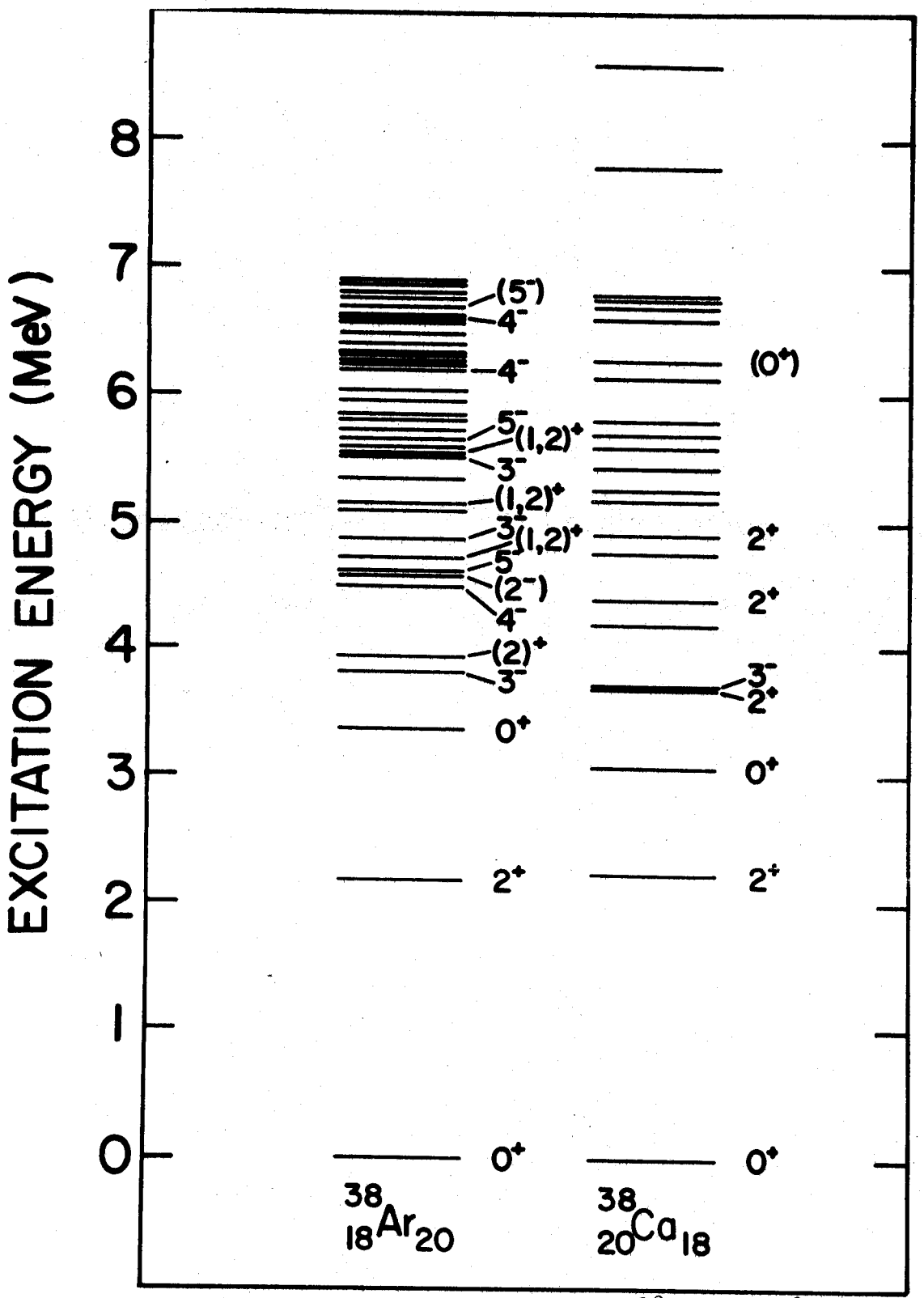

Figure 13.--Energy levels of ^{38}Ar and ^{38}Ca.

^{34}S, and ^{38}Ar are taken from the compilation of P. M. Endt and C. Van der Leun[En67].

CHAPTER 7

DISTORTED WAVE CALCULATIONS

7.1 The Optical Model

The Distorted Wave Method of calculating direct reactions uses an optical model to describe the elastic scattering in the entrance and exit channels. The optical model takes the form of a potential which, when put into the Schroedinger Equation, produces the distorted waves (wave functions) which represent the scattering. The form of the particular optical model potential that was used in the code JULIE is given in equation (7.1.1).

$$U_{OM}(r) = V_c(r) - V_o \frac{1}{1 + e^{x}} - (W_o - 4W_D \frac{d}{dx'})\frac{1}{1 + e^{x'}}$$

$$+ (\frac{\hbar}{m_\pi c})^2 V_s \frac{1}{r} \frac{d}{dr} (\frac{1}{1 + e^{x''}}) \vec{\ell}\cdot\vec{\sigma} \qquad (7.1.1)$$

The first term is the Coulomb potential of a uniformly charged sphere of radius $R_c = r_{oc}A^{1/3}$. The parameter x, x' and x" in the rest of the terms have the form $x=(r-r_oA^{1/3})/a$. For spin 1/2 particles $\vec{\sigma} = 2\vec{s}$.

A search of recent literature was made to obtain optical model parameters for protons and tritons in the appropriate energy range. This corresponds to about 40 MeV for the protons and 20 MeV for the tritons. There is, of course, no elastic scattering data for tritons on the nuclei which are the final state of the (p,t) reactions studied since they are all unstable. Also there is in general little triton elastic scattering at all. It was therefore decided to consider the possibility of using ^{3}He parameters.

Since elastic scattering data were not available for the precise nuclei and energies studied in this experiment, it was decided that it would be best to use optical model parameters which were consistent and relatively constant over the range of nuclear masses studied. Several sets of recent parameters were found, and the ones considered here are listed in Table 7. The geometries are average geometries over a range of A. The potential depths are essentially averages over the range of A pertinent to this work, the exact determinations of which will be discussed later in this section. Variation of potential depths with A given in the literature was small and not smooth as a function of A, and therefore no variation was used. When considering triton and ^{3}He optical parameters, it is found that ambiguities exist(Ka68a, Fl69). For example the elastic data can be

TABLE 7.--Optical model parameters.

Set Particle	V_o (MeV)	W_o (MeV)	W_D (MeV)	V_s (MeV)	r_o (f)	a (f)	r'_o (f)	a' (f)	r''_o (f)	a'' (f)	r_{oc} (f)	Reference
I Proton	42.6	3.7	2.7	6.04	1.16	0.75	1.37	0.63	1.064	0.734	1.25	(Fr67)
II Proton*	42	0	8.5	7.5	1.18	0.7	1.04	0.7	1.18	0.7	1.2	(Fr65)
III Proton	40	7	0	7.5	1.18	0.7	1.40	0.7	1.18	0.7	1.2	(Fr65)
IV Triton	150	26.3	0	0	1.24	0.678	1.45	0.841			1.25	(Ha67)
V Triton*	168	17	0	0	1.16	0.752	1.498	0.817			1.25	(Fl69)

*Final sets used in all calculations.

fit for any reasonable value of r_o by proper choice of V_o and other parameters. A study of the literature indicates that reaction data is usually best fit with parameters where r_o is in the range of 1.15 f to 1.25 f and V_o is in the corresponding range of 170 MeV to 150 MeV[F169]. The choice of optical parameters to be considered for this work was therefore limited to this range.

In order to determine which set of parameters to use, distorted wave calculations were made for the six L=0 ground state to ground state transitions. The form factor used was based on the pickup of a pair of neutrons from the last shell in the simplest j-j coupled shell model configuration. For example for $^{20}Ne(p,t)^{18}Ne(G.S.)$, the pickup of two $d_{5/2}$ neutrons coupled to zero angular momentum was assumed, for $^{40}Ca(p,t)^{38}Ca(G.S.)$ two $d_{3/2}$ neutrons were used, and so on. These should be the dominant terms derived from a more extensive shell model wave function of these nuclei. As will be seen later in this chapter, the shape of the angular distribution is most greatly dominated by the L transfer and secondly, and much more weakly, by the major pickup configuration. From the three sets of proton parameters and two sets of triton parameters, various combinations were tried, and the pair which gave the best average fit to the experimental shape for all six

cases, as determined by visual inspection, was chosen. This was sets II and V of Table 7. Small variations in the real and imaginary well depths were made within reasonable limits as determined by the scatter in the values of the well depths given in the literature for fits to actual elastic scattering data. Again the best average fit to all six cases was used to determine the final value of the depths given in Table 7. The strongest dependence of the shape of the angular distribution was found to be on the imaginary well depths of both the protons and the tritons. All distorted wave calculations shown in this work are based on this final set of optical model parameters.

7.2 The Ground State Transitions

As was mentioned in Section 7.1, distorted wave calculations were made for the six 0^+ to 0^+ ground state transitions assuming the pickup of a pair of neutrons coupled to angular momentum zero from the last shell in the simple j-j coupled shell model picture. Each individual proton shell and neutron shell was assumed coupled to zero angular momentum. In calculating the form factor described in Chapter 3, the wave functions of the individual neutrons were taken to be those of a particle bound in a Woods-Saxon well of the form given in equation (7.2.1).

$$U(r) = -V_o \frac{1}{1 + e^x} + \left(\frac{\hbar}{m_{\pi^o} C}\right)^2 V_s \frac{1}{r} \frac{d}{dr} \left(\frac{1}{1 + e^x}\right) \vec{\ell}\,\vec{\sigma} \qquad (7.2.1)$$

In the above expression, $\vec{\sigma} = 2\vec{s}$ for these spin 1/2 particles. The parameter x is equal to $(r-r_o A^{1/3})/a$, where A was the mass of the target minus the mass of one neutron. The values of r_o and a were chosen to be 1.25 f and 0.65 f as suggested by Bayman et al.(Ba68). V_s was taken as 6 MeV, which is typical of single nucleon spin-orbit strengths. The real well depth V_o was adjusted so the individual neutrons were bound by one-half the two neutron separation energy as suggested in references Dr66 and Ba68. These Woods-Saxon wave functions were then expanded in terms of a series of harmonic oscillator wave functions whose strength parameters α was chosen by the code TWOFRM to maximize the convergence of this expansion and was usually about 0.3 f^{-2}. This expansion had the form of equation (7.2.2).

$$\phi_{\gamma\ell}(\vec{r}) = \sum_{\mu=0} a_\gamma^\mu \Theta_{\mu\ell}(\alpha, \vec{r}) \qquad (7.2.2)$$

Multiplying both sides of equation (7.2.2) by $\Theta^*_{\mu',\ell}(\alpha, \vec{r})$ and integrating over $d\vec{r}$, and expression for the coefficients can be found.

$$a_\gamma^\mu = \int \Theta^*_{\mu\ell}(\alpha, \vec{r})\, \phi_{\gamma\ell}(\vec{r})\, d\vec{r} \qquad (7.2.3)$$

Both wave functions have the same angular dependence, and this can be integrated out.

$$a_\gamma^\mu = \int R_{\mu\ell}(\alpha r^2)\, U_{\gamma\ell}(r)\, r^2\, dr \qquad (7.2.4)$$

The a_γ^μ's were calculated by numerically evaluating the integral of equation (7.2.4).

Since these are orthonormal wave functions, the following restriction exists for the a_γ^μ's.

$$\sum_{\mu=0}^{\infty} |a_\gamma^\mu|^2 = 1 \qquad (7.2.5)$$

The sum over μ was cut off at $\mu=\mu_{max}$, where μ_{max} was determined by the following criterion. The first requirement is given in equation (7.2.6).

$$\sum_{\mu=0}^{\mu_{max}} |a_\gamma^\mu|^2 \geq 0.9996 \qquad (7.2.6)$$

The final cutoff was determined by minimizing the quantity Q defined in equation (7.2.7).

$$Q \equiv \int \left| u_{\gamma\ell}(r) - \sum_{\mu=0}^{\mu_{max}} a_\gamma^\mu\, R_{\mu\ell}(\alpha r^2) \right|^2 r^2\, dr \qquad (7.2.7)$$

Formally Q should go to zero as μ_{max} gets infinitely large, but because of numerical problems in evaluating the integral of equation (7.2.4), Q does not go to zero,

but reaches a minimum. Typically μ_{max} was between 5 and 8, Q was about 4×10^{-6} and $\sum_{\mu=0}^{\mu_{max}} |a_\gamma^\mu|^2$ was about 0.99998. This corresponded to fitting the Woods-Saxon wave functions to better than 2% out to a radius of about $2.6\ A^{1/3} f$ and better than 10% out to about $3.2\ A^{1/3} f$. Since the well had a size parameter of $1.25\ A^{1/3} f$, this corresponds to fitting to 2% out to twice the nuclear radius and to 10% to 2 1/2 times the nuclear radius. At twice the nuclear radius, the form factor has already dropped off by 3 or 4 orders of magnitude.

According to the results of Chapter 3, the theoretical differential cross-section should be proportional to the cross-section calculated with JULIE.

$$\frac{d\sigma}{d\Omega})_{theory} = \frac{K}{5014}\ \sigma(\text{JULIE}) \qquad (7.2.8)$$

The proportionality factor, K should be constant for all the (p,t) reactions studied if the proper wave functions and thus parentage factors are used, along with the proper distorted waves. Since the simple wave functions described above are most probably not adequate, the factor K cannot be expected to be constant, and it is not. Figure 14 shows the data for these six 0^+ to 0^+ ground state transitions along with the distorted wave calculations based on these simplest of wave

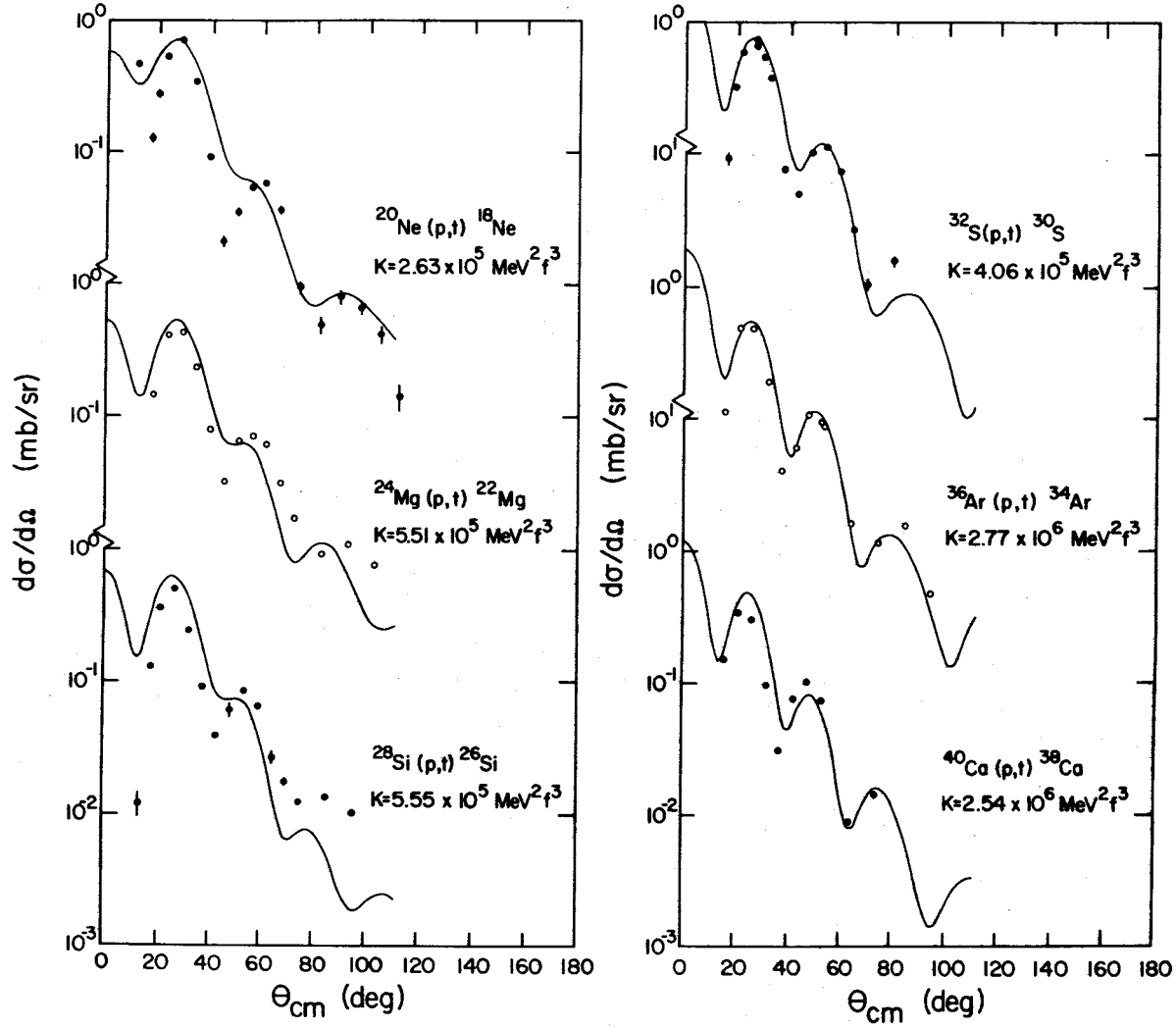

Figure 14.--0^+ to 0^+ ground state transitions.

functions. The value of K was chosen to give the best average fit to the two maxima of the data, and the value of K is given in the figure.

Another method of calculating (p,t) angular distributions using distorted waves is to treat the reaction as a transfer of a rigid cluster. In this method the two neutrons are treated as if they were an elementary particle of spin zero and mass 2 with no internal structure present in the target nucleus as such. With this picture, the calculation can be carried out exactly the same way as single nucleon transfer such as (p,d). In distorted wave calculations of (p,d), the form factor is usually taken to be the bound state wave function of the neutron in a Woods-Saxon well. Such a cluster transfer calculation was carried out using the wave function of a mass 2 particle with quantum numbers L=0, S=0 and J=0. The principle quantum number, which is somewhat arbitrary for such a calculation, was chosen to be 3. This choice is based on the fact that in the expression for the form factor (equation 3.3.2), in the more detailed model of Chapter 3, the dominant term is the one corresponding to N=3. Calculations were also made with N=1 and 2 and little difference in shape was observed. The cluster was assumed to be bound in a well of the form given in equation (7.2.9)

$$U(r) = V_o \frac{1}{1 + e^x} \; ; \; x = (r - 1.25 \; A^{1/3} \; f)/0.65 \; f \qquad (7.2.9)$$

In this expression A was taken to be the mass of the residual nucleus, and V_o was chosen to reproduce the experimental two neutron separation energy. The calculations show that the general shape of the angular distributions are reproduced but not nearly as well as with the more detailed calculations.

In order to compare in a systematic way, the data with these calculations, it can be noted that over the range that the distributions were observed, there are two peaks in the cross-section. The first one at about 25° will be denoted by θ_1 and σ_1 where θ_1 is the center of mass angle at which the peak occurs and σ_1 is the cross-section at this peak. The second peak at about 55° can be denoted by θ_2 and σ_2. Figures 15, 16 and 17 show the value of θ_1, θ_2, and σ_1/σ_2 respectively as a function of target mass number (A) for the data and the two methods of distorted wave calculations. Of interest is the fact that the general trend of σ_1/σ_2 is reproduced fairly well by the two nucleon transfer theory, but that the cluster model does not reproduce it as well. The same single set of optical model parameters was used throughout.

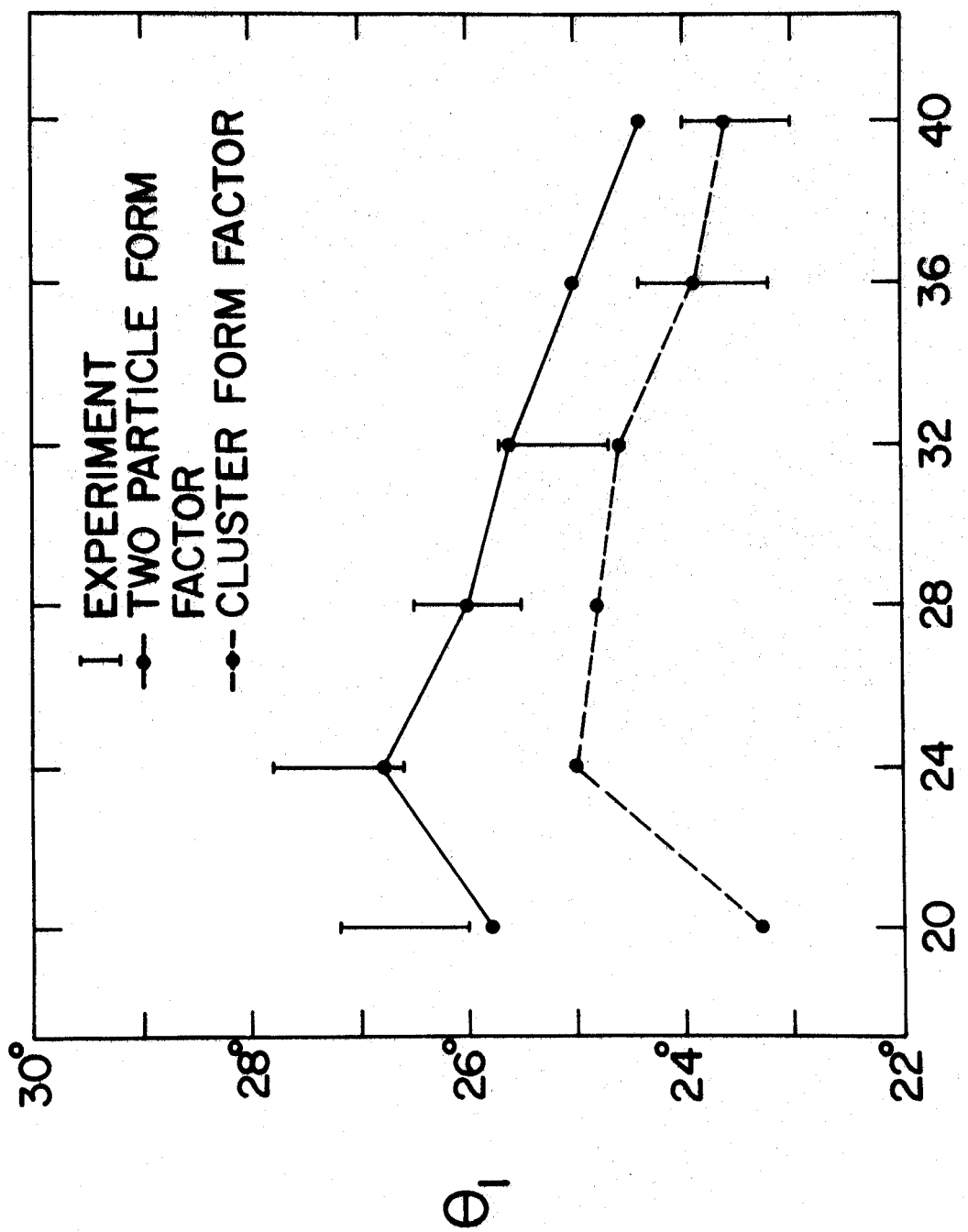

Figure 15.--Position of first peak for the ground state transitions.

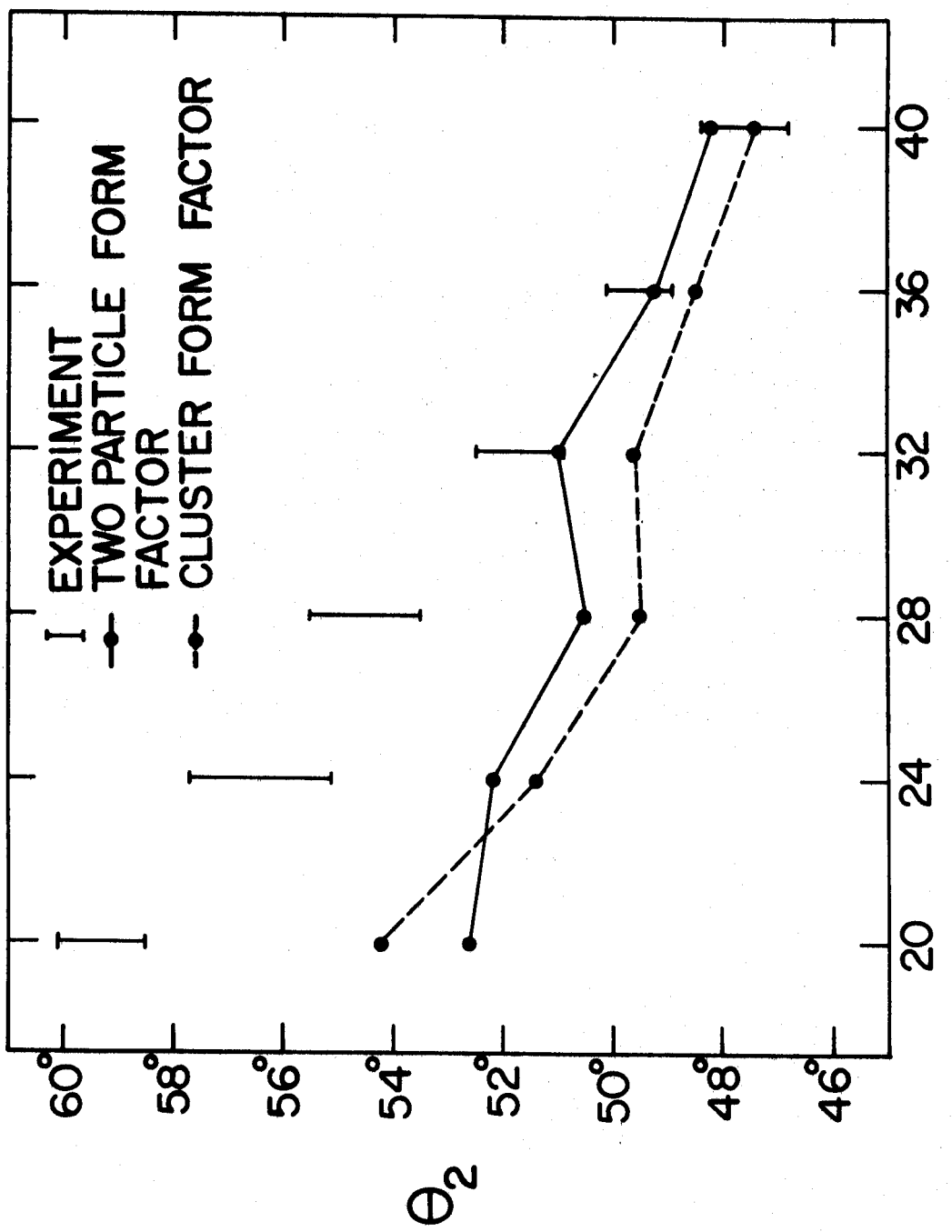

Figure 16.--Position of second peak for the ground state transitions.

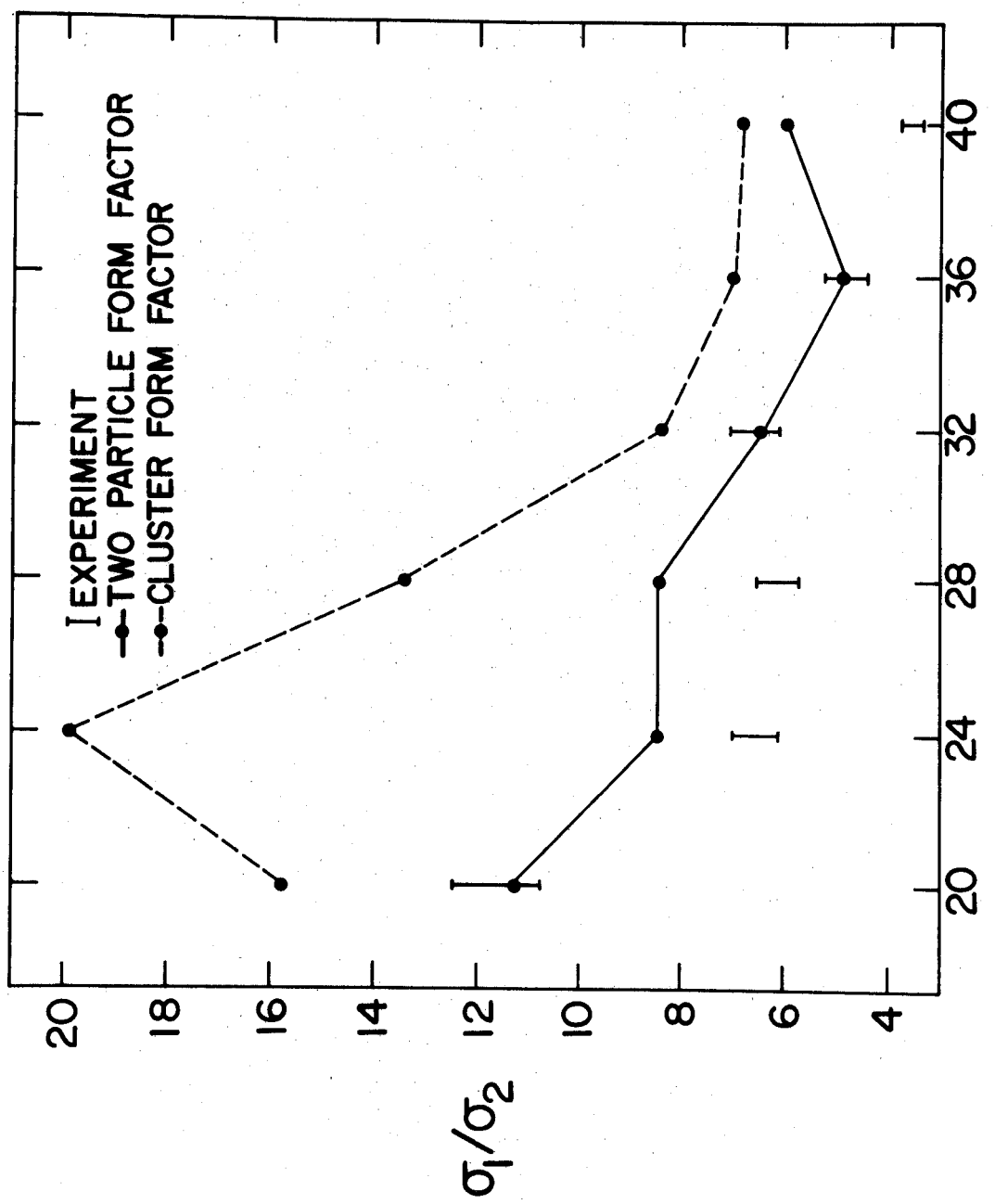

Figure 17.--Ratio of peak cross-sections for the ground state transitions.

In some cases the second maximum in the calculation does not appear as a peak, but as a plateau, in which case θ_2 was defined as the angle where the slope of the cross-section with θ was a minimum. The data is represented as bars which denote approximate limits on the quantities as determined from the data. They were arrived at by sketching the reasonable limits of smooth curves through the actual data points of the angular distributions.

7.3 Dependence on the Bound State Well

The dependence of the calculations on the bound state well of the individual transferred neutrons was also investigated. The $^{32}S(p,t)^{30}S(G.S.)$ transition was chosen for an example. The values of r_o and a of the Woods-Saxon well were varied to investigate their effects. The overall shape was found to vary only slightly. The parameters θ_1 and θ_2 were not effected at all with any reasonable variation of r_o or a. The integrated cross-section (integrated over the angular range of the calculation, 0° to 111°) denoted as σ_{tot} was found to vary greatly and σ_1/σ_2 was also found to vary. When a was varied by 0.10 f from 0.65 f, σ_1/σ_2 changed by about 6% and σ_{tot} by 40 to 50%. When r_o was increased by 0.10 f from 1.25 f, σ_1/σ_2 changed by 20% and σ_{tot} by 115%. This large variation in the magnitude of

the cross-section with small variations in a and r_o indicates the necessity of good values of parameters in order to calculate magnitudes of cross-section reliably. Variations in σ_1/σ_2 (the shape) were observed but were small. Therefore, we again conclude that the shape is mostly dominated by the L-transfer.

In the selection of optical model parameters, as mentioned in Section 7.1, several sets were tried. Although not investigated in detail, variations in σ_1/σ_2 and σ_{tot} of the same order of magnitude as mentioned in the discussion of bound state parameters were observed, along with some variations in θ_1 and θ_2. This indicates the need of good optical parameters in order to carry out distorted wave calculations which are meaningful in detail.

7.4 Dependence on Configuration Mixing

The exact calculation of an angular distribution by the two nucleon transfer distorted wave theory involves the use of complete wave functions for the initial and final states. Since these are not well known in general, the complete calculation cannot be made. Even if they were known, the calculation of the appropriate parentage factors as described even in the simplest general case of Section 3.4 are very involved

and include sums over single particle c.f.p.'s, Clebsh-Gordan coefficients, Racah coefficients, and 9-J symbols.

In order to study the dependence of the distorted wave calculations on the inclusion of configuration mixed wave functions, the case of $^{40}Ca(p,t)^{38}Ca(G.S.)$ will be considered. This is possibly the simplest case since ^{40}Ca is doubly magic nucleus whose ground state to 0^{th} order might be considered a doubly closed shell. The ^{38}Ca ground state might then be considered as a closed proton shell and a mixture of a term with two neutron holes coupled to zero in the $1d_{3/2}$ shell, and a term with the neutron holes in the $2s_{1/2}$ shell. Therefore, the (p,t) reaction to the ^{38}Ca ground state could go by either the pickup of two $d_{3/2}$ neutrons coupled to zero, or two $s_{1/2}$ neutrons coupled to zero, and in general by some mixture of the two. Figure 18 shows the distorted wave calculations for these two extreme cases. The shapes are quite similar. In the case of $(d_{3/2})^2$ pickup, σ_1/σ_2 equals 6.0 and in the case of $(s_{1/2})^2$ pickup σ_1/σ_2 equals 6.8. The maxima (θ_1 and θ_2) fall at essentially the same angles in both cases. The magnitudes are quite different and are in the ratio of about 1.00/0.67. In order to study the effects of mixing these two possible components, calculations were made as a function of percentage mixture of $(s_{1/2})^2$ pickup with the $(d_{3/2})^2$, both in phase and out of phase.

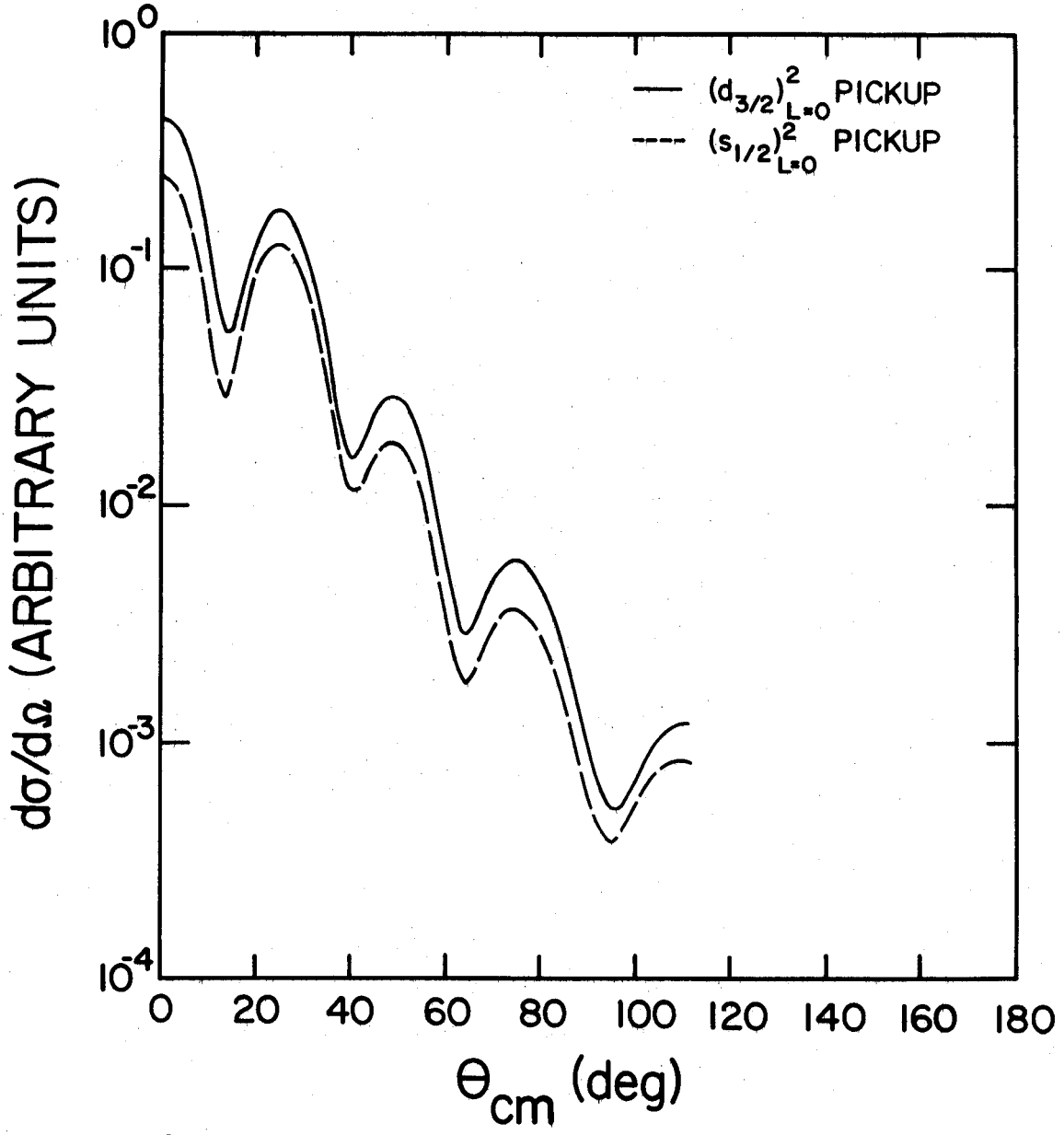

Figure 18.--Distorted wave calculations for pure pickup in the $^{40}Ca(p,t)^{38}Ca$ ground state transition.

Figure 19 shows the percentage change in the integrated cross-section (σ_{tot}) with respect to pure $(d_{3/2})^2$ pickup as a function of this admixture. It should be noted that certain admixtures can enhance the cross-section by a factor of about 1.7 and if out of phase, the cross-section can drop to essentially zero. Therefore, admixtures and their relative phases can have a very drastic effect on the magnitude of the cross-section predicted. It also should be noted that this effect is strongest for very small admixtures, that is the greatest rate of change of σ_{tot} as a function of admixture occurs at small admixtures. Figure 20 shows the effect on σ_1/σ_2 (shape) as a function of in phase admixture. An effect is noted, but it is not as drastic as the effect on the magnitude. Looking at Figure 18, the effect on shape is almost not detectable on the semi-log plot of differential cross-section versus angle.

According to the above analysis, it can be concluded that the two nucleon transfer reaction is very sensitive to the actual wave functions only in magnitude, the shapes being mostly dominated by the L-transfer and the distorted waves. It can also be concluded that the magnitude of the cross-section is so strongly dependent on small admixtures that the wave functions would have to be known in great detail and to great accuracy in

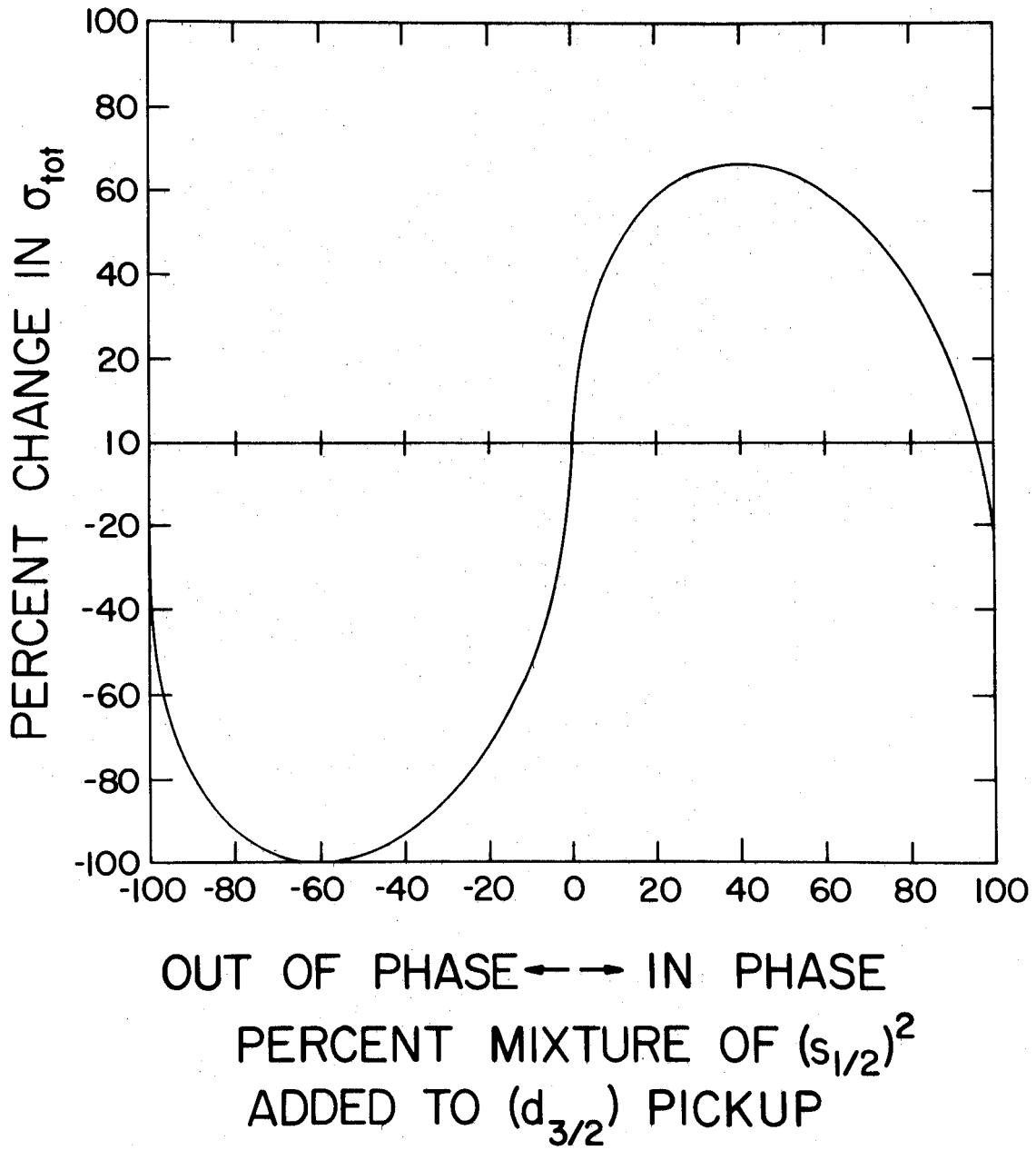

Figure 19.--Change in σ_{tot} as a function of configuration mixing.

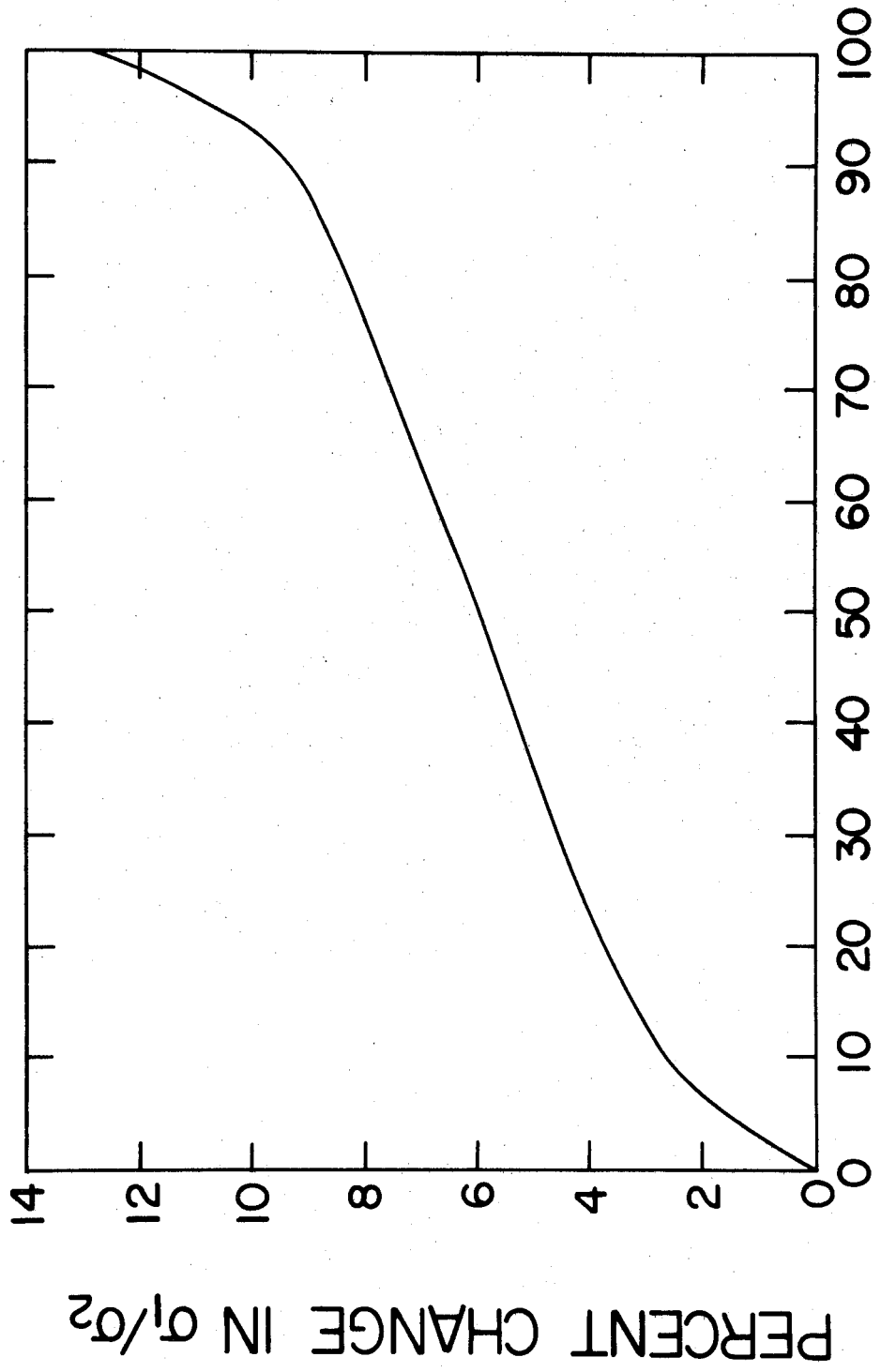

Figure 20.--Change in σ_1/σ_2 as a function of configuration mixing.

order to calculate magnitudes of cross-sections that are at all meaningful.

7.5 The Transitions to the First Excited 2^+ States

All six nuclei studied show a fairly well populated first excited state which is well isolated from any other nearby excited states that are populated. This state is either known or expected to be a $J^\pi=2^+$ state. Two nucleon transfer distorted wave calculations were made for these states also. Again the wave functions for the initial and final states were assumed to be the very simplest. In particular, calculations were made assuming the pickup of a pair of neutrons from the same shell coupled to J=2. This was the $d_{5/2}$ shell for Ne, Mg, and Si and the $d_{3/2}$ shell for Ar and Ca. In the case of $^{32}S(P,t)^{30}S(1^{st}2^+)$, this is not possible since if there are two neutrons in the $2s_{1/2}$ shell they must be coupled to zero. The ^{32}S ground state might be expected to contain admixtures of particles in the $d_{3/2}$ as well as the $s_{1/2}$ shell. Therefore, for this simple calculation of the L=2 shape, a pickup of one $S_{1/2}$ particle and one $d_{3/2}$ particle was assumed. The experimental distributions along with the results of the above calculations are shown in Figure 21. The calculations are arbitrarily normalized to the first and second peaks of the data.

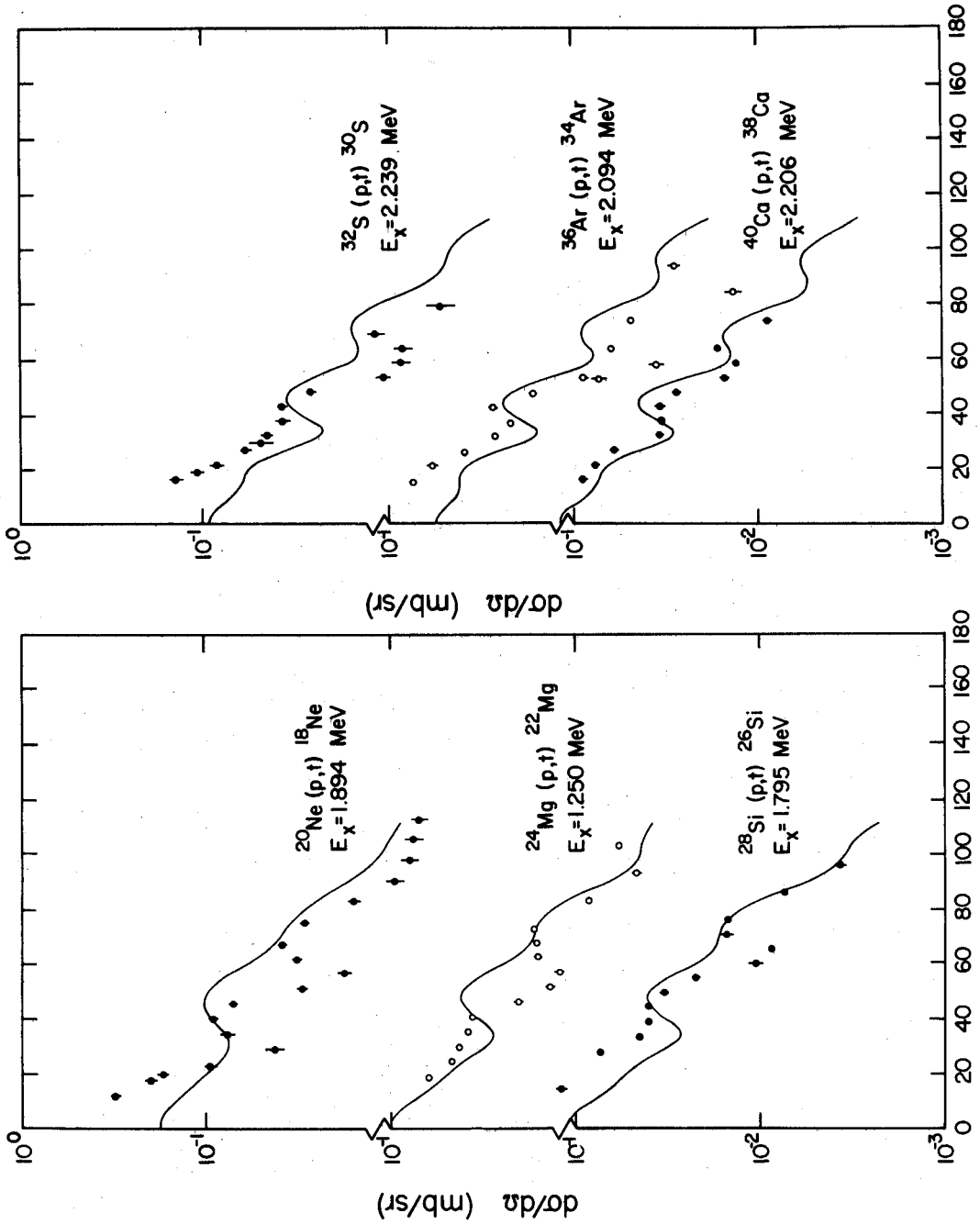

Figure 21.--Transitions to the first 2^+ states.

Again a θ_1, θ_2, and σ_1/σ_2 can be defined as was done for the L=0 shape. In the case of the L=2 transition, the first peak (at θ_1) is not usually well defined by the data. Figures 22 and 23 show σ_1/σ_2 and θ_2 versus target mass number for the data and these calculations. The optical model parameters and the bound state well geometries were the same as for the L=0 ground state calculations. The depth of the bound state well was chosen so that the individual neutrons would be bound by an energy ε defined in equation (7.5.1).

$$\varepsilon = 1/2(|B.E.(2n)| + E_x) \qquad (7.5.1)$$

In this expression B.E.(2n) is the separation energy of the last two neutrons, and E_x is the excitation energy of the excited state.

7.6 Transitions to States in ^{18}Ne

Two nucleon transfer distorted wave calculations were made for those transitions where the experimental angular distributions were clear enough to indicate L-transfer and for transitions to states where J^π assignments have been made by other workers. The results are shown in Figure 24 along with the configuration of the two picked up neutrons assumed for purposes of calculation. This assumed configuration has little meaning since it has been shown that shapes have only a small dependence

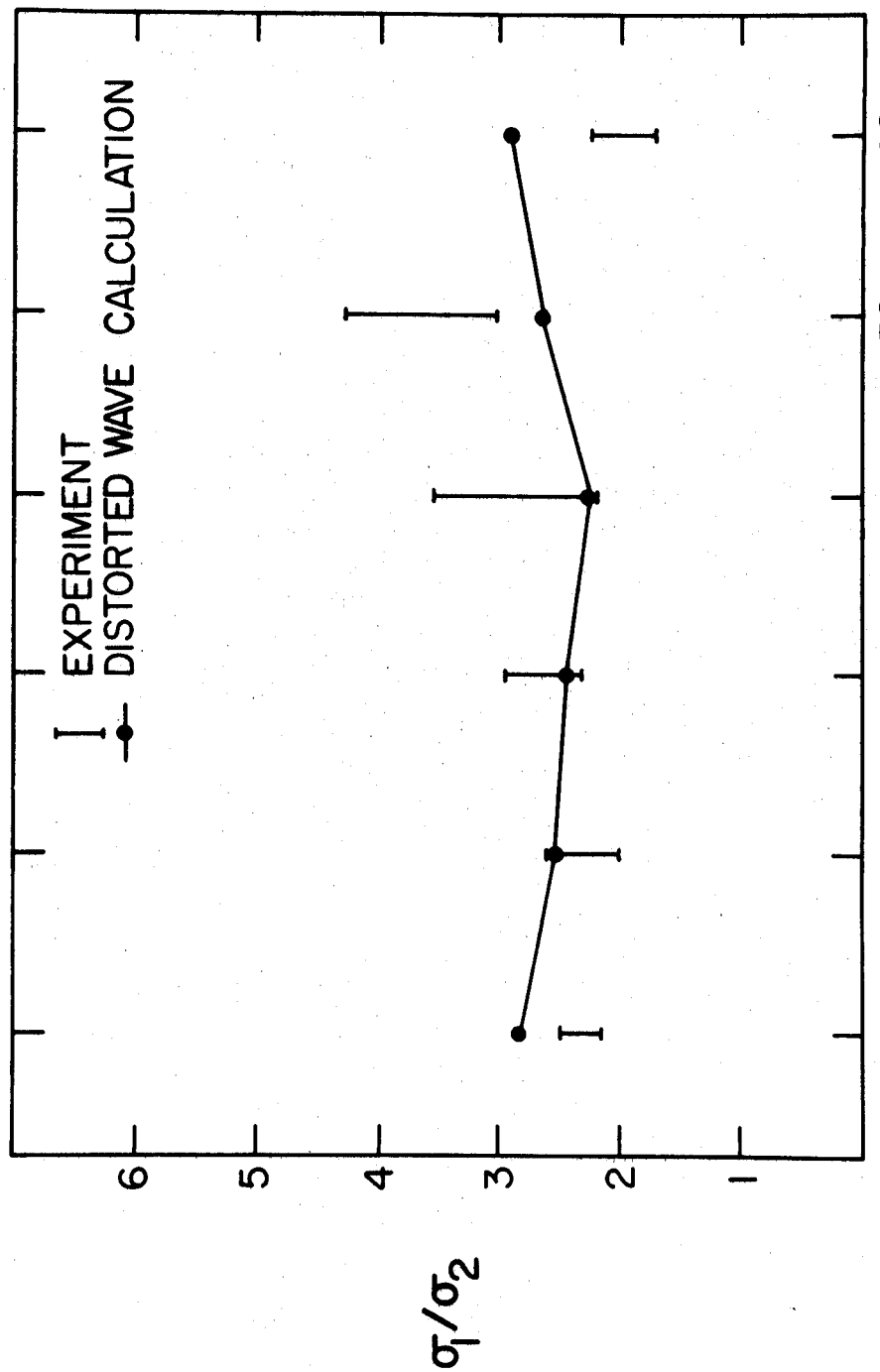

Figure 22.--Ratio of peak cross-sections for the first L=2 transitions.

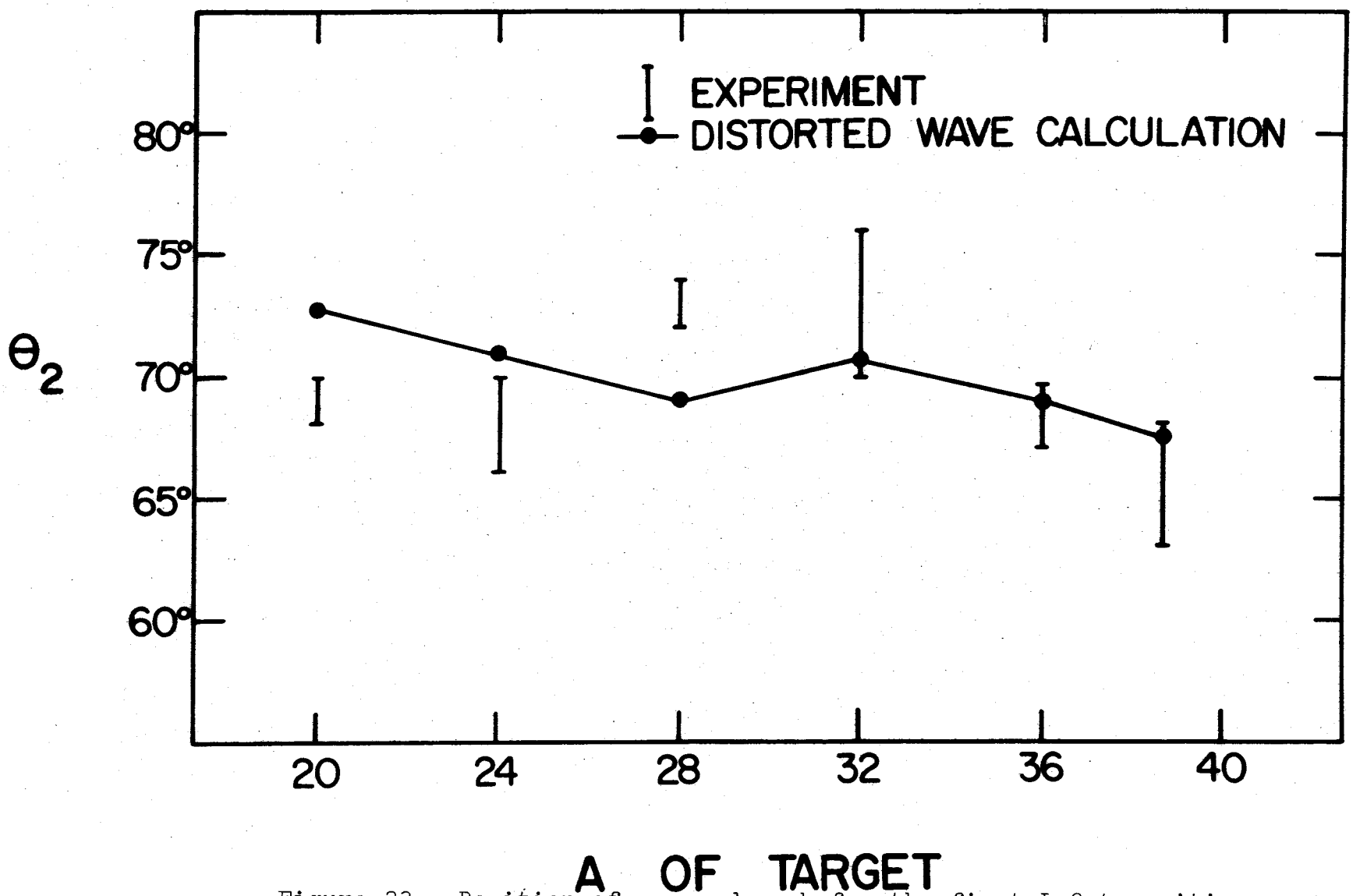

Figure 23.--Position of second peak for the first L=2 transition.

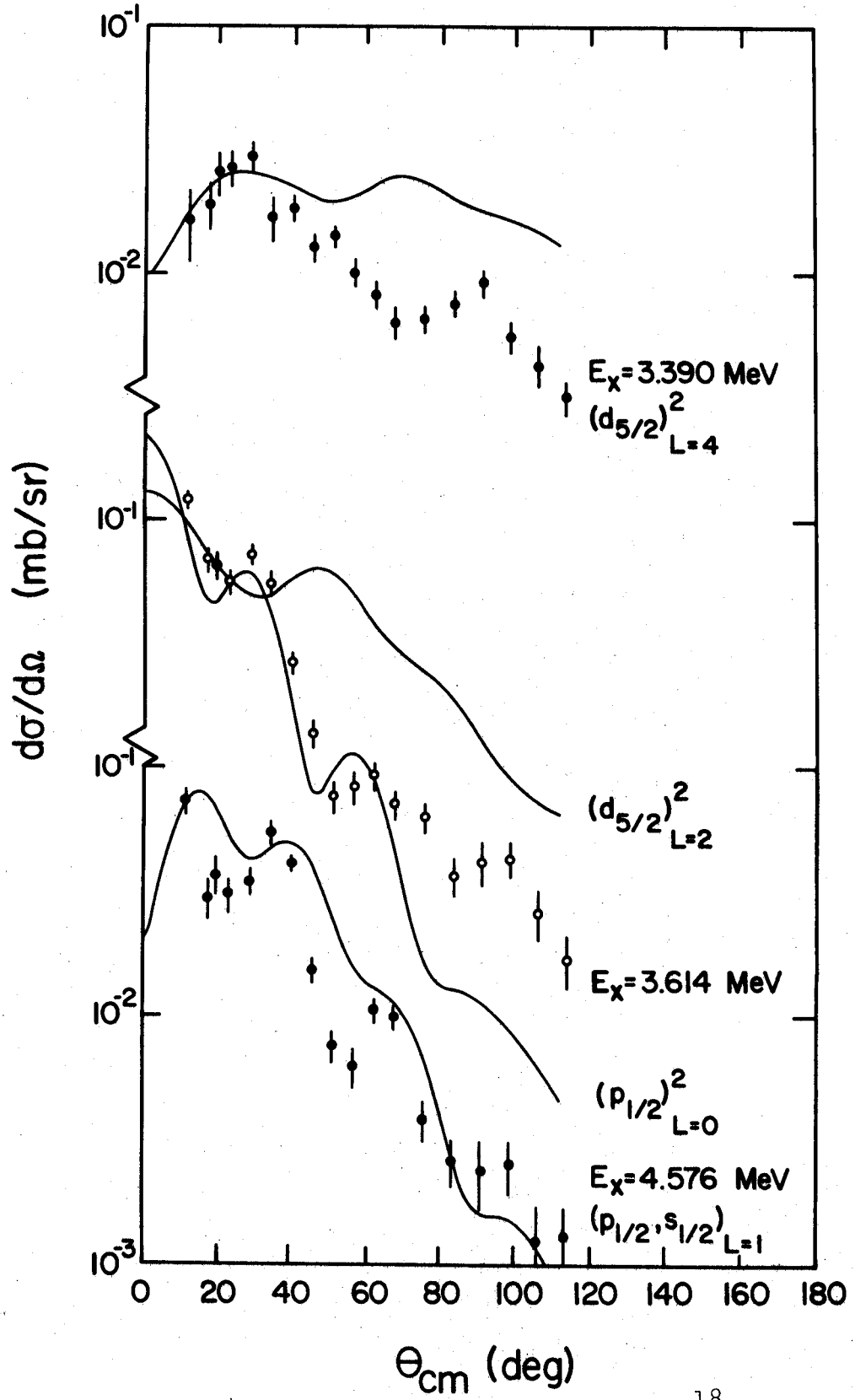

Figure 24.--Transitions to states in ^{18}Ne.

on the configuration and are dominated by the L-transfer. The calculations are arbitrarily normalized to make comparisons of shape with data easier.

The experimental shape of the distribution to the state at 3.390 MeV is not well reproduced by the L=4 calculation which is shown with it in Figure 24. The L=4 assignment is best verified by comparison with the experimental distribution to the 3.323 MeV state in ^{22}Mg which is most probably a 4^+ by comparison with the level structure of its mirror nucleus ^{22}Ne (see Figure 9). This is the basis for the tentative 4^+ assignment to this level at 3.390 MeV in ^{18}Ne.

The level at 3.614 MeV has been previously identified as a 2^+ (see Table 1). The present data is very well fit by the L=0 shape. Figure 24 shows both an L=0 and an L=2 calculation for comparison. The present experiment therefore calls for an 0^+ assignment to the state at 3.614 MeV in ^{18}Ne.

The general features of the angular distribution to the level at 4.576 MeV are well reproduced by an L=1 calculation as shown in Figure 24. This state is therefore assigned a J^π value of 1^-.

7.7 Transitions to States in ^{22}Mg

The state at 3.323 MeV in ^{22}Mg is tentatively assigned $J^\pi=4^+$ although the shape is not well reproduced

by the L=4 calculation shown in Figure 25. This assignment is primarily based on a comparison with the known level structure of ^{22}Ne, the mirror nucleus to ^{22}Mg (see Figure 9).

The levels at 4.417 MeV and 5.507 MeV exhibit the features of an L=2 transition. Comparison with the transition to the known 2^+ at 1.250 MeV verifies this (see Figure 21). These two states are therefore tentatively assigned $J^\pi=2^+$.

The state at 5.738 MeV has previously been very tentatively assumed to be a 0^+ (see Table 2). An L=0 calculation is shown with the data in Figure 25, but there is very little similarity at all. No attempt has been made to make a further assignment to this state.

The level at 6.061 MeV is assigned a J^π value of 0^+. The angular distribution to this state is quite well represented by the L=0 calculation shown in Figure 25.

7.8 Transitions to States in ^{26}Si

The angular distributions to the state at 2.790 MeV in ^{26}Si is not complete enough to make a definite J^π assignment. It does exhibit some of the features of an L=2 distribution (see Figure 26) and so a tentative 2^+ assignment is made. This is in agreement with the previous assignment (see Table 3).

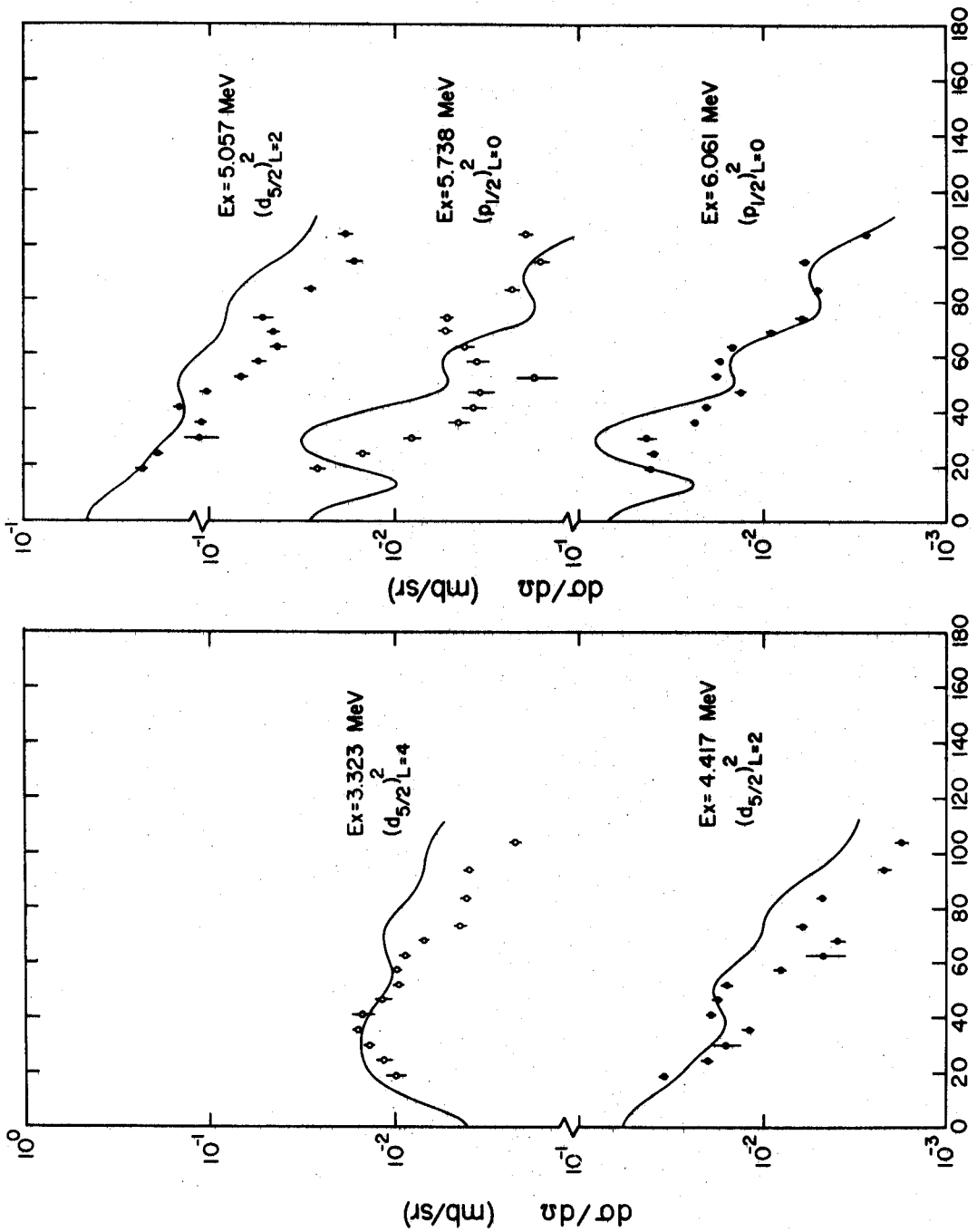

Figure 25.--Transitions to states in ^{22}Mg.

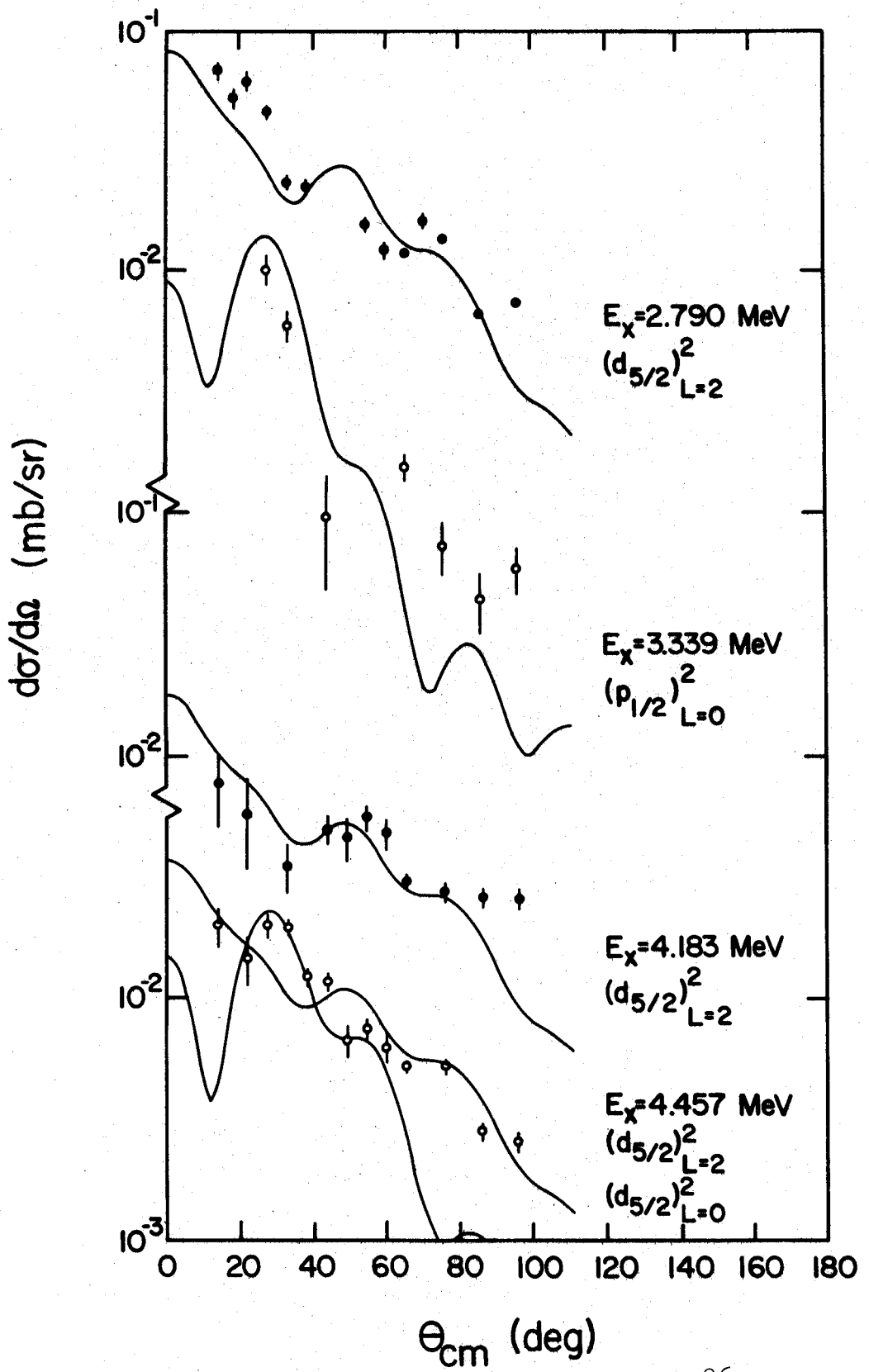

Figure 26.--Transitions to states in ^{26}Si.

The level at 3.339 MeV is very weakly excited. Its angular distribution is not inconsistent with the previous tentative J=0 assignment[Ro68], but no definite assignment can be made.

The shape of the distribution to the state at 4.183 MeV in ^{26}Si is quite well reproduced by an L=2 calculation but the state is only weakly excited and so only a tentative 2^+ assignment can be made.

Figure 26 shows both an L=0 and an L=2 calculation for the state at 4.457 MeV. The L=0 shape appears to give the better fit, but no definite assignment is made.

7.9 Transitions to States in ^{30}S

The shape of the angular distribution to the state at 3.438 MeV in ^{30}S is fairly well reproduced by an L=2 calculation as shown in Figure 27. This state is therefore assigned a J^π value of 2^+.

The state at 3.707 MeV is only weakly excited. The angles at which it was excited enough to extract a cross-section correspond to the maxima of the L=0 ground state transition distribution to ^{30}S (see Figure 14). Only a very tentative assignment of 0^+ can be made.

7.10 Transitions to States in ^{34}Ar

The ^{36}Ar(p,t)^{34}Ar has not previously been reported. The angular distribution to the state at 3.288 MeV in ^{34}Ar exhibits very definite L=2 character. Comparison

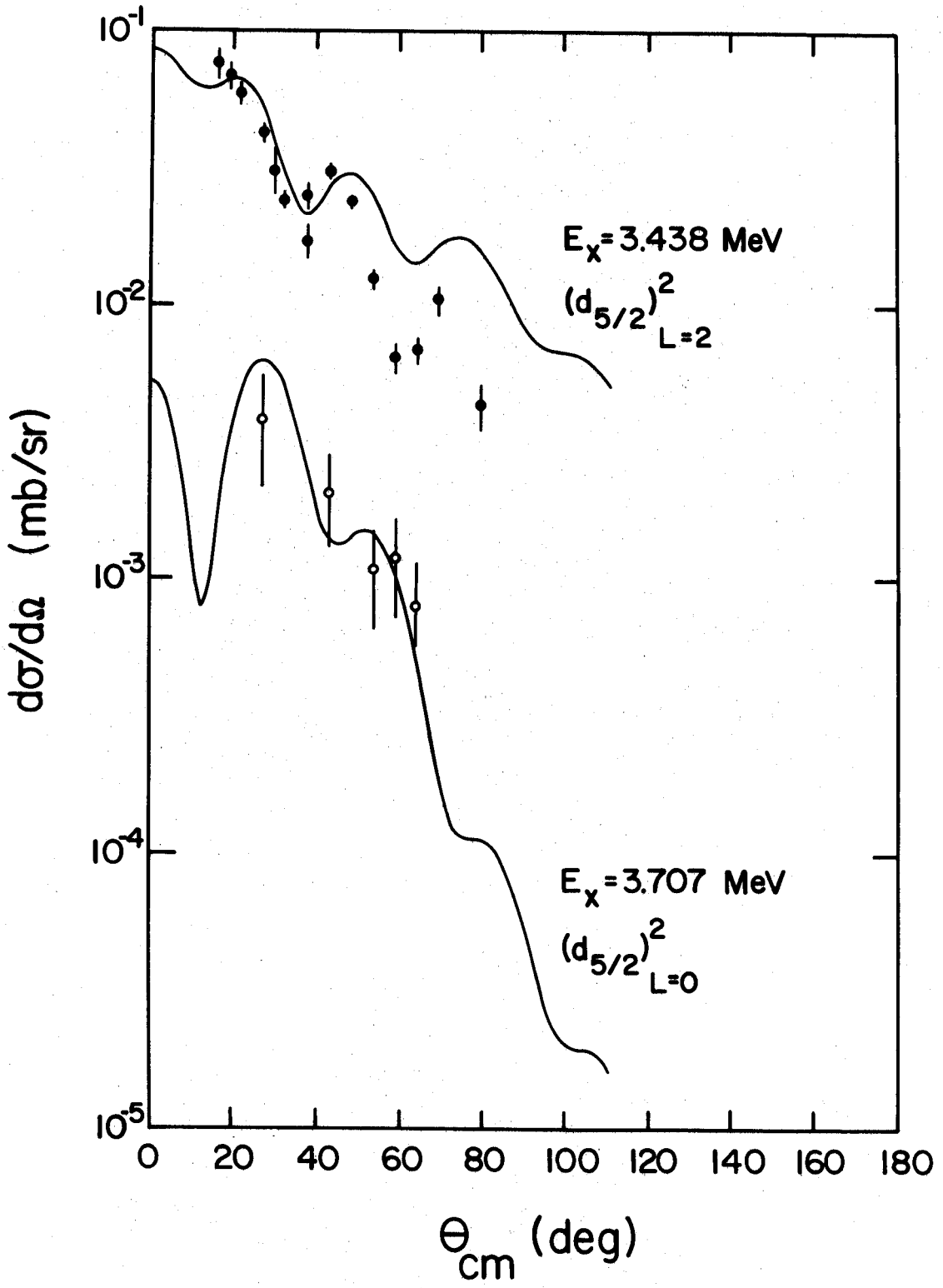

Figure 27.--Transitions to states in ^{30}S.

with the L=2 calculation shown in Figure 28 and comparison with the distribution to the first 2^+ state in ^{34}Ar (see Figure 21) both demonstrate this. A J^π value of 2^+ is therefore assigned to this state.

During many of the runs the level at 3.879 MeV and 4.050 MeV were not resolved. When it was possible to resolve them, it was obvious that the state at 3.879 MeV was more strongly excited by far. Figure 28 shows the angular distribution to the sum of these two states, along with an L=0 distorted wave calculation. The shape of the distribution is very well reproduced by this calculation and so an 0^+ assignment can be made for the state at 3.879 MeV in ^{34}Ar.

The states at 5.909 MeV and 6.074 MeV were also often not resolved, and the sum of the distributions to these two states is shown in Figure 28. When these two states were resolved, it was not possible to say that one was much more strongly excited than the other. The total angular distribution does exhibit some L=2 character, and therefore possibly one or both states are 2^+'s, but no definite assignment can be made.

7.11 Transitions to States in ^{38}Ca

A level in ^{38}Ca at 3.72 MeV has been reported by Hardy et al.(Ha66) using the (p,t) reaction. This level was assigned a J^π value of 3^-. Recently Shapiro

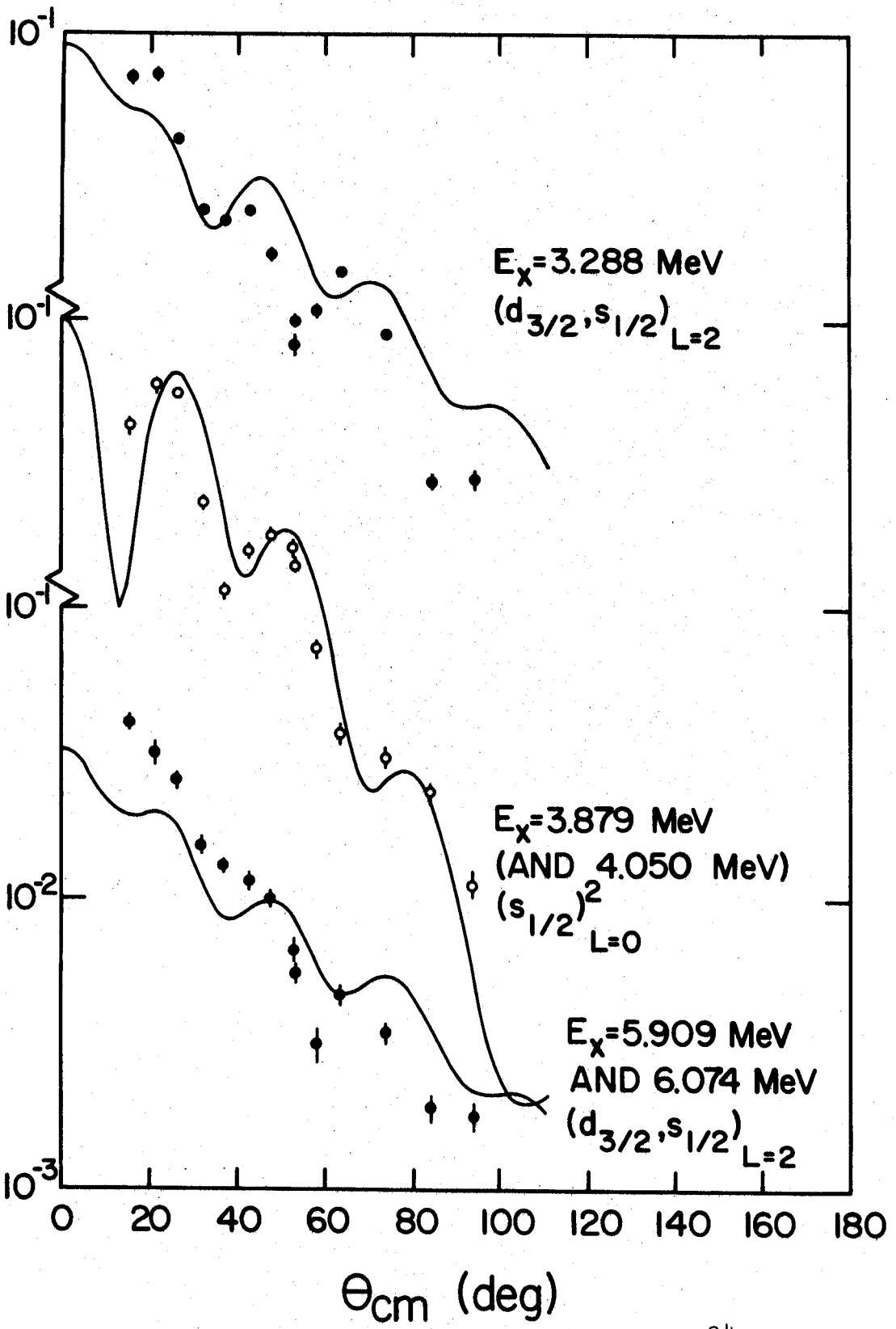

Figure 28.--Transitions to states in ^{34}Ar.

et al.[Sh69b] have reported a 2^+ level at 3.69 MeV in ^{38}Ca seen by the (^{3}He,n) reaction. In the present experiment, a level at 3.695 MeV was observed. The angular distribution to this state is shown in Figure 29. An L=3 distorted wave calculation is shown along with it, but an L=2 shape fits it nearly as well. If the two states previously reported are actually the same, the present experiment does not resolve the discrepancy. The 0^+ state at 3.06 MeV reported by Shapiro et al.[Sh69b] was not observed at all in the present experiment.

The angular distribution to the states at 4.381 MeV and 4.899 MeV both resemble an L=2 shape (see Figure 29) but the distributions are not complete enough to make a definite assignment.

The level at 6.280 MeV in ^{38}Ca was only weakly excited by the (p,t) reaction. The distribution to this state resembles an L=0 transition as shown in Figure 29. The transition is too weak, and the distribution is not complete enough to make any more than a tentative 0^+ assignment to this level.

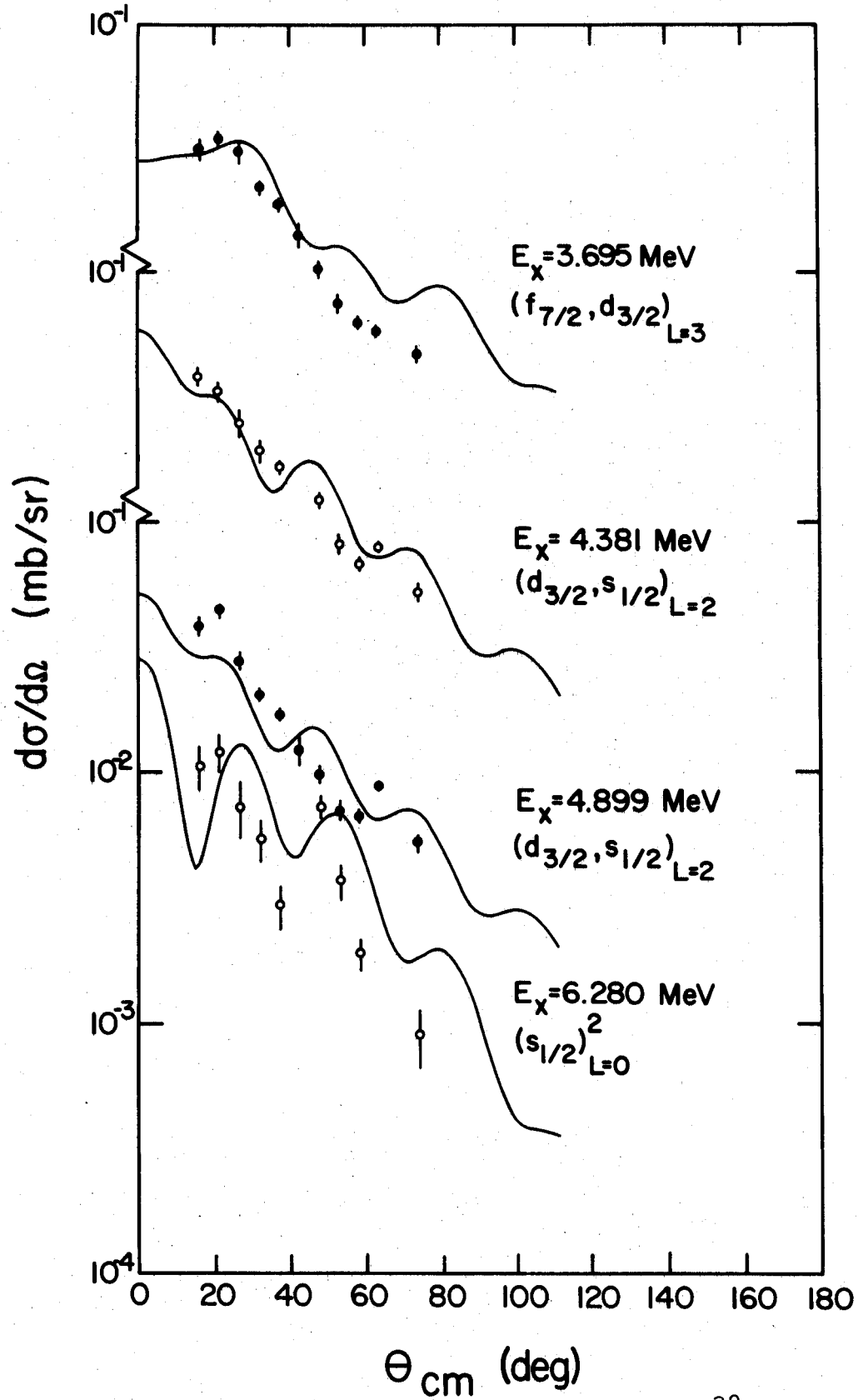

Figure 29.--Transitions to states in ^{38}Ca.

CHAPTER 8

SUMMARY AND CONCLUSIONS

In this work it has been found that the (p,t) reaction is useful as a method of studying the energy levels of nuclei. It is particularly useful in studying nuclei two nucleons away from stability. The energies of the tritons from the (p,t) reaction have been used to locate levels in the nuclei ^{18}Ne, ^{22}Mg, ^{26}Si, ^{30}S, ^{34}Ar, and ^{38}Ca and to assign values of excitation energy to them. The shapes of the angular distribution were found to be dominantly characterized by the angular momentum transfer, and this quality was used to make spin-parity assignments to some of the nuclear levels observed.

The two nucleon transfer theory of Glendenning[gl65] and the distorted wave method was also studied. It was found that the shapes of the experimental angular distributions were fairly well reproduced, and this was used as mentioned above to make angular momentum transfer and spin-parity assignments. The magnitudes of the predicted cross-sections were found to be influenced very greatly by the optical model parameters, the bound state parameters, and, most importantly, the presence of small admixtures in the shell model wave functions of the

initial and final nuclear states. It is concluded that these strong dependences make the prediction of magnitudes of cross-section for the (p,t) reaction extremely difficult. The detailed calculation of parentage factors from very accurate shell model wave functions would be needed along with well determined distorted wave and bound state parameters. Such detailed calculations and studies would involve such an extensive project that the present understanding of the two nucleon transfer process might not warrant it.

APPENDICES

APPENDIX A

$^{20}Ne(p,t)^{18}Ne$ EXPERIMENTAL DATA

Abs. Norm. Error	2.8%
Angle Error	0.15 deg.
Proton Energy	44.965 MeV
Ground State Q-Value	-20.0218 MeV ±0.0048 MeV

NE20(P,T)NE18

EX= 0.000 MEV

ANG(CM) (DEG)	SIGMA(CM) (MB/SR)	ERROR (%)
11.6	4.63 E-1	4.2
17.2	1.28 E-1	7.8
19.5	2.77 E-1	5.9
22.9	5.33 E-1	3.5
28.5	7.09 E-1	2.7
34.0	3.42 E-1	4.4
39.5	9.29 E-2	4.8
45.0	2.12 E-2	9.8
50.5	3.50 E-2	6.7
56.0	5.40 E-2	5.1
61.3	5.90 E-2	4.2
66.7	3.69 E-2	5.3
74.6	9.66 E-3	10.3
82.5	5.02 E-3	14.8
90.0	8.16 E-3	12.0
97.7	6.73 E-3	11.6
105.1	4.28 E-3	15.8
112.4	1.45 E-3	23.4

NE20(P,T)NE18

EX= 1.894 MEV
+/- 0.010 MEV

ANG(CM) (DEG)	SIGMA(CM) (MB/SR)	ERROR (%)
11.7	3.14 E-1	5.3
17.3	2.00 E-1	6.2
19.6	1.75 E-1	7.5
23.0	9.63 E-2	8.5
28.7	4.34 E-2	11.8
34.2	7.80 E-2	9.2
39.7	9.25 E-2	4.8
45.3	7.26 E-2	4.7
50.7	3.05 E-2	6.9
56.3	1.81 E-2	9.4
61.6	3.27 E-2	5.7
67.0	3.89 E-2	5.2
74.9	2.96 E-2	5.5
82.8	1.60 E-2	7.8
90.4	9.6 E-3	11.6
98.0	7.91 E-3	11.4
105.4	7.52 E-3	11.9
112.7	6.98 E-3	10.2

NE20(P,T)NE18

EX= 3.390 MEV
+/- 0.014 MEV

ANG(CM) (DEG)	SIGMA(CM) (MB/SR)	ERROR (%)
11.7	1.65 E-2	33.8
17.4	1.94 E-2	22.7
19.6	2.61 E-2	20.6
23.1	2.73 E-2	17.0
28.8	3.04 E-2	14.8
34.3	1.71 E-2	20.8
39.9	1.87 E-2	12.5
45.4	1.29 E-2	13.0
50.9	1.42 E-2	10.3
56.5	1.02 E-2	13.4
61.8	8.3 E-3	12.4
67.2	6.44 E-3	15.1
75.2	6.64 E-3	13.0
83.0	7.61 E-3	12.0
90.7	9.2 E-3	11.8
98.3	5.60 E-3	14.2
105.7	4.27 E-3	17.6
113.0	3.20 E-3	15.5

NE20(P,T)NE18

EX= 3.614 MEV
+/- 0.013 MEV

ANG(CM) (DEG)	SIGMA(CM) (MB/SR)	ERROR (%)
11.7	1.21 E-1	8.8
17.4	6.96 E-2	11.1
19.7	6.57 E-2	12.5
23.1	5.64 E-2	11.4
28.8	7.28 E-2	8.9
34.3	5.56 E-2	11.2
39.9	2.68 E-2	9.9
45.5	1.38 E-2	12.6
51.0	7.7 E-3	15.3
56.5	8.4 E-3	15.4
61.9	9.4 E-3	12.2
67.3	7.12 E-3	13.8
75.2	6.29 E-3	13.3
83.1	3.66 E-3	18.1
90.7	4.14 E-3	19.7
98.4	4.27 E-3	16.4
105.8	2.60 E-3	22.6
113.0	1.68 E-3	24.0

NE20(P,T)NE18

EX= 4.576 MEV
+/- 0.017 MEV

ANG(CM) (DEG)	SIGMA(CM) (MB/SR)	ERROR (%)
11.8	7.30 E-2	12.0
17.4	2.95 E-2	18.7
19.7	3.68 E-2	18.0
23.2	3.05 E-2	16.4
28.9	3.45 E-2	13.8
34.4	5.48 E-2	11.6
40.0	4.09 E-2	7.4
45.6	1.53 E-2	12.1
51.1	7.6 E-3	15.5
56.7	6.3 E-3	18.6
62.0	1.06 E-2	12.0
67.4	9.9 E-3	11.6
75.4	3.84 E-3	18.9
83.3	2.60 E-3	22.6
90.9	2.40 E-3	30.5
98.6	2.53 E-3	24.0
106.0	1.25 E-3	36.4
113.2	1.32 E-3	29.3

NE20(P,T)NE18

EX= 5.150 MEV
+/- 0.014 MEV

ANG(CM) (DEG)	SIGMA(CM) (MB/SR)	ERROR (%)
11.8	9.1 E-2	11.2
17.5	1.146E-1	8.4
19.8	1.02 E-1	10.0
23.2	1.112E-1	8.2
29.0	1.103E-1	7.3
34.5	6.82 E-2	10.3
40.1	5.39 E-2	6.4
45.7	4.01 E-2	6.8
51.2	4.61 E-2	5.5
56.8	3.23 E-2	6.9
62.2	1.95 E-2	8.2
67.5	1.10 E-2	10.9
75.5	1.09 E-2	9.8
83.4	9.1 E-3	11.5
91.0	6.6 E-3	15.3
98.7	3.01 E-3	20.8
106.1	1.47 E-3	34.4
113.3	2.18 E-3	23.7

NE20(P,T)NE18

EX= 6.326 MEV
+/- 0.018 MEV

ANG(CM) (DEG)	SIGMA(CM) (MB/SR)	ERROR (%)
17.6	2.36 E-2	21.6
19.9	2.82 E-2	21.6
23.3	2.34 E-2	21.3
29.1	2.08 E-2	18.1
34.6	1.36 E-2	31.7
40.3	1.05 E-2	18.5
45.9	6.2 E-3	22.2
51.4	1.21 E-2	12.6
57.0	1.12 E-2	13.7
62.4	6.2 E-3	17.6
75.8	4.82 E-3	17.7
83.7	4.87 E-3	17.4
91.3	4.90 E-3	19.9
99.0	2.79 E-3	25.2

NE20(P,T)NE18

EX= 7.957 MEV
+/- 0.025 MEV

ANG(CM) (DEG)	SIGMA(CM) (MB/SR)	ERROR (%)
40.5	9.6 E-3	23.6
46.2	1.00 E-2	17.8
51.8	4.9 E-3	26.5
57.3	7.3 E-3	21.7
68.2	6.5 E-3	18.6
76.2	6.3 E-3	17.0

NE20(P,T)NE18

EX= 9.215 MEV
+/- 0.020 MEV

ANG(CM) (DEG)	SIGMA(CM) (MB/SR)		ERROR (%)
12.0	6.59	E-2	14.5
17.8	5.88	E-2	14.4
20.1	5.14	E-2	17.6
23.6	3.30	E-2	19.2
29.5	3.16	E-2	18.0
35.1	2.51	E-2	22.8
40.8	1.94	E-2	17.0
46.4	1.55	E-2	16.5
52.0	1.76	E-2	12.0
57.7	1.25	E-2	16.7
63.1	9.2	E-3	16.7
68.6	5.8	E-3	21.3
76.6	5.4	E-3	19.5
84.6	6.2	E-3	18.3
92.2	4.0	E-3	25.8

APPENDIX B

$^{24}Mg(p,t)^{22}Mg$ EXPERIMENTAL DATA

Abs. Norm. Error	6.9%
Angle Error	0.15 deg.
Proton Energy	41.875 MeV
Ground State Q-Value	-21.1820 MeV ±0.0096 MeV

MG24(P,T)MG22

EX= 0.000 MEV

ANG(CM) (DEG)	SIGMA(CM) (MB/SR)	ERROR (%)
18.5	1.428E-1	2.8
24.0	4.044E-1	1.4
29.5	4.23 E-1	3.3
35.0	2.306E-1	1.5
40.5	7.68 E-2	2.7
45.9	3.16 E-2	3.9
51.3	6.41 E-2	2.5
56.8	6.97 E-2	2.4
62.0	6.06 E-2	2.5
67.3	3.048E-2	2.8
72.6	1.673E-2	3.8
82.9	9.00 E-3	4.1
93.1	1.065E-2	3.5
103.0	7.46 E-3	3.9

MG24(P,T)MG22

EX= 3.323 MEV
+/- 0.021 MEV

ANG(CM) (DEG)	SIGMA(CM) (MB/SR)	ERROR (%)
18.7	9.9 E-3	12.7
24.3	1.15 E-2	10.2
29.8	1.364E-2	6.8
35.4	1.580E-2	5.9
40.9	1.49 E-2	14.6
46.4	1.16 E-2	10.0
51.8	9.45 E-3	6.9
57.3	9.65 E-3	6.9
62.6	8.69 E-3	6.8
67.9	6.88 E-3	6.2
73.2	4.41 E-3	8.1
83.5	4.06 E-3	6.5
93.7	3.90 E-3	6.2
103.7	2.21 E-3	7.8

MG24(P,T)MG22

EX= 1.250 MEV
+/- 0.008 MEV

ANG(CM) (DEG)	SIGMA(CM) (MB/SR)	ERROR (%)
18.6	6.30 E-2	4.3
24.1	4.69 E-2	4.1
29.6	4.29 E-2	3.5
35.1	3.85 E-2	3.6
40.6	3.64 E-2	3.9
46.1	2.05 E-2	4.9
51.5	1.380E-2	5.5
57.0	1.235E-2	6.0
62.6	1.603E-2	4.9
67.5	1.626E-2	3.9
72.8	1.693E-2	3.8
83.1	8.49 E-3	4.2
93.3	4.65 E-3	5.5
103.3	5.79 E-3	4.5

MG24(P,T)MG22

EX= 4.417 MEV
+/- 0.027 MEV

ANG(CM) (DEG)	SIGMA(CM) (MB/SR)	ERROR (%)
18.8	3.44 E-2	6.0
24.4	2.00 E-2	7.3
29.9	1.59 E-2	17.2
35.5	1.192E-2	7.1
41.0	1.91 E-2	5.5
46.5	1.760E-2	5.3
52.0	1.571E-2	5.4
57.5	8.05 E-3	7.6
62.8	4.7 E-3	24.4
68.1	3.96 E-3	9.0
73.4	6.14 E-3	6.9
83.8	4.79 E-3	5.9
94.0	2.20 E-3	8.6
103.9	1.77 E-3	9.0

MG24(P,T)MG22

EX= 5.057 MEV
+/- 0.031 MEV

ANG(CM) (DEG)	SIGMA(CM) (MB/SR)	ERROR (%)
18.8	2.29 E-2	7.4
24.4	1.89 E-2	7.4
30.0	1.13 E-2	21.2
35.6	1.106E-2	7.4
41.1	1.451E-2	6.4
46.6	1.034E-2	7.2
52.1	6.73 E-3	9.0
57.6	5.40 E-3	9.6
62.9	4.28 E-3	10.9
68.3	4.53 E-3	8.2
73.5	5.16 E-3	13.0
84.0	2.82 E-3	7.9
94.2	1.65 E-3	10.3
104.1	1.83 E-3	9.1

MG24(P,T)MG22

EX= 5.738 MEV
+/- 0.035 MEV

ANG(CM) (DEG)	SIGMA(CM) (MB/SR)	ERROR (%)
18.9	2.57 E-2	10.0
24.5	1.46 E-2	9.2
30.1	7.96 E-3	11.0
35.7	4.45 E-3	13.2
41.2	3.70 E-3	15.1
46.8	3.40 E-3	15.7
52.2	1.73 E-3	25.0
57.8	3.53 E-3	14.0
63.1	4.13 E-3	11.7
68.4	5.19 E-3	7.9
73.7	5.12 E-3	8.0
84.1	2.28 E-3	9.4
94.3	1.60 E-3	10.8
104.3	1.93 E-3	8.8

MG24(P,T)MG22

EX= 5.313 MEV
+/- 0.032 MEV

ANG(CM) (DEG)	SIGMA(CM) (MB/SR)	ERROR (%)
18.8	1.79 E-2	8.7
24.4	1.12 E-2	10.1
30.0	1.57 E-2	18.2
35.6	1.351E-2	6.6
41.2	9.44 E-3	8.4
46.7	6.89 E-3	9.5
52.2	4.66 E-3	11.0
57.7	5.22 E-3	10.5
63.0	3.52 E-3	12.1
68.3	3.39 E-3	9.5
104.2	1.14 E-3	11.8

MG24(P,T)MG22

EX= 6.061 MEV
+/- 0.037 MEV

ANG(CM) (DEG)	SIGMA(CM) (MB/SR)	ERROR (%)
18.9	4.09 E-2	5.6
24.5	3.95 E-2	6.9
30.1	4.34 E-2	12.5
35.7	2.35 E-2	4.8
41.3	2.05 E-2	5.4
46.8	1.327E-2	6.5
52.3	1.807E-2	5.2
57.9	1.715E-2	5.2
63.2	1.471E-2	5.4
68.5	9.08 E-3	5.6
73.8	6.22 E-3	7.1
84.2	5.09 E-3	5.9
94.4	5.99 E-3	5.1
104.4	2.80 E-3	7.2

MG24(P,T)MG22

EX= 6.281 MEV
+/- 0.033 MEV

ANG(CM) (DEG)	SIGMA(CM) (MB/SR)	ERROR (%)
18.9	1.10 E-2	12.6
24.5	9.8 E-3	12.9
30.2	1.00 E-2	11.0
35.8	1.108E-2	7.5
41.3	9.09 E-3	10.0
46.9	7.64 E-3	9.9
52.4	6.55 E-3	9.8
57.9	7.91 E-3	8.8
63.2	7.12 E-3	8.7
68.6	6.12 E-3	7.4
73.9	6.31 E-3	7.3
84.3	4.19 E-3	7.0
94.5	3.60 E-3	7.2
104.5	3.11 E-3	6.8

MG24(P,T)MG22

EX= 6.836 MEV
+/- 0.044 MEV

ANG(CM) (DEG)	SIGMA(CM) (MB/SR)	ERROR (%)
30.3	5.08 E-3	18.0
35.9	3.49 E-3	15.2
41.4	6.09 E-3	12.0
47.0	3.52 E-3	17.4
52.5	5.43 E-3	13.0

MG24(P,T)MG22

EX= 6.645 MEV
+/- 0.044 MEV

ANG(CM) (DEG)	SIGMA(CM) (MB/SR)	ERROR (%)
30.2	2.52 E-3	25.5
41.4	2.68 E-3	19.5
46.9	3.41 E-3	20.0
52.5	2.39 E-3	18.6
94.6	1.54 E-3	11.8

MG24(P,T)MG22

EX= 7.257 MEV
+/- 0.044 MEV

ANG(CM) (DEG)	SIGMA(CM) (MB/SR)	ERROR (%)
19.0	1.97 E-2	8.6
24.7	2.35 E-2	6.7
30.3	2.95 E-2	10.0
35.9	2.59 E-2	4.7
41.5	1.69 E-2	6.5
47.1	7.94 E-3	11.0
52.6	8.39 E-3	8.4
58.2	8.39 E-3	10.0
63.5	9.15 E-3	10.0
68.9	5.52 E-3	8.2
74.2	5.24 E-3	8.5
84.6	4.21 E-3	6.9
94.8	3.91 E-3	6.9
104.8	3.52 E-3	6.5

MG24(P,T)MG22

EX= 7.961 MEV
+/- 0.049 MEV

ANG(CM) (DEG)	SIGMA(CM) (MB/SR)	ERROR (%)
19.1	1.09 E-2	13.1
24.8	7.9 E-3	13.2
30.4	6.12 E-3	15.0
36.1	9.36 E-3	8.6
41.7	7.50 E-3	10.9
47.3	5.09 E-3	13.8
52.8	6.55 E-3	10.2
58.4	3.30 E-3	16.3
63.7	2.58 E-3	18.0
69.1	2.06 E-3	16.0
74.4	3.07 E-3	16.0
84.9	1.85 E-3	12.5
95.1	1.58 E-3	13.0
105.0	1.99 E-3	10.2

APPENDIX C

$^{28}Si(p,t)^{26}Si$ EXPERIMENTAL DATA

Abs. Norm. Error	11 %
Angle Error	0.15 deg.
Proton Energy	42.06 MeV
Ground State Q-Value	-22.010 MeV ±0.011 MeV

SI28(P,T)SI26

EX= 0.000 MEV

ANG(CM) (DEG)	SIGMA(CM) (MB/SR)	ERROR (%)
14.0	1.16 E-2	22.3
18.3	1.267E-1	4.7
22.0	3.54 E-1	3.5
27.3	4.883E-1	1.9
32.8	2.385E-1	1.9
38.1	8.74 E-2	2.6
43.6	3.83 E-2	4.0
48.8	6.02 E-2	13.0
54.2	8.38 E-2	2.9
59.5	6.32 E-2	3.3
64.9	2.62 E-2	12.0
70.0	1.71 E-2	7.4
75.3	1.211E-2	4.4
85.5	1.315E-2	3.5
95.6	9.94 E-3	4.3

SI28(P,T)SI26

EX= 2.790 MEV
+/- 0.012 MEV

ANG(CM) (DEG)	SIGMA(CM) (MB/SR)	ERROR (%)
14.1	6.67 E-2	8.5
18.4	5.13 E-2	9.7
22.1	6.04 E-2	9.0
27.5	4.51 E-2	6.0
33.1	2.29 E-2	6.6
38.4	2.18 E-2	5.7
54.6	1.53 E-2	7.1
59.9	1.196E-2	8.2
65.3	1.166E-2	3.6
70.4	1.58 E-2	7.8
75.7	1.330E-2	4.3
86.0	6.52 E-3	5.2
96.1	7.22 E-3	5.1

SI28(P,T)SI26

EX= 1.795 MEV
+/- 0.011 MEV

ANG(CM) (DEG)	SIGMA(CM) (MB/SR)	ERROR (%)
14.1	1.205E-1	6.1
27.4	7.39 E-2	4.5
32.9	4.49 E-2	4.4
38.3	4.00 E-2	4.0
43.8	4.02 E-2	4.0
49.0	3.29 E-2	5.4
54.5	2.21 E-2	5.6
59.7	1.054E-2	8.9
65.1	8.63 E-3	4.2
70.3	1.51 E-2	8.0
75.6	1.482E-2	4.1
85.8	7.31 E-3	4.8
95.9	3.64 E-3	7.3

SI28(P,T)SI26

EX= 3.339 MEV
+/- 0.019 MEV

ANG(CM) (DEG)	SIGMA(CM) (MB/SR)	ERROR (%)
27.5	9.9 E-3	14.8
33.1	5.80 E-3	15.3
44.0	9.4 E-4	50.2
65.4	1.53 E-3	12.3
75.8	7.2 E-4	25.4
86.1	4.3 E-4	27.9
96.2	5.8 E-4	21.6

SI28(P,T)SI26

EX= 4.183 MEV
+/- 0.011 MEV

ANG(CM) (DEG)	SIGMA(CM) (MB/SR)	ERROR (%)
14.2	7.7 E-3	33.8
22.2	5.8 E-3	40.9
33.2	3.51 E-3	22.5
44.1	5.00 E-3	13.5
49.4	4.62 E-3	20.1
54.8	5.61 E-3	12.4
60.1	4.83 E-3	14.7
65.5	3.05 E-3	8.2
76.0	2.77 E-3	10.6
86.3	2.61 E-3	8.9
96.4	2.57 E-3	9.2

SI28(P,T)SI26

EX= 4.821 MEV
+/- 0.013 MEV

ANG(CM) (DEG)	SIGMA(CM) (MB/SR)	ERROR (%)
22.2	1.52 E-2	20.7
33.3	9.7 E-3	11.4
44.2	7.86 E-3	10.5
49.5	6.66 E-3	14.7
54.9	5.29 E-3	12.9
60.2	2.47 E-3	27.7
65.7	2.70 E-3	9.1
86.4	2.08 E-3	10.3
96.5	1.76 E-3	11.4

SI28(P,T)SI26

EX= 4.457 MEV
+/- 0.013 MEV

ANG(CM) (DEG)	SIGMA(CM) (MB/SR)	ERROR (%)
14.2	1.96 E-2	17.6
22.2	1.43 E-2	22.2
27.6	1.95 E-2	10.4
33.3	1.92 E-2	7.4
38.6	1.20 E-2	8.9
44.2	1.155E-2	8.1
49.4	6.6 E-3	15.3
54.8	7.42 E-3	10.5
60.2	6.24 E-3	13.0
65.6	5.22 E-3	5.8
76.1	5.24 E-3	7.3
86.3	2.82 E-3	8.4
96.4	2.57 E-3	9.1

SI28(P,T)SI26

EX= 5.229 MEV
+/- 0.012 MEV

ANG(CM) (DEG)	SIGMA(CM) (MB/SR)	ERROR (%)
14.2	2.03 E-3	19.6
44.3	1.065E-2	9.0
55.0	5.51 E-3	13.6
65.7	2.64 E-3	9.7
76.2	2.65 E-3	12.6
96.6	2.48 E-3	9.7

SI28(P,T)SI26

EX= 5.562 MEV
+/- 0.028 MEV

ANG(CM) (DEG)	SIGMA(CM) (MB/SR)	ERROR (%)
44.3	8.16 E-3	10.5
55.0	4.26 E-3	15.9
65.8	1.64 E-3	14.1
76.3	1.62 E-3	17.5
96.7	1.94 E-3	11.1

SI28(P,T)SI26

EX= 6.381 MEV
+/- 0.020 MEV

ANG(CM) (DEG)	SIGMA(CM) (MB/SR)	ERROR (%)
33.5	6.4 E-3	16.1
44.5	6.60 E-3	11.8
66.0	3.01 E-3	9.6
76.5	3.07 E-3	10.1
86.8	2.04 E-3	11.6
96.9	1.43 E-3	13.8

SI28(P,T)SI26

EX= 5.960 MEV
+/- 0.022 MEV

ANG(CM) (DEG)	SIGMA(CM) (MB/SR)	ERROR (%)
33.4	2.87 E-3	33.9
55.1	5.12 E-3	13.9
65.9	1.97 E-3	13.1
76.4	1.96 E-3	14.1
86.7	1.16 E-3	15.5

SI28(P,T)SI26

EX= 6.786 MEV
+/- 0.029 MEV

ANG(CM) (DEG)	SIGMA(CM) (MB/SR)	ERROR (%)
22.4	5.2 E-3	51.3
55.3	3.26 E-3	18.9
66.1	1.94 E-3	13.6
76.6	4.19 E-3	8.7
86.9	3.09 E-3	9.7
97.0	1.79 E-3	13.5

SI28(P,T)SI26

EX= 7.150 MEV
+/- 0.015 MEV

ANG(CM) (DEG)	SIGMA(CM) (MB/SR)	ERROR (%)
33.6	2.53 E-3	34.8
44.6	1.26 E-3	39.1
76.7	1.15 E-3	23.7
87.1	1.58 E-3	16.4

SI28(P,T)SI26

EX= 7.695 MEV
+/- 0.031 MEV

ANG(CM) (DEG)	SIGMA(CM) (MB/SR)	ERROR (%)
14.4	1.91 E-2	20.8
22.5	1.54 E-2	24.8
33.7	1.33 E-2	10.7
97.3	1.88 E-3	15.3

SI28(P,T)SI26

EX= 7.476 MEV
+/- 0.020 MEV

ANG(CM) (DEG)	SIGMA(CM) (MB/SR)	ERROR (%)
14.4	8.7 E-3	34.3
22.5	8.1 E-3	35.4
33.6	8.6 E-3	15.3
44.7	1.24 E-2	8.5
55.5	6.38 E-3	14.5
66.3	3.65 E-3	9.5
76.8	4.25 E-3	10.0
97.3	3.83 E-3	9.1

SI28(P,T)SI26

EX= 7.902 MEV
+/- 0.021 MEV

ANG(CM) (DEG)	SIGMA(CM) (MB/SR)	ERROR (%)
14.4	2.81 E-2	15.7
22.6	1.80 E-2	21.0
33.7	1.11 E-2	12.7
87.3	1.57 E-3	19.1
97.4	1.81 E-3	15.3

SI28(P,T)SI26

EX= 7.476 MEV AND
EX= 7.695 MEV AND
EX= 7.902 MEV

ANG(CM) (DEG)	SIGMA(CM) (MB/SR)	ERROR (%)
14.4	5.59 E-2	12.1
22.5	4.32 E-2	14.6
33.7	3.31 E-2	7.1
44.7	3.23 E-2	5.2
55.5	2.06 E-2	8.1
66.4	9.28 E-3	6.2
76.9	1.118E-2	6.1
87.2	7.60 E-3	7.2
97.3	7.55 E-3	6.9

APPENDIX D

$^{32}S(p,t)^{30}S$ EXPERIMENTAL DATA

Abs. Norm. Error	2.3%
Angle Error	0.15 deg.
Proton Energy	39.915 MeV
Ground State Q-Value	-19.593 MeV ±0.012 MeV

S32(P,T)S30

EX= 0.000 MEV

ANG(CM) (DEG)	SIGMA(CM) (MB/SR)	ERROR (%)
16.1	9.3 E-2	11.1
18.8	3.21 E-1	4.9
21.5	5.89 E-1	2.8
26.8	7.32 E-1	1.8
27.0	6.51 E-1	1.8
29.5	5.36 E-1	4.5
32.2	3.740E-1	2.0
37.5	7.67 E-2	6.4
42.8	5.00 E-2	5.3
48.2	1.031E-1	2.7
53.6	1.121E-1	2.5
58.7	7.39 E-2	3.4
63.9	2.70 E-2	5.7
69.2	1.04 E-2	11.3
79.4	1.56 E-2	9.2

S32(P,T)S30

EX= 3.438 MEV
+/- 0.014 MEV

ANG(CM) (DEG)	SIGMA(CM) (MB/SR)	ERROR (%)
16.3	7.72 E-2	12.8
19.0	6.95 E-2	11.5
21.6	5.98 E-2	9.8
27.1	4.27 E-2	7.7
29.7	3.11 E-2	19.6
32.4	2.43 E-2	7.3
37.7	1.72 E-2	15.6
37.8	2.51 E-2	11.7
43.1	3.09 E-2	7.0
48.6	2.41 E-2	5.9
53.9	1.24 E-2	8.2
59.1	6.42 E-3	13.1
64.3	6.79 E-3	12.2
69.6	1.04 E-2	11.8
79.8	4.30 E-3	19.1

S32(P,T)S30

EX= 2.239 MEV
+/- 0.018 MEV

ANG(CM) (DEG)	SIGMA(CM) (MB/SR)	ERROR (%)
16.2	1.41 E-1	9.0
18.9	1.087E-1	8.8
21.6	8.48 E-2	8.1
27.0	5.99 E-2	6.7
29.6	4.92 E-2	15.5
32.3	4.55 E-2	7.7
37.7	3.74 E-2	9.7
43.0	3.78 E-2	6.2
48.4	2.61 E-2	5.7
53.8	1.060E-2	9.3
58.9	8.53 E-3	11.5
64.2	8.36 E-3	10.8
69.4	1.17 E-2	10.6
79.6	5.24 E-3	16.8

S32(P,T)S30

EX= 3.707 MEV
+/- 0.025 MEV

ANG(CM) (DEG)	SIGMA(CM) (MB/SR)	ERROR (%)
27.0	3.8 E-3	44.0
43.1	2.06 E-3	37.2
53.9	1.08 E-3	39.2
59.1	1.19 E-3	40.2
64.3	7.9 E-4	44.6

S32(P,T)S30

EX= 5.207 MEV
+/- 0.022 MEV

ANG(CM) (DEG)	SIGMA(CM) (MB/SR)	ERROR (%)
54.2	8.14 E-3	10.7
64.6	7.89 E-3	11.3

S32(P,T)S30

EX= 5.207 MEV AND
EX= 5.306 MEV

ANG(CM) (DEG)	SIGMA(CM) (MB/SR)	ERROR (%)
19.1	2.71 E-2	25.0
21.8	3.40 E-2	14.9
27.1	3.52 E-2	10.1
27.3	4.32 E-2	8.4
32.6	3.02 E-2	7.7
43.3	2.51 E-2	8.1
48.8	1.84 E-2	6.9
54.2	1.43 E-2	7.9
59.3	1.32 E-2	8.9
64.6	1.30 E-2	8.6
69.9	1.31 E-2	10.7
80.1	7.2 E-3	14.8

S32(P,T)S30

EX= 5.306 MEV
+/- 0.025 MEV

ANG(CM) (DEG)	SIGMA(CM) (MB/SR)	ERROR (%)
54.2	6.14 E-3	12.7
64.6	5.14 E-3	14.2

S32(P,T)S30

EX= 5.426 MEV
+/- 0.025 MEV

ANG(CM) (DEG)	SIGMA(CM) (MB/SR)	ERROR (%)
16.4	3.59 E-2	21.1
19.1	2.87 E-2	21.3
21.8	2.56 E-2	15.9
27.2	3.04 E-2	10.7
27.3	1.68 E-2	13.6
32.6	1.06 E-2	11.6
43.3	9.0 E-3	15.6
48.8	7.62 E-3	11.8
54.2	8.06 E-3	10.9
59.4	9.6 E-3	10.8
64.7	7.08 E-3	12.3
69.9	5.51 E-3	16.9
80.2	4.42 E-3	19.2

S32(P,T)S30

EX= 5.207 MEV AND
EX= 5.306 MEV AND
EX= 5.426 MEV

ANG(CM) (DEG)	SIGMA(CM) (MB/SR)	ERROR (%)
37.9	2.95 E-2	14.2
38.0	3.79 E-2	10.1

S32(P,T)S30

EX= 6.108 MEV
+/- 0.029 MEV

ANG(CM) (DEG)	SIGMA(CM) (MB/SR)	ERROR (%)
32.7	3.16 E-3	27.7

S32(P,T)S30

EX= 5.897 MEV
+/- 0.027 MEV

ANG(CM) (DEG)	SIGMA(CM) (MB/SR)	ERROR (%)
27.2	4.8 E-3	43.3
27.4	6.1 E-3	30.3
32.7	6.3 E-3	18.3

S32(P,T)S30

EX= 6.223 MEV
+/- 0.030 MEV

ANG(CM) (DEG)	SIGMA(CM) (MB/SR)	ERROR (%)
32.7	3.35 E-3	28.7

S32(P,T)S30

EX= 6.415 MEV
+/- 0.040 MEV

ANG(CM) (DEG)	SIGMA(CM) (MB/SR)	ERROR (%)
21.8	6.4 E-3	46.1
27.3	1.21 E-2	19.9
32.7	7.5 E-3	15.8
49.0	3.91 E-3	19.7
54.4	5.51 E-3	14.4
59.5	6.62 E-3	13.9
64.8	3.53 E-3	19.5

S32(P,T)S30

EX= 7.185 MEV
+/- 0.035 MEV

ANG(CM) (DEG)	SIGMA(CM) (MB/SR)	ERROR (%)
16.5	1.62 E-2	36.6
21.9	6.6 E-3	39.5
27.3	1.09 E-2	19.0
32.8	8.9 E-3	14.9
38.1	7.1 E-3	29.9
43.6	7.3 E-3	18.3
49.1	5.53 E-3	15.8
54.5	4.50 E-3	17.8
59.7	3.65 E-3	19.8
65.0	3.45 E-3	21.0

S32(P,T)S30

EX= 6.861 MEV
+/- 0.040 MEV

ANG(CM) (DEG)	SIGMA(CM) (MB/SR)	ERROR (%)
16.4	2.86 E-2	22.5
19.2	1.95 E-2	25.5
21.9	1.96 E-2	20.9
27.4	3.11 E-2	9.7
32.8	2.76 E-2	6.9
38.1	1.84 E-2	15.8
43.5	1.30 E-2	12.2
49.0	1.06 E-2	10.7
54.4	8.17 E-3	11.4
59.6	7.09 E-3	12.7
64.9	6.28 E-3	13.5
80.5	5.7 E-3	18.7

S32(P,T)S30

EX= 7.570 MEV
+/- 0.045 MEV

ANG(CM) (DEG)	SIGMA(CM) (MB/SR)	ERROR (%)
27.4	9.7 E-3	22.1
27.5	1.30 E-2	17.4

APPENDIX E

$^{36}Ar(p,t)^{34}Ar$ EXPERIMENTAL DATA

Abs. Norm. Error	4.8%
Angle Error	0.15 deg.
Proton Energy	39.9 MeV
Ground State Q-Value	-19.523 MeV ±0.011 MeV

AR36(P,T)AR34

EX= 0.000 MEV

ANG(CM) (DEG)	SIGMA(CM) (MB/SR)	ERROR (%)
15.6	1.134E-1	3.8
21.4	4.880E-1	1.8
26.2	4.840E-1	1.3
32.0	1.905E-1	1.7
36.9	4.03 E-2	2.8
42.6	6.04 E-2	2.7
47.4	1.065E-1	1.8
52.6	9.25 E-2	2.5
53.1	8.68 E-2	1.4
57.9	4.87 E-2	2.4
63.5	1.615E-2	3.2
73.8	1.143E-2	3.0
84.0	1.528E-2	2.5
93.7	4.72 E-3	5.1

AR36(P,T)AR34

EX= 3.288 MEV
+/- 0.014 MEV

ANG(CM) (DEG)	SIGMA(CM) (MB/SR)	ERROR (%)
15.7	7.01 E-2	5.0
21.5	7.18 E-2	5.6
26.4	4.26 E-2	4.7
32.2	2.42 E-2	5.3
37.1	2.230E-2	3.9
42.9	2.42 E-2	4.4
47.7	1.704E-2	4.7
52.9	8.24 E-3	8.9
53.4	9.97 E-3	5.1
58.2	1.078E-2	5.5
63.9	1.460E-2	3.5
74.2	8.88 E-3	3.7
84.4	2.76 E-3	6.5
94.1	2.80 E-3	7.2

AR36(P,T)AR34

EX= 2.094 MEV
+/- 0.011 MEV

ANG(CM) (DEG)	SIGMA(CM) (MB/SR)	ERROR (%)
15.6	7.42 E-2	4.8
21.5	5.84 E-2	7.7
26.4	3.90 E-2	4.9
32.2	2.67 E-2	4.9
37.0	2.200E-2	3.9
42.8	2.70 E-2	4.2
47.6	1.660E-2	4.7
52.8	7.29 E-3	9.6
53.3	8.77 E-3	5.4
58.1	3.55 E-3	10.0
63.8	6.19 E-3	5.6
74.1	4.86 E-3	4.9
84.3	1.35 E-3	10.2
94.0	2.81 E-3	7.1

AR36(P,T)AR34

EX= 3.879 MEV
+/- 0.015 MEV

ANG(CM) (DEG)	SIGMA(CM) (MB/SR)	ERROR (%)
25.0	6.06 E-2	12.8
27.7	5.21 E-2	3.8
37.2	6.20 E-3	8.4
49.1	1.42 E-2	9.8
58.3	5.99 E-3	7.7

AR36(P,T)AR34

EX= 4.050 MEV
+/- 0.014 MEV

ANG(CM) (DEG)	SIGMA(CM) (MB/SR)	ERRBR (%)
25.0	7.4 E-3	49.8
27.7	1.50 E-2	7.5
37.2	5.28 E-3	9.7
49.1	9.2 E-3	13.1
58.3	1.25 E-3	21.1

AR36(P,T)AR34

EX= 4.522 MEV
+/- 0.014 MEV

ANG(CM) (DEG)	SIGMA(CM) (MB/SR)	ERRBR (%)
15.7	2.29 E-2	9.6
26.5	2.00 E-2	7.4
27.8	2.17 E-2	6.3
47.8	8.79 E-3	7.2
49.2	7.9 E-3	13.6

AR36(P,T)AR34

EX= 3.879 MEV AND
EX= 4.050 MEV

ANG(CM) (DEG)	SIGMA(CM) (MB/SR)	ERRBR (%)
15.7	4.29 E-2	7.4
21.6	5.93 E-2	6.5
26.5	5.51 E-2	4.1
32.3	2.32 E-2	5.4
37.2	1.150E-2	6.1
42.9	1.578E-2	6.1
47.8	1.832E-2	4.6
53.0	1.62 E-2	6.3
53.4	1.397E-2	4.1
58.3	7.23 E-3	7.1
64.0	3.70 E-3	8.4
74.3	3.10 E-3	7.6
84.5	2.32 E-3	7.9
94.2	1.11 E-3	12.6

AR36(P,T)AR34

EX= 4.651 MEV
+/- 0.014 MEV

ANG(CM) (DEG)	SIGMA(CM) (MB/SR)	ERRBR (%)
15.7	1.68 E-2	12.9
26.5	1.85 E-2	8.2
27.8	1.76 E-2	7.3
47.9	7.70 E-3	7.7
49.2	8.0 E-3	13.8

AR36(P,T)AR34

EX= 4.522 MEV AND
EX= 4.651 MEV

ANG(CM) (DEG)	SIGMA(CM) (MB/SR)	ERROR (%)
15.7	3.97 E-2	7.3
21.6	4.01 E-2	8.2
26.5	3.85 E-2	5.1
32.3	2.99 E-2	4.6
37.2	2.627E-2	3.6
43.0	2.06 E-2	5.0
47.8	1.648E-2	4.9
53.1	1.207E-2	7.3
53.5	1.194E-2	4.5
58.4	1.000E-2	5.8
64.0	1.037E-2	4.4
74.4	6.31 E-3	4.6
84.6	4.78 E-3	5.0
94.3	4.04 E-3	6.0

AR36(P,T)AR34

EX= 4.985 MEV
+/- 0.014 MEV

ANG(CM) (DEG)	SIGMA(CM) (MB/SR)	ERROR (%)
27.8	1.78 E-2	6.9
49.2	7.3 E-3	14.7
53.1	5.80 E-3	10.8
58.4	3.49 E-3	10.9

AR36(P,T)AR34

EX= 4.867 MEV
+/- 0.014 MEV

ANG(CM) (DEG)	SIGMA(CM) (MB/SR)	ERROR (%)
27.8	9.4 E-3	10.6
49.2	3.03 E-3	25.3
58.4	1.16 E-3	21.1

AR36(P,T)AR34

EX= 4.867 MEV AND
EX= 4.985 MEV

ANG(CM) (DEG)	SIGMA(CM) (MB/SR)	ERROR (%)
21.6	1.88 E-2	13.6
26.5	2.09 E-2	7.1
32.4	1.68 E-2	6.4
37.2	1.098E-2	5.9
43.0	8.30 E-3	8.7
47.9	7.96 E-3	7.4
53.1	5.80 E-3	10.8
53.6	6.11 E-3	6.8
58.4	4.66 E-3	9.1
84.7	1.17 E-3	11.9
94.4	7.0 E-4	16.3

AR36(P,T)AR34

EX= 5.307 MEV
+/- 0.013 MEV

ANG(CM) (DEG)	SIGMA(CM) (MB/SR)	ERROR (%)
21.6	6.9 E-3	26.1
26.6	1.18 E-2	10.7
32.4	1.052E-2	8.9
37.3	8.94 E-3	7.0
43.1	7.37 E-3	9.6
47.9	6.11 E-3	8.6
53.2	5.53 E-3	11.5
53.6	4.95 E-3	8.1
58.5	4.54 E-3	9.8
64.2	4.49 E-3	7.4
74.5	2.11 E-3	10.2
84.7	2.18 E-3	8.3
94.4	1.30 E-3	11.6

AR36(P,T)AR34

EX= 6.074 MEV
+/- 0.011 MEV

ANG(CM) (DEG)	SIGMA(CM) (MB/SR)	ERROR (%)
27.9	2.09 E-2	6.6
43.2	6.75 E-3	10.2
49.4	6.4 E-3	16.1
53.3	4.07 E-3	14.1
58.6	2.19 E-3	15.4
94.6	1.05 E-3	13.9

AR36(P,T)AR34

EX= 5.909 MEV
+/- 0.012 MEV

ANG(CM) (DEG)	SIGMA(CM) (MB/SR)	ERROR (%)
27.9	5.90 E-3	15.7
43.1	4.88 E-3	12.3
49.3	1.55 E-3	44.1
53.2	2.60 E-3	18.1
58.6	1.01 E-3	27.0
94.5	7.6 E-4	17.6

AR36(P,T)AR34

EX= 5.909 MEV AND
EX= 6.074 MEV

ANG(CM) (DEG)	SIGMA(CM) (MB/SR)	ERROR (%)
15.8	4.06 E-2	7.4
21.7	3.19 E-2	10.0
26.6	2.58 E-2	6.7
32.4	1.54 E-2	7.4
37.4	1.298E-2	5.8
43.2	1.160E-2	7.6
48.0	1.010E-2	6.9
53.3	6.69 E-3	10.6
53.7	5.59 E-3	8.4
58.6	3.19 E-3	13.2
64.2	4.69 E-3	8.1
74.6	3.47 E-3	8.1
84.8	1.93 E-3	10.7
94.6	1.80 E-3	10.7

AR36(P,T)AR34

EX= 6.525 MEV
+/- 0.009 MEV

ANG(CM) (DEG)	SIGMA(CM) (MB/SR)	ERROR (%)
26.6	4.7 E-3	22.6
32.5	4.12 E-3	20.0
37.4	2.35 E-3	17.2
48.1	2.63 E-3	16.3
53.3	2.17 E-3	21.3
58.7	1.25 E-3	25.5

AR36(P,T)AR34

EX= 7.322 MEV
+/- 0.006 MEV

ANG(CM) (DEG)	SIGMA(CM) (MB/SR)	ERROR (%)
15.8	2.76 E-2	9.6
21.8	1.82 E-2	13.8
26.7	2.43 E-2	7.0
37.5	1.286E-2	6.0
43.3	1.113E-2	8.0
49.5	7.4 E-3	14.7

AR36(P,T)AR34

EX= 6.794 MEV
+/- 0.011 MEV

ANG(CM) (DEG)	SIGMA(CM) (MB/SR)	ERROR (%)
15.8	1.39 E-2	16.9
21.7	7.3 E-3	28.0
26.7	1.01 E-2	12.8
32.5	5.74 E-3	15.6
37.4	6.41 E-3	10.0
43.2	6.13 E-3	12.4
48.1	4.26 E-3	12.6
53.4	4.56 E-3	15.0
53.8	3.62 E-3	13.1
58.7	2.97 E-3	14.8
64.4	4.80 E-3	8.6
74.8	2.13 E-3	11.7
85.0	1.34 E-3	14.5
94.7	1.82 E-3	11.0

AR36(P,T)AR34

EX= 7.499 MEV
+/- 0.004 MEV

ANG(CM) (DEG)	SIGMA(CM) (MB/SR)	ERROR (%)
15.9	8.6 E-3	23.6
21.8	1.57 E-2	15.3
26.7	1.67 E-2	8.8
37.5	1.248E-2	6.2
43.3	8.15 E-3	10.1
49.6	9.7 E-3	12.5

AR36(P,T)AR34

EX= 7.322 MEV AND
EX= 7.499 MEV

ANG(CM) (DEG)	SIGMA(CM) (MB/SR)	ERROR (%)
15.9	3.62 E-2	8.8
21.8	3.38 E-2	10.0
26.7	4.10 E-2	5.3
32.6	2.60 E-2	5.9
37.5	2.53 E-2	4.2
43.3	1.92 E-2	6.2
48.2	1.530E-2	5.8
53.5	1.21 E-2	8.7
53.9	1.013E-2	6.7
58.8	8.91 E-3	7.4
64.5	8.52 E-3	5.6
74.9	5.71 E-3	6.2
85.1	4.86 E-3	6.1
94.8	3.91 E-3	7.4

AR36(P,T)AR34

EX= 7.925 MEV
+/- 0.005 MEV

ANG(CM) (DEG)	SIGMA(CM) (MB/SR)	ERROR (%)
15.9	1.94 E-2	12.9
21.8	2.06 E-2	14.2
26.8	2.12 E-2	7.9
32.6	1.47 E-2	9.1
37.6	1.553E-2	5.6
43.4	9.00 E-3	10.4
48.3	9.56 E-3	7.9
53.6	5.57 E-3	15.1
54.0	3.94 E-3	13.1
58.9	4.72 E-3	10.8
64.6	5.01 E-3	8.2
75.0	3.87 E-3	8.9
85.2	3.14 E-3	9.0
95.0	2.34 E-3	11.5

APPENDIX F

$^{40}Ca(p,t)^{38}Ca$ EXPERIMENTAL DATA

Abs. Norm. Error	7.3%
Angle Error	0.15 deg.
Proton Energy	40.14 MeV
Ground State Q-Value	-20.428 MeV ±0.010 MeV

CA40(P,T)CA38

EX= 0.000 MEV

ANG(CM) (DEG)	SIGMA(CM) (MB/SR)	ERROR (%)
16.0	1.524E-1	3.8
21.3	3.383E-1	2.5
26.6	3.017E-1	2.5
32.1	9.81 E-2	4.0
37.1	3.09 E-2	4.3
42.4	7.59 E-2	4.6
47.6	1.029E-1	2.0
52.9	7.37 E-2	2.7
58.1	3.002E-2	2.6
63.3	8.94 E-3	4.2
73.5	1.449E-2	4.3

CA40(P,T)CA38

EX= 3.695 MEV
+/- 0.005 MEV

ANG(CM) (DEG)	SIGMA(CM) (MB/SR)	ERROR (%)
16.1	3.15 E-2	9.6
21.5	3.45 E-2	7.8
26.8	3.05 E-2	10.0
32.3	2.21 E-2	7.0
37.4	1.89 E-2	5.7
42.7	1.42 E-2	11.2
47.9	1.036E-2	8.1
53.2	7.52 E-3	9.0
58.5	6.32 E-3	6.2
63.6	5.82 E-3	5.6
73.9	4.68 E-3	8.2

CA40(P,T)CA38

EX= 2.206 MEV
+/- 0.005 MEV

ANG(CM) (DEG)	SIGMA(CM) (MB/SR)	ERROR (%)
16.1	8.87 E-2	5.2
21.4	7.67 E-2	5.1
26.7	6.02 E-2	5.0
32.2	3.40 E-2	5.0
37.3	3.38 E-2	4.1
42.6	3.40 E-2	6.9
47.8	2.77 E-2	5.0
53.1	1.512E-2	6.0
58.3	1.317E-2	4.1
63.5	1.655E-2	3.1
73.7	8.87 E-3	5.7

CA40(P,T)CA38

EX= 4.191 MEV
+/- 0.005 MEV

ANG(CM) (DEG)	SIGMA(CM) (MB/SR)	ERROR (%)
21.5	4.0 E-3	35.8
32.4	2.18 E-3	35.0
53.3	1.23 E-3	26.4
58.5	5.9 E-4	28.2
63.7	7.7 E-4	22.4

CA40(P,T)CA38

EX= 4.381 MEV
+/- 0.005 MEV

ANG(CM) (DEG)	SIGMA(CM) (MB/SR)	ERROR (%)
16.1	3.81 E-2	8.5
21.5	3.31 E-2	8.2
26.9	2.47 E-2	12.0
32.4	1.91 E-2	10.0
37.4	1.64 E-2	6.3
48.0	1.219E-2	7.0
53.3	8.15 E-3	8.7
58.5	6.77 E-3	6.1
63.7	7.91 E-3	4.7
74.0	5.19 E-3	7.7

CA40(P,T)CA38

EX= 4.899 MEV
+/- 0.005 MEV

ANG(CM) (DEG)	SIGMA(CM) (MB/SR)	ERROR (%)
16.2	3.82 E-2	8.4
21.5	4.43 E-2	7.0
26.9	2.78 E-2	8.0
32.4	2.03 E-2	7.0
37.5	1.69 E-2	6.1
42.8	1.22 E-2	12.7
48.1	9.80 E-3	8.0
53.4	7.10 E-3	9.2
58.6	6.70 E-3	6.1
63.8	8.84 E-3	4.5
74.1	5.26 E-3	7.6

CA40(P,T)CA38

EX= 4.748 MEV
+/- 0.005 MEV

ANG(CM) (DEG)	SIGMA(CM) (MB/SR)	ERROR (%)
16.2	1.85 E-2	13.3
21.5	1.04 E-2	17.2
26.9	7.9 E-3	30.0
32.4	6.49 E-3	15.0
37.5	3.99 E-3	14.3
53.3	2.99 E-3	15.3
58.6	1.92 E-3	12.9
63.8	1.54 E-3	13.0
74.1	1.25 E-3	19.2

CA40(P,T)CA38

EX= 5.159 MEV
+/- 0.007 MEV

ANG(CM) (DEG)	SIGMA(CM) (MB/SR)	ERROR (%)
16.2	5.6 E-3	31.0
21.5	3.6 E-3	34.5
26.9	3.3 E-3	35.0
32.4	3.42 E-3	19.0
37.5	2.93 E-3	18.5
48.1	1.46 E-3	27.5
58.6	1.33 E-3	16.7
63.8	8.6 E-4	19.8
74.1	6.9 E-4	26.8

CA40(P,T)CA38

EX= 5.264 MEV
+/- 0.005 MEV

ANG(CM) (DEG)	SIGMA(CM) (MB/SR)	ERROR (%)
16.2	9.2 E-3	20.9
21.5	1.05 E-2	17.4
26.9	8.0 E-3	18.0
32.5	6.47 E-3	15.0
37.5	4.71 E-3	13.0
48.1	1.78 E-3	24.0
58.6	1.28 E-3	17.0
63.8	2.06 E-3	11.2
74.2	6.8 E-4	30.4

CA40(P,T)CA38

EX= 5.598 MEV
+/- 0.007 MEV

ANG(CM) (DEG)	SIGMA(CM) (MB/SR)	ERROR (%)
16.2	1.00 E-2	21.5
32.5	3.95 E-3	19.0
37.5	3.99 E-3	15.4
48.1	2.73 E-3	19.6
53.4	1.67 E-3	21.8
63.9	1.61 E-3	13.8
74.2	1.54 E-3	17.8

CA40(P,T)CA38

EX= 5.427 MEV
+/- 0.006 MEV

ANG(CM) (DEG)	SIGMA(CM) (MB/SR)	ERROR (%)
32.5	2.26 E-3	27.0
37.5	1.22 E-3	30.7

CA40(P,T)CA38

EX= 5.698 MEV
+/- 0.005 MEV

ANG(CM) (DEG)	SIGMA(CM) (MB/SR)	ERROR (%)
32.5	3.51 E-3	25.0
37.6	2.61 E-3	19.7
48.2	2.10 E-3	22.6
53.5	3.44 E-3	14.9

CA40(P,T)CA38

EX= 5.810 MEV
+/- 0.005 MEV

ANG(CM) (DEG)	SIGMA(CM) (MB/SR)	ERROR (%)
16.2	1.31 E-2	17.5
21.6	1.48 E-2	15.4
27.0	9.8 E-3	15.0
32.5	6.6 E-3	17.0
37.6	7.67 E-3	10.2
42.9	4.15 E-3	23.9
48.2	4.12 E-3	15.1
53.5	4.03 E-3	13.1
58.7	2.76 E-3	10.6
74.2	1.68 E-3	16.6

CA40(P,T)CA38

EX= 6.280 MEV
+/- 0.008 MEV

ANG(CM) (DEG)	SIGMA(CM) (MB/SR)	ERROR (%)
16.2	1.04 E-2	20.0
21.6	1.18 E-2	17.7
27.0	7.2 E-3	26.0
32.5	5.4 E-3	20.0
37.6	2.90 E-3	19.9
48.2	7.20 E-3	10.9
53.5	3.65 E-3	15.6
58.8	1.87 E-3	14.9
74.3	8.8 E-4	26.3

CA40(P,T)CA38

EX= 6.136 MEV
+/- 0.006 MEV

ANG(CM) (DEG)	SIGMA(CM) (MB/SR)	ERROR (%)
16.2	4.7 E-3	35.0
21.6	4.6 E-3	33.7
32.5	2.97 E-3	24.0
37.6	3.62 E-3	16.8
48.2	1.77 E-3	24.9
53.5	1.09 E-3	33.7
74.3	7.6 E-4	30.3

CA40(P,T)CA38

EX= 6.598 MEV
+/- 0.007 MEV

ANG(CM) (DEG)	SIGMA(CM) (MB/SR)	ERROR (%)
27.0	1.07 E-2	15.0
32.6	5.75 E-3	15.0
37.6	3.28 E-3	17.9
43.0	4.0 E-3	26.8
48.3	5.19 E-3	13.1
53.6	5.83 E-3	11.1
58.8	2.32 E-3	12.0
64.0	1.86 E-3	14.0

CA40(P,T)CA38

EX= 6.702 MEV
+/- 0.010 MEV

ANG(CM) (DEG)	SIGMA(CM) (MB/SR)	ERROR (%)
16.2	2.60 E-2	10.9
32.6	6.8 E-3	15.5
37.7	6.08 E-3	12.2
43.0	4.0 E-3	25.9
48.3	5.02 E-3	14.0
53.6	3.10 E-3	15.7
58.9	2.45 E-3	11.7
64.1	1.89 E-3	13.2

CA40(P,T)CA38

EX= 6.801 MEV
+/- 0.012 MEV

ANG(CM) (DEG)	SIGMA(CM) (MB/SR)	ERROR (%)
37.7	1.18 E-3	34.0
48.3	1.15 E-3	35.2
53.6	1.66 E-3	25.8

CA40(P,T)CA38

EX= 6.768 MEV
+/- 0.015 MEV

ANG(CM) (DEG)	SIGMA(CM) (MB/SR)	ERROR (%)
21.6	2.17 E-2	11.2
32.6	4.7 E-3	25.5

CA40(P,T)CA38

EX= 7.208 MEV
+/- 0.015 MEV

ANG(CM) (DEG)	SIGMA(CM) (MB/SR)	ERROR (%)
74.5	1.50 E-3	19.6

CA40(P,T)CA38

EX= 7.800 MEV
+/- 0.012 MEV

ANG(CM) (DEG)	SIGMA(CM) (MB/SR)	ERROR (%)
16.3	1.48 E-2	19.4
21.7	1.02 E-2	18.7
37.8	4.29 E-3	16.5
53.8	4.35 E-3	15.2
59.0	2.99 E-3	13.6
64.3	2.04 E-3	14.6

CA40(P,T)CA38

EX= 8.595 MEV
+/- 0.010 MEV

ANG(CM) (DEG)	SIGMA(CM) (MB/SR)	ERROR (%)
16.4	1.18 E-2	23.9
21.8	6.6 E-3	29.5
27.2	5.6 E-3	37.1
32.8	4.3 E-3	25.8
37.9	4.28 E-3	19.6
48.6	3.83 E-3	19.8
53.9	3.46 E-3	18.8
64.4	1.60 E-3	19.1

LIST OF REFERENCES

LIST OF REFERENCES

Ab66 A. Y. Abul-Magd, and M. El Nadi, Nucl. Phys. 77, 182 (1966).

Ad67 Eric George Adelberger, Thesis - Calif. Inst. of Tech. - 1967, from abstract in Nucl. Science Abstracts 22, 1225 (1968).

Ad68 J. M. Adams, A. Adams, and J. M. Calvert, J. Phys. A (London) 1, 549 (1968), from abstract in Nucl. Science Abstracts 22, 4923 (1968).

Aj59 F. Ajzenberg-Selove, and T. Lauritsen, Nucl. Phys. 11, 1 (1959).

Aj60 F. Azenberg-Selove, and K. L. Dunning, Phys. Rev. 119, 1681 (1960).

Ar68 A. Arima, S. Cohen, R. D. Lawson, and M. H. Macfarlane, Nucl. Phys. A108, 94 (1968).

Ba62 R. H. Bassel, R. M. Drisko, and G. R. Satchler, Oak Ridge National Laboratory Report ORNL-3240, 1962 (unpublished) and "Oak Ridge National Laboratory Memorandum to the Users of the Code JULIE," 1966 (unpublished).

Ba64a G. Bassani, Norton M. Hintz, and C. D. Kavaloski, Phys. Rev. 136, B1006 (1964).

Ba64b B. Bayman, Argonne National Laboratory Report ANL-6878, 335 (1964).

Ba65 G. Bassani, N. M. Hintz, C. D. Kavaloski, J. R. Maxwell, and G. M. Reynolds, Phys. Rev. 139, B830 (1965).

Ba68 B. F. Bayman, and Norton M. Hintz, Phys. Rev. 172, 1113 (1968).

Ba69 D. Bayer, and W. Benenson (to be published).

Be66 R. Benenson, and I. J. Taylor, Bull. Am. Phys. Soc., 11, 737 (1966).

Bl62 J. M. Blatt, G. H. Derrick, and J. N. Lyness, Phys. Rev. Letters 8, 323 (1962).

Br60 T. A. Brody, and M. Moshinsky, "Tables of Transformation Brackets," Monografias del Instituto de Fisica, Mexico (1960).

Br62 D. M. Brink, and G. R. Satchler, "Angular Momentum" (1962).

Br67 R. A. Broglia, and C. Riedel, Nucl. Phys. A92, 145 (1967) and Nucl. Phys. A93, 241 (1967).

Bu67 S. Buhl, D. Pelte, and B. Pouh, Nucl. Phys. A91, 319 (1967).

Ce64 J. Cerny, R. H. Pehl, and G. T. Garvey, Phys. Letters 12, 234 (1964).

Ce66 J. Cerny, S. W. Cosper, G. W. Butler, R. H. Pehl, F. S. Goulding, D. A. Landis, and C. Détraz, Phys. Rev. Letters 16, 469 (1966).

Da67 W. G. Davies, J. C. Hardy, D. J. Skyrme, D. G. Montague, K. Ramavataram, and T. A. Hodges, Rutherford Laboratory Report PLA-Dec. 1967.

Dr66 R. M. Drisko, and F. Rybicki, Phys. Rev. Letters 16, 275 (1966).

En67 P. M. Endt, and C. Van Der Leun, Nucl. Phys. A105, 1 (1967).

Fa68 W. R. Falk, R. J. Kidney, G. K. Tandon, and P. Kulisic, Bull. Am. Phys. Soc. 13, 1464 (1968).

Fl67 Donald George Fleming, Thesis - Univ. of Calif., Berkeley - 1967.

Fl68 D. G. Fleming, J. Cerny, C. Maples, and N. Glendenning, Phys. Rev. 166, 1012 (1968).

Fl69 E. R. Flynn, D. D. Armstrong, J. G. Beery, and A. G. Blair, Los Alamos Scientific Laboratory of the Univ. of Calif. (to be published).

Fr65 M. P. Fricke, and G. R. Satchler, Phys. Rev. 139, B567 (1965).

Fr67 M. P. Fricke, E. E. Gross, B. J. Morton, and A. Zucker, Phys. Rev. 156, 1207 (1967).

Ga61 N. H. Gale, J. B. Garg, and K. Ramavataram, Nucl. Phys. 22, 500 (1961).

Ga64 G. T. Garvey, J. Cerny, and R. Pehl, Phys. Rev. Letters 12, 726 (1964).

Ga67 N. K. Ganguly, A. A. Rush, E. J. Burge, and D. A. Smith, Rutherford Laboratory Report PLA-Dec. 1967, and Bull. Am. Phys. Soc. 12, 664 (1967).

Gi68 R. D. Gill, B. C. Robertson, J. L'Ecuyer, R. A. I. Bell, and H. J. Rose, Phys. Letters 28B, 116 (1968).

Gl62 N. K. Glendenning, Nucl. Phys. 29, 109 (1962).

Gl64 P. W. M. Glaudemans, G. Wiechers, and P. J. Brussaard, Nucl. Phys. 56, 529 (1964).

Gl65 Norman K. Glendenning, Phys. Rev. 137, B102 (1965).

Go64 F. S. Goulding, D. A. Landis, J. Cerny, and R. H. Pehl, Nucl. Inst, Methods 31, 1 (1964).

Ha66 J. C. Hardy, D. J. Skyrme, and I. S. Towner, Phys. Letters 23, 487 (1966).

Ha67 J. C. Hafele, E. R. Flynn, and A. G. Blair, Phys. Rev. 155, 1238 (1967).

Ha68 M. Hagen, K. H. Maier, and R. Michaelsen, Phys. Letters 26B, 432 (1968).

He64a E. M. Henley, and D. V. L. Yu, Phys. Rev. 133B, 1445 (1964).

He64b P. Hewka, R. Middleton, and J. Wiza, Phys. Letters 10, 93 (1964).

Hi64 N. M. Hintz, Argonne National Laboratory Report ANL-6878, 429 (1964).

Ja68 R. L. Jaffe, and W. J. Gerace, Princeton Univ. PUC-937-329, July, 1968 (unpublished).

Ka68a H. Kattenborn, C. Mayer-Böricke, and B. Mertens, Nucl. Phys. A119, 559 (1968).

Ka68b R. W. Kavanagh, A. Gallmann, E. Aslanides, F. Jundt, and E. Jacobs, Phys. Rev. 175, 1426 (1968).

Ko67 Raymond L. Kozub, Thesis - Michigan State Univ. - 1967.

Kr66 Merlyn Krick, G. J. F. Legge, Nucl. Phys. 89, 63 (1966).

La60 R. D. Lawson, and M. Goeppert-Mayer, Phys. Rev. 117, 174 (1960).

La62 T. Lauritsen, and F. Ajzenberg-Selove, Nuclear Data Sheets - Energy Levels of Light Nuclei (1962).

Le67 F. D. Lee, R. W. Krone, and F. W. Prosser, Jr., Nucl. Phys. A96, 209 (1967).

Li64 C. L. Lin, and S. Yoshida, Prog. Theo. Phys. (Tokyo) 32, 885 (1964).

Li66 C. L. Lin, Prog. Theo. Phys. (Tokyo) 36, 251 (1966).

Ma65 J. H. E. Mattauch, W. Thiele, and A. H. Wapstra, Nucl. Phys. 67, 1 (1965).

Ma66a Robert Golden Matlock, Thesis - Univ. of Colorado - 1966, from abstract in Nucl. Science Abstracts 22, 994 (1968).

Ma66b J. R. Maxwell, G. M. Reynolds, and N. M. Hintz, Phys. Rev. 151, 1000 (1966).

Ma67 G. Mackenzie, E. Kashy, M. M. Gordan, and H. G. Blosser, I.E.E.E. Trans. on Nuclear Science 450, NS-14, No. 3 (1967).

Mc65 W. R. McMurray, P. Van Der Merwe, and I. J. Van Heerden, Phys. Letters 18, 319 (1965).

Mc67 W. R. McMurray, P. Van Der Merwe, and I. J. Van Heerden, Nucl. Phys. A92, 401 (1967).

Mi64 R. Middleton, and D. J. Pullen, Nucl. Phys. 51, 63 (1964).

Mi66 R. G. Miller, and R. W. Kavanagh, Phys. Letters 22, 461 (1966).

Mi67 R. G. Miller, and R. W. Kavanagh, Nucl. Phys. A94, 261 (1967).

Mo59 M. Moshinsky, Nucl. Phys. 13, 104 (1959).

Ol65 R. W. Ollerhead, J. S. Lopes, A. R. Poletti, M. F. Thomas, and E. K. Warburton, Nucl. Phys. 66, 161 (1965).

Ol67 J. W. Olness, A. R. Poletti, and E. K. Warburton, Pys. Rev. 161, 1131 (1967).

Ol68 D. K. Olsen, and R. E. Brown, John H. Williams Laboratory of Nuclear Physics, Univ. of Minnesota, Annual Report COO-1265-67, 86 (1968).

Pa69 R. A. Paddock, S. M. Austin, W. Bensenson, I. D. Proctor, and F. St. Amant, Phys. Rev. (in press).

Pe64 D. Pelte, B. Pouh, and W. Scholz, Nucl. Phys. 52, 333 (1964).

Re67 G. M. Reynolds, J. R. Maxwell, and Norton M. Hintz, Phys. Rev. 153, 1283 (1967).

Ro67 R. R. Roy, and B. P. Nigam, Nuclear Physics (1967).

Ro68 C. Rolfs, and W. Trost, Nucl. Phys. A122, 633 (1968).

Sh63 A. de-Shalit, and I. Talmi, Nuclear Shell Theory (1963).

Sa64 G. R. Satchler, Nucl. Phys. 55, 1 (1964).

Sh68 M. H. Shapiro, Univ. of Rochester (private communication).

Sh69a M. H. Shapiro, A. Adams, C. Moss, and W. M. Denny, Bull. Am. Phys. Soc. 14, 530 (1969).

Sh69b M. H. Shapiro, C. Moss, and W. M. Denny, Nucl. Phys. A128, 73 (1969).

Si59 E. Silverstein, Nucl. Inst. Methods 4, 53 (1959).

To68 J. H. Towle, and G. J. Wall, Nucl. Phys. A118, 500 (1968).

Wi66 C. F. Williamson, J. Boujot, and J. Picard, Centre d'Etudes Nucléaire de Saclay, Report CEA-R3042 (1966).